Acta Medica Marisiensis

Volume 63 | Number 2 | 2017

Contents

Acta Medica Marisiensis

Acta Medica Marisiensis (ISSN: 2068-3324) is the official publication of the University of Medicine and Pharmacy of Tirgu-Mures, being published by University Press, Tîrgu Mureş.

The journal publishes high-quality articles on various subjects related to research and medical practice from the all the medical and pharmaceutical fields, ranging from basic to clinical research and corresponding to different article types such as: reviews, original articles, case reports, case series, letter to editor or brief reports. The journal also publishes short information or editorial notes in relation to different aspects of the medical and academic life.

Information for contributors

Manuscripts must be submitted via editorial manager system, available online at **www.editorialmanager.com/amma**

Correspondence

All correspondence should be addressed to the Editorial Office:

Acta Medica Marisiensis

University of Medicine and Pharmacy of Tîrgu Mureş

38, Gh. Marinescu St, 540139 Tîrgu Mureş, Romania

Managing Editor Associate Professor Adrian Man

or sent by e-mail to ammjournal@umftgm.ro

Acta Medica Marisiensis is indexed in the following international databases:

· Celdes
· CNKI Scholar
· CNPIEC
· EBSCO Discovery Service (since 01 July 2010, first indexed number - no.4/2010)
· Google Scholar
· J-Gate
· Primo Central (ExLibris)
· ReadCube
· Summon (Serials Solutions/ProQuest)
· TDOne (TDNet)
· WorldCat (OCLC)

DTP and Website Management

Editura Prisma

Disclaimer

The views expressed in this journal represent those of the authors or advertisers only.
In no way can they be construed necessarily to reflect the view of either the Editors or the Publishers.

This journal is printed on environmentally-friendly ECF (elemental chlorine free) woodfree paper.

Fresh or Frozen Berry Fruits?

Andrei-Şerban Gâz-Florea*
Editor

Recent studies suggest that diet rich in fruits and vegetables could be associated with reduced risk of coronary hard disease, stroke and even cancer [1]. Both fruits and vegetables are important sources of vitamins (e.g. group of vitamins B and C), minerals and fibers. Berry fruits are considered the healthiest, being also called the "*super fruits*". They are rich in anthocyanins, catechins, ellagic acid, vitamin C, flavonoids and antioxidants.

Catechins are flavonols that support the antioxidant defense system, while anthocyanins (water-soluble colored pigments that depending on their pH, could have red, blue or purple color) are associated with a low risk of certain cancers, prevent aging, improve memory function and the urinary tract health. Both catechins and anthocyanins have antioxidant properties [2].

Antioxidants are substances that protect the body by neutralizing free radicals or unstable molecules of oxygen that are major sources of disease and aging and can damage the body cells. They reduce the inflammation, neurodegenerative oxidative stress and macular degeneration, improve cardiovascular functions and decrease the risk of cancer.

However, both anthocyanins and catechins are not completely stable, therefore after harvesting, these compounds undergo different transformations during processing and storage, which may alter the biological activity [3]. In general, bioactive polyphenols are easily oxidized by polyphenol oxidase enzymes present in berry fruits (e.g. blueberries). The enzymes convert the polyphenols to the corresponding quinones, which furthermore is rapidly polymerized giving the red, brown or black pigment that cause fruits browning.

Recent studies assessed the storage effect of berry fruits, especially blueberries [4,5]. Although freezing of fruits is considered to be one of the best option for preservation, in the case of blueberries and bilberries there is a high decrease in the concentration of total phenols and anthocyanins after only three months of storage, even at low temperature (-20°C). In addition, there were no significant differences between fruits deposited at -20°C or -50°C, suggesting that lowering the temperature will not improve the preservation of bioactive compounds, especially the anthocyanins.

As a conclusion, freezing the berry fruits is not enough for anthocyanins to be preserved, since there is a retention of about 50%. On the other hand, no statistically significant loss of total polyphenols was noticed in the first 30 days for frozen fruits, while both anthocyanins and total polyphenols losses were significant at +6°C after less than 15 days (e.g. for total of polyphenols, the retention is about 34%).

Though the berry fruits are considered "*super fruits*" due to their high antioxidant properties, it is recommended to consume them fresh and to avoid processed fruits as much as possible.

The article „Short Period Storage Impact on Bioactive Constituents from Bilberries and Blueberries" published in this issue, present the antioxidant and antibacterial effects of these "*super fruits*" and the content of their specific bioactive compounds.

Conflict of interest

None to declare.

References

1. Giampieri F, Forbes-Hernandez TY, Gasparrini M, Afrin S, Cianciosi D, Reboredo-Rodriguez P, et al. The healthy effects of strawberry bioactive compounds on molecular pathways related to chronic diseases. Ann NY Acad Sci. 2017; doi: 10.1111/nyas.13373
2. Konarska A, Domaciuk M. Differences in the fruit structure and the location and content of bioactive substances in Viburnum opulus and Viburnum lantana fruits. Protoplasma. 2017 Jun 10;1–17
3. Rossi M, Giussani E, Morelli R, Lo Scalzo R, Nani RC, Torreggiani D. Effect of fruit blanching on phenolics and radical scavenging activity of highbush blueberry juice. Food Research International. 2003 Jan 1;36(9):999–1005
4. Mallik AU, Hamilton J. Harvest date and storage effect on fruit size, phenolic content and antioxidant capacity of wild blueberries of NW Ontario, Canada. J Food Sci Technol. 2017 May 1;54(6):1545–54
5. Srivastava A, Akoh CC, Yi W, Fischer J, Krewer G. Effect of Storage Conditions on the Biological Activity of Phenolic Compounds of Blueberry Extract Packed in Glass Bottles. J Agric Food Chem. 2007 Apr 1;55(7):2705–13

* Correspondence to: Andrei-Şerban Gâz-Florea
E-mail: andrei.gaz@umftgm.ro

DE GRUYTER OPEN

Acta Medica Marisiensis 2017;63(2):52-55 DOI: 10.1515/amma-2017-0021

REVIEW

Analytical Methodologies for the Stereoselective Determination of Sibutramine: An Overview

Alexandru Robert Vlad[1], Gabriel Hancu[1*], Hajnal Kelemen[1], Diana Ciurcă[2], Amelia Tero-Vescan[3]

1 Department of Pharmaceutical Chemistry, Faculty of Pharmacy, University of Medicine and Pharmacy, Tîrgu Mureș, Romania
2 Department of Organic Chemistry, Faculty of Pharmacy, University of Medicine and Pharmacy, Tîrgu Mureș, Romania
3 Department of Biochemistry, Faculty of Pharmacy, University of Medicine and Pharmacy, Tîrgu Mureș, Romania

Sibutramine is a chiral anti-obesity drug which decreases food intake and increases energy expenditure. In therapy it is used as a racemic mixture; however both pharmacokinetic and pharmacodynamic data have revealed enantioselective behavior of sibutramine and its major active metabolites. Several chromatographic and electrophoretic analytical methods have been published so far for the chiral determination of sibutramine from pharmaceutical preparations and biological samples. The current paper aims to provide a systematic review of the stereochemical aspects and analytical methods used for the enantiodetermination of sibutramine and its active enantiomers covering the last 15 years.

Keywords: sibutramine; chirality; enantioseparation; high perfomance liquid chromatography; capillary electrophoresis

Received 7 May 2017 / Accepted 13 June 2017

Introduction

Sibutramine [(±)-1-(p-chlorophenyl)a-isobutyl-N,N dimethyl cyclobutane methylamine hydrochloride] (SIB) is an oral anorexiant which inhibits central reuptake of serotonin, norepinephrine, and to a lesser extent dopamine; prescribed in the treatment of obesity along with a reduced calorie diet. Unlike other anorexiant agents, like amphetamine, SIB does not affect the release of neurotransmitters [1].

SIB pharmacological mechanism of action by which it exerts its weight-loss effect is due to a combination of feelings of satiety, reduced appetite and induction of thermogenesis [2]. SIB is prescribed as an adjunct in the management of exogenous obesity along with exercise and diet [3].

SIB has a chiral carbon in its molecule and consequently exists in the form of two enantiomers, *R*-SIB and *S*-SIB (figure 1). The substance is marketed as a racemic mixture, but pharmacodynamic and pharmacokinetic profile has revealed the enantioselective behavior of SIB, as *R*-SIB presents a better anorexic effect than racemic SIB or its *S*-enantiomer [4].

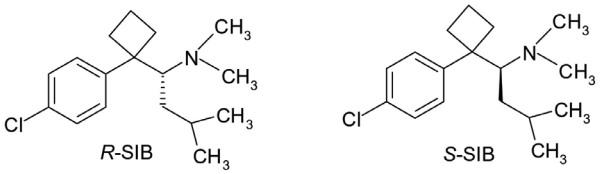

Fig. 1. Chemical structure of SIB enantiomers

SIB undergoes first-pass demethylation to active metabolites, mono-desmethylsibutramine (MDS) and di-desmethylsibutramine (DDS) which are primarily responsible for its pharmacologic effects (figure 2). The active metabolites are biotransformed further in the liver and excreted primarily in the urine [5]. SIB metabolites are also chiral, and exhibit enantioselecive effects; as *R*-SIB metabolites exhibit higher potency than the *S*-SIB metabolites; also *R*-SIB metabolites were present at lower concentrations in the body because of their fast metabolization to hydroxylated and carbamoylglucuronized forms and their fast urinary excretion [6]. Additionaly, another pharmacokinetic study demonstrates that *R*-SIB is biotransformed preferentially over *S*-SIB in primary cultures of rat hepatocytes and in rat liver microsomes [7].

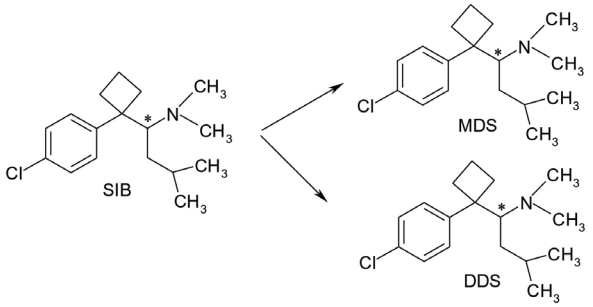

Fig. 2. SIB metabolism (* denotes the chiral centers)

Initially, at doses of 10-20 mg per day, SIB was considered to present good safety profile, as it does not induce cardiovascular adverse effects or pulmonary hypertension, in comparison with other previously used antiobesity agents [8]. However, the results of SCOUT (Sibutramine Cardiovascular and Diabetes Outcome Study) clinical trial, a study designed to evaluate the efficacy/safety ratio of SIB in high-risk patients, showed that long-term treatment with SIB exposed patients with pre-existing cardiovascular disease to a statistically significant increased risk for stroke and myocardial infarction [9]. The European Medicines

* Correspondence to: Gabriel Hancu
E-mail: gabriel.hancu@umftgm.ro

Agency (EMA) recommended in 2010 the suspension of marketing authorizations for SIB across EU countries, taking in consideration reports considering that the cardiovascular risks of SIB seems to outweigh the benefits as a weight-loss agent. In the same year Abbot Laboratories announced the withdrawing SIB from the US market under pressure from the Food and Drug Administration (FDA), citing concerns over therapeutic efficiency coupled with increased risk of adverse cardiovascular adverse effects [10].

Nowadays SIB is still used in more than 40 countries from Asia and Central and South America. Also, the illicit addition of SIB in counterfeit slimming products has been reported, which represents a serious public health problem [11].

The enantioselective behavior of SIB enantiomers and its two major active metabolites have been of great interest from pharmacodynamic and pharmacokinetic point of view. For the development of SIB as a chiral drug and for pharmacokinetic and pharmacologic studies, the enantioselective separation and determination of SIB become of major importance.

A variety of analytical methods (chromatographic, electrophoretic) have been reported in the past decade for the determination of SIB in pharmaceutical preparations and in biological materials. However the large majority of the published methods report achiral analysis of SIB by reversed-phase liquid chromatography (RP-LC) in pharmaceutical products [12], ultra-high-pressure liquid chromatography with diode-array detection in adulterated weight-loss formulations [13], column-switching high performance liquid chromatography (HPLC) in rat serum [14] or liquid chromatography–mass spectrometry (LC-MS/MS) in human plasma [15]. Despite the pharmaceutical importance of the stereoselective analysis of this compound, only a few studies have been reported for chiral separation of SIB and its metabolites.

In the current review, we have summed up the previously published methods in the literature for enantiodetermination of SIB and its active metabolites.

Determination of absolute configuration

Single crystal X-ray crystallography is considered to be the most powerful structural method for the determination of 3D structures of the molecules; however while the results of a routine diffraction experiment provides unambiguous determination of the relative configuration of the stereogenic centers in the molecule, determination of absolute configuration can be a more challenging task.

In the literature we can find a few reports for the preparation of SIB or its metabolites enantiomers using: resolution of the racemate with a chiral acid; asymmetric synthesis and chiral column HPLC separation.

Racemic SIB was resolved with dibenzoyl-D-tartaric acid, and the absolute stereochemistry of SIB was determined by single crystal X-ray crystallography of the dibenzoyl D-tartrate. The major active metabolite, MDS, was obtained by demethylation of SIB with diethyl azodicarboxylate, a complete retention of the configuration was observed. Based on single crystal X-ray structural analysis, the (+)-isomer of SIB salt has the R configuration, the same as the (+)-MDS salt obtained by demethylation. Enantiomeric purity of SIB was verified by HPLC using a chiral stationary phase column (ES-OVM) [16].

Because of the potentially explosive diethyl azodicarboxylate, application of the SIB demethylation method to the mass production of MDS cannot be viable a solution. Consequently another synthesis method of the enantiomerically pure *R*-MDS and *S*-MDS was developed along with an improved alternative synthesis of the racemic MDS. This route was used for kilo-scale production of enantiomerically pure *R*- and *S*- MDS. Racemic MDS was resolved with either *R*- or *S*-mandelic acid, and the absolute stereochemistry of MDS was determined by single X-ray crystallography of its mandelate salt. Based on single-crystal X-ray structural analysis, the same results were obtained as in the previous study, as the (+)-isomer of the MDS salt presented *R*-configuration [17].

In order to find an efficient high yielding synthesis method for *R*-MDS, efforts were focused towards the development of a catalytic asymmetric method. The key step in the asymmetric synthesis of *R*-MDS was the enantioselective catalytic addition of iBuLi to aldimine 3 derived from methyl amine and 1-(4-chlorophenyl) cyclobutanecarboxaldehyde [18].

The synthesis of the other enantiopure metabolite DDS was also resolved by combining isolation, purification, and salt formation resolution in one-step, in which chemically pure racemic DDS was isolated from the reaction mixture as a tartaric acid salt, to perform simple crystallizations, in order to provide both enantiopure *R*- and *S*-DDS [19].

Chiral separation of sibutramine by chromatographic methods

Two HPLC techniques can be used for the chiral separation of pharmaceutical substances: indirect and direct ones. The indirect HPLC technique involves the use of a chiral derivatization reagent with the formation of two diastereomer, which can be separated using achiral chromatographic conditions. On the other hand, the direct HPLC technique utilizes a chiral selector added either in the chiral stationary phase or in the mobile phase, and are the most frequently used methods because of their simplicity and rapidity [20].

Several reports have been published for the chiral determination of SIB by HPLC techniques, using protein based chiral stationary phase [21], Chiracel OD column [22] or Chiralcel AGP-stationary phase column [23,24].

The enantioseparation of SIB was achieved by direct HPLC on a Chiralcel OD column (250 × 4.6 mm, 10 μm) using a mobile phase consisting of hexane:ethanol:trifloroacetic acid (93:7:0.05, v/v/v) and a flow rate of 1 mL/min. The chiral separation of the two

enantiomers was obtained within 15 minutes with UV detection at a wavelength of 225 nm [22].

A rapid and simple chromatographic method for the separation of *R*- and *S*-isomers of SIB, MDS, and DDS in rat plasma by LC-MS/MS using a Chiral-AGP stationary-phase column (chiral stationary-phase based on bonding to α-acid glycoprotein -AGP) (100 × 2.0 mm, 5 μm) has been also reported. The enantiomers of SIB and its two major active metabolites were extracted from rat plasma using diethyl ether and n-hexane under alkaline conditions. After evaporation the organic layer, the residue was reconstituted in the mobile phase (10 mM ammonium acetate buffer adjusted to pH 4.03 with acetic acid:acetonitrile, 94:6, v/v). The method was used to characterize the plasma concentrations of the stereoisomers of SIB and its metabolites in rat plasma, following the oral administration of a single oral dose of 10 mg/kg of racemic SIB [23].

The same optimized LC-MS/MS method was then applied for the determination of SIB and its two active metabolites in human plasma. The method was validated in accordance with FDA regulations for the validation of bioanalytical methods. The method was successfully applied to quantify SIB and its metabolites stereoisomers plasma concentration in healthy volunteers [24].

Chiral separation of sibutramine by electrophoretic methods

The use of chiral capillary electrophoresis (CE) in enantiomeric separations has gained momentum in the chiral analysis of pharmaceutical substances, with advantages related to the rapid method development and high separation efficiency; CE is also a highly flexible and versatile analytical method, with a minimal use of chiral selectors and analytes, and usually uses a direct method of separation by simply adding the chiral selector to the background electrolyte [25].

Cyclodextrins (CDs) are the most frequently used chiral selectors in enantiomeric separations by CE, because several useful properties in chiral CE such as good complexation ability of various analytes, acceptable solubility in water, low UV absorption, commercial availability, relatively low price and good chemical stability [26].

Capillary zone electrophoresis (CZE) using derivatized neutral CD - methyl-β-CD (M-β-CD) or derivatized ionized CD - carboxymethyl- β-CD as chiral (CM-β-CD) selectors was the first-choice method used in several studies for the enantioseparation of SIB enantiomers [27-30].

Separation of SIB enantiomers by CE was accomplished using a mixed buffer composition containing a mixture of 20 mM phosphate and 10 mM citrate and either 5 mM M-β-CD (pH 4.3) or 5 mM CM-β-CD (pH 6.5) as chiral selectors. The separation was achieved on a 50 cm × 50 μm fused silica capillary, UV detection was used at 223 nm. During the method optimization, the mixed buffer showed superior separation results in comparison with single component buffers. The stability constants of *R*- and *S*-SIB demonstrated that the resolution of SIB enantiomers was primarily due to the difference in the stability constants of the complexes. The optimized CE method was used for the determination of SIB enantiomers in pharmaceutical formulations [27].

Proton nuclear magnetic resonance spectroscopy (^{1}H-NMR) and CE have been used to discriminate SIB enantiomers using different CD derivatives as chiral selectors. Possible correlations between ^{1}H-NMR and CE results were examined; good correlation between the H-NMR shift non-equivalence data for SIB and the enantioseparation by CE was observed. Separation of SIB enantiomers by CE was achieved using a 50 mM of phosphate buffer at pH 3.0 and 10 mM of M-β-CD as chiral selector. The CE method was optimized by a complex study regarding the influence of buffer concentration, buffer pH, CD concentration, and system temperature on the chiral resolution of SIB enantiomers. The analytical performance of the method was verified; the method was validated according to ICH guidelines and was applied for the quantitative determination of SIB enantiomers in pharmaceutical formulations. On a 600 MHz ^{1}H-NMR analysis, enantiomer signal separation of SIB was obtained by fast diastereomeric interaction with the chiral selector. Using ^{1}H-NMR and 2D ROESY studies a structure of the inclusion complex was also proposed [28].

In another study a complex screening of a large number of native and derivatized, neutral and ionized CD derivatives was performed in order to establish the optimum chiral selector for the enantiodetermination of SIB. During the optimization process, the effects of buffer composition, background electrolyte concentration and pH, CD type and concentration, applied voltage, capillary temperature and injection parameters on the chiral resolution were studied. The best results on a short fused silica capillary of 30 cm × 50 μm were obtained using a 50 mM phosphate buffer containing 10 mM randomly methylated β-CD (RAMEB) as chiral selector at a pH of 4.50 with UV detection at 220 nm; the separation of enantiomers was achieved in approximately 5 minutes [29].

SIB was used as the model substance in order to demonstrate the reversal of enantiomer migration order in CE separations in correlation with CD concentration. In the presence of M-β-CD and 2-hydroxypropyl-β-CD (HP-β-CD) overlapping of migration for SIB enantiomers was observed, while reversal of enantiomer migration order was observed in the case of β-CD and acetyl-β-CD (A- β-CD) when increasing CD concentration. The reversal of enantiomer migration order could be explained in terms of the opposing effects of the stability and the limiting complex mobility of the SIB-CD complexes while the enantioseparation of SIB with M- and HP-β-CD was based on the differences in the binding constants of the SIB-CD complexes while [30].

SIB was one of the ten model compounds used for the testing of an open-tubular capillary electrochromatogra-

phy column prepared by chemically immobilized β-CD modified gold nanoparticles onto a new surface with pre-derivatization of (3-mercaptopropyl)-trimethoxysilane. To improve enantioselectivity, β-CD was used as chiral additive in order to identify synergistic effects and increase chiral resolution [31].

Conclusions

In therapy, SIB has been used as a racemic mixture, while the pure enantiomers of the compound have not been available. For efficiency and safety reasons, maybe SIB may have been developed and administered as a pure enatiomer, and for the evaluation of pharmacokinetic and pharmacodynamic profile enantioselective determination of SIB enantiomers is needed. Without doubt HPLC methods have proven to be the most reliable and versatile analytical techniques for chiral measurements of pharmaceutical substances, however CE has become a viable alternative and a complementary technique for certain applications because of its high separation efficiency, relatively short analysis time, and low consumption of samples and reagents.

References

1. Luque CA, Rey JA - The discovery and status of sibutramine as an anti-obesity drug. Eur J Pharmacol. 2002;(2-3):119-128.
2. Finer N. - Sibutramine: its mode of action and efficacy. Int J Obes Relat Metab Disord. 2002;26(4):29-33.
3. Nisoli E, Carruba MO - An assessment of the safety and efficacy of sibutramine, an anti-obesity drug with a novel mechanism of action. Obes Rev. 2000;1(2):127-139.
4. Bodhankar SL, Thakurdesai PA, Singhal S, et al. - Anorexic effect of (R)-sibutramine: comparison with (RS)-sibutramine and (S)-sibutramine. Indian J Physiol Pharmacol. 2007;51(2):175-178.
5. Filippatos TD, Kiortsis DN, Liberopoulos EN, et al. - A review of the metabolic effects of sibutramine. Curr Med Res Opin. 2005;21(3):457-468.
6. Glick SD, Haskew RE, Maisonneuve IM, et al. - Enantioselective behavioral effects of sibutramine metabolites. Eur J Pharmacol. 2000;397:93-102.
7. Noh K, Bae K, Min B, et al. - Enantioselective pharmacokinetics of sibutramine in rat. Arch Pharm Res. 2010;33:267-273.
8. Tyczynski JE, Oleske DM, Klingman D, et al. - Safety assessment of an anti-obesity drug (sibutramine): a retrospective cohort study. Drug Saf. 2012;35(8):629-644.
9. Maggioni AP, Caterson ID, Urso R, et al. - Relation between weight loss and causes of death in patients with cardiovascular disease: finding from the SCOUT trial. J Cardiovasc Med. 2017;18(3):144-151.
10. Scheen AJ - Cardiovascular risk-benefit profile of sibutramine. Am J Cardiovasc Drugs. 2010; 10(5):321-334.
11. Dunn JD, Gryniewicz-Ruzicka CM, Kauffman JF, et al.- Using a portable ion mobility spectrometer to screen dietary supplements for sibutramine. J Pharm Biomed Anal. 2011; 54(3):469-474.
12. Diefenbach IC, Friedrich M, Dos Santos MR, et al. - Development and validation of a column high-performance liquid chromatographic method for determination of sibutramine in capsules. J AOAC Int. 2009; 92(1):148-151.
13. Rebiere H, Guinot P, Civade C, et al. - Detection of hazardous weight-loss substances in adulterated slimming formulations using ultra-high-pressure liquid chromatography with diode-array detection. Food Addit Contam Part A Chem Anal Control Expo Risk Assess. 2012;29(2):161-171.
14. Um SY, Kim KB, Kim SH, et al. - Determination of the active metabolites of sibutramine in rat serum using column-switching HPLC. J Sep Sci. 2008;31(15):2820-2826.
15. Bae JW, Choi CI, Jang CG, et al. - Simultaneous determination of sibutramine and its active metabolites in human plasma by LC-MS/MS and its application to a pharmacokinetic study. Biomed Chromatogr. 2011;25(11):1181-1188.
16. Fang QK, Senanayake CH, Han Z, et al. - First preparation of enantiomerically pure sibutramine and its major metabolite, and determination of their absolute configuration by single crystal X-ray analysis. Tetrahedron Asymmetry, 1999; 10:4477-4480.
17. Han Z, Krishnamurthy D, Pflum D, et al. - First practical synthesis of enantiomerically pure (R)- and (S)-desmethylsibutramine (DMS) and unambiguous determination of their absolute configuration by single-crystal X-ray analysis. Tetrahedron Asymmetry, 2002;13(2):107-109.
18. Krishnamurthy D, Han Z, Wald SA, et al. - First asymmetric synthesis of (R)-desmethylsibutramine. Tetrahedron Asymmetry, 2002;43(13):2331-2333.
19. Han Z, Krishnamurthy D, Fang QF, et al. - New resolution approach for large-scale preparation of enantiopure didesmethylsibutramine (DDMS). Tetrahedron Asymmetry, 2003;14(22):3533-3536.
20. Bojarski J, Aboun-Enein HY, Ghanem A - What's new in chromatographic enantioseparations. Curr Anal Chem. 2005;1:59–97.
21. Singh AK, Pedro LG, Gomes FP, et al. - Development and validation of sensitive methods for determination of sibutramine hydrochloride monohydrate and direct enantiomeric separation on a protein-based chiral stationary phase. J. AOAC Int. 2008; 91(3):572-579.
22. Radhakrishna T, Lakshmi-Narayana C, Sreenivas-Rao D, et al. - LC method for the determination of assay and purity of sibutramine hydrochloride and its enantiomers by chiral chromatography. J Pharm Biomed Anal. 2000;22:627-639.
23. Bae K, Noh K, Jang K, et al. - Analysis of enantiomers of sibutramine and its metabolites in rat plasma by liquid chromatography–mass spectrometry using a chiral stationary-phase column. J Pharm Biomed Anal. 2009;50(2):267-70.
24. Kang W, Bae K, Noh K - Enantioselective determination of sibutramine and its active metabolites in human plasma. J Pharm Biomed Anal. 2009; 51:264-267.
25. Scriba GK - Differentiation of enantiomers by capillary electrophoresis. Top Curr Chem. 2013; 340:209-275.
26. Rezanka P, Navrátilová K, Rezanka M, et al. - Application of cyclodextrins in chiral capillary electrophoresis. Electrophoresis. 2014; 35(19):2701-2721.
27. Zhu H, Wu E, Chen J, et al. - Enantioseparation and determination of sibutramine in pharmaceutical formulations by capillary electrophoresis. Bull. Korean Chem. Soc. 2010; 31:1496-1500.
28. Lee YJ, Choi S, Lee J, et al. - Chiral discrimination of sibutramine enantiomers by capillary electrophoresis and proton nuclear magnetic resonance spectroscopy. Arch Pharm Sci Res. 2012;35(4):671-681.
29. Hancu G, Hilochie A, Vlad RA, et al. - Enantiomeric separation of sibutramine by capillary zone electrophoresis. J Braz Chem Soc. 2016;27(6):1116-1120.
30. Zhu H, Wu E, Chen J, et al. - Reverse migration order of sibutramine enantiomers as a function of cyclodextrin concentration in capillary electrophoresis. J Pharm Biomed Anal. 2011; 54:1007-1112.
31. Fang L, Yu J, Jiang Z, et al. - Preparation of a β-cyclodextrin-based open-tubular capillary electrochromatography column and application for enantioseparations of ten basic drugs. PLoS One. 2016; 15(1): e0146292.

DE GRUYTER OPEN

Acta Medica Marisiensis 2017;63(2):56-61 DOI: 10.1515/amma-2017-0011

RESEARCH ARTICLE

Evaluation of Mechanical Properties of Nonsteroidal Anti-Inflammatory Matrix Type Transdermal Therapeutic Systems

Paula Antonoaea[1], Nicoleta Todoran[1]*, Emőke Rédai[1], Adriana Ciurba[1], Cătălina Bogdan[2], Mirela Moldovan[2], Daniela Lucia Muntean[3]

1 Department of Pharmaceutical Technology, University of Medicine and Pharmacy of Tîrgu Mureș, Romania
2 Department of Dermatopharmacy and Cosmetics, "Iuliu Haţieganu" University of Medicine and Pharmacy Cluj-Napoca, Romania
3 Department of Analytical Chemistry and Drug Analysis, University of Medicine and Pharmacy of Tîrgu Mureș, Romania

Objective: Transdermal therapeutic systems (TTSs) represent an intensely studied alternative to oral delivery of non-steroid anti-inflammatory drugs (NSAIDs) in the treatment of rheumatic diseases due to its ability of avoiding the side effects of the oral route. This study aims to present the evaluation of the mechanical properties of three NSAIDs (meloxicam, tenoxicam and indomethacin) individually included in four type of polymeric matrixes, as part of new formulations development process. **Methods**: 12 products in form of TTS matrixes were prepared by solvent casting evaporation technique, using hydroxypropyl methylcellulose (HPMC 15000, HPMC E5) and/or ethylcellulose as matrix-forming polymers. Each of the resulted products was evaluated by determining the water vapor absorption, desorption or transmission in controlled atmosphere humidity (evaluation of porosity); the elongation capacity, tensile strength and bioadhesiveness (evaluation of mechanical properties). **Results**: The analysis of three groups of the experimental data expressed as averages on each group was necessary, in order to identify the parameters which statistically are critically influenced by the ingredients associated in the TTSs matrix compositions. Analysis by normality tests, variance and correlation tests (Anova, Pearson) enabled evaluation of the effect of NSAID type vs. the effect of polymer matrix type on the parameters of the NSAID TTS matrix. **Conclusions**: Meloxicam incorporated in the structure of HPMC 15000 polymeric matrix favors its viscoelastic structure. Ethylcellulose functions as plasticizer and supports the matrix bioadhesiveness. HPMC E5 does not meet the requirements for TTS preparation in the used experimental conditions.

Keywords: transdermal therapeutic system, matrix type, non-steroid anti-inflammatory, mechanical properties, bioadhesiveness

Received 28 February 2017 / Accepted 13 April 2017

Introduction

Transdermal therapeutic systems (TTSs) represent an important therapeutic progress for both healthcare professionals and patients, as the absorption of pharmaceutical active ingredients by the transdermal route has the main advantage of minimize their side effects [1-3]. The transdermal route is also preferable in case of oral intolerance, or to enable patients to self-administrate their medication [4]. Although the efficacy of nonsteroidal anti-inflammatory drugs (NSAIDs) in rheumatic diseases is well known, their gastric side effects cannot be neglected. Considering this, in the last years the interest to incorporate NSAIDs into TTSs has grown, as it results from the latest published data for: indomethacin [5,6], meloxicam [7,8], tenoxicam [7,9], lornoxicam [10,11], naproxen [12], ketoprofen [13].

In order to study and describe the dissolution process of the active ingredient from a TTS, several properties of the matrix system need to be evaluated, such as: physical appearance, folding endurance, tensile strength, moisture vapors absorption, moisture vapors loss. These properties depend on the composition, compatibility and amount of used ingredients [14-16]. In addition, the ability of the NSAIDs to be released from a transdermal therapeutic system is fundamentally influenced by certain mechanical properties [14,17] that must be provided to the bioadhesive matrix by a suitable formulation.

This study aims to present the evaluation of the mechanical properties of three NSAIDs individually included in four type of polymeric matrix, as part of the formulation development process of new TTSs.

Methods

Preparation of NAIDs TTS matrix:

-Chemicals: meloxicam - MX (Techno Drugs & Intermediates Ltd. Mumbai, India), tenoxicam - TX (Nantong Chemding Chephar Co. Ltd. Jiangsu, China) and indomethacin - IND (Sigma Aldrich Milan, Italy). Three types of cellulose ethers polymers were used as matrix formers in ultrapure water (Millipore Direct-Q S. water distiller): hydroxypropyl methylcellulose - HPMC 15000 (Metolose 90SH - 15000 mPa·s, Shin-Etsu Chemical Co., Ltd. Tokyo, Japan), hydroxypropyl methylcellulose - HPMC E5 (Methocel *E5 - 5* mPa·s, Dow *Chemical Co.,* Midland, USA) and ethyl cellulose - EC 10 (EC 10 mPa·s, Sigma Aldrich Co., Germany). Auxiliary substances: propylene glycol - PG (Scharlau Chemie, Barcelona, Spain); tween 20 (Sigma Aldrich Co., France); absolute ethanol and chloroform (Chemical Company, Romania).

-Formulation of NSAIDs TTS matrix: 12 compositions containing each 0.5 % of NSAID were formulated using

* Correspondence to: Nicoleta Todoran
E-mail: nicoleta.todoran@umftgm.ro

three different NSAIDs (MX, TX or IND), each of them being included in four variants of polymeric liquid dispersions (table I).

- TTS matrix preparation technique: 0.5% NSAID dissolved in ethanol - propylene was mixed with 1% tween 20 (previously dispersed in the corresponding amount of water). The film former polymer/s (dissolved in a minimum amount of chloroform, in the case of EC 10) has been added to the mixture under continuous stirring to obtain a homogeneous dispersion which was then poured into Petri dishes (diameter of 9.8 cm) and kept 24 hours into an oven at 40°C, for solvent evaporation.

Evaluation of bulk viscoelastic properties (sample size/performed test):

-Samples of 75.39 cm² (∅ 9.8 cm): Physical appearance was visually evaluated in terms of appearance, color, clarity and smoothness of the surface. *Weight uniformity – m (g)* was determined by weighing three samples of each product and then expressed as the calculated average. *Thickness – T (mm)* was determined using a digital micrometer and expressed as average of the values determined in five different points on the surface of the each product.

-Sample of 4.0 cm² (2.0 cm/2.0 cm): Folding endurance - FE (x) was determined by repeatedly folding the sample (twice for a pair) in the same place (middle line) and expressed as the number (x) of fold pairs to which the product resisted until the break.

-Samples of 6 cm² (4.0 cm length/1.5 cm width): Tensile strength - TS ($N \cdot mm^{-2}$) was determined by subjecting the sample, kept fixed at the upper end, to increasing downwards tensile forces generated by 10 g weights successively attached to the lower end, until the break of the sample. $TS\ (N \cdot mm^{-2}) = (M \cdot g)/(W \cdot T)$, wherein M - is the weight that generated the tensile force (Kg), g - the gravitational acceleration (9.8 N/Kg), W - the width of sample (mm) and T – the thickness of sample (mm). *Elongation to break – Eb (%)*: $Eb\ (\%) = (L_f - L_i) \cdot 100/L_i$, wherein L_i – is the initial length of sample (cm) and L_f – the final length of sample (cm) recorded before break. The pairs of data (elongation as a result of tensile strength) recorded during each determination were then used to evaluate the viscoelastic behavior by graphical and statistical correlation analysis.

-Samples of 4.15 cm² (∅ 2.3 cm): Moisture vapor absorption - WVA (%) was determined by keeping the sample for 72 hours in desiccator containing a saturated solution of potassium chloride (relative humidity - RH ≈ 80%) and expressed as the moisture uptake: $WVA\ (\%) = (m_f - m_i) \cdot 100/m_i$, wherein m_i - is the initial mass of the sample (g), m_f - the final mass of the sample (g). *Moisture vapor loss - WVL (%)* was determined by keeping the sample for 72 hours in desiccator containing anhydrous calcium chloride (RH ≈ 0%) and expressed as the calculated moisture lost: $WVL\ (\%) = (m_i - m_f) \cdot 100/m_i$, wherein m_i - is the initial mass of the sample (g), m_f - the final mass of the sample (g). *Water vapor transmission rate - WVTR ($g \cdot cm^{-2} \cdot h^{-1}$)* was determined by weighting an assemble consisting of a glass flask (internal volume of 6 cm³) containing 1.000 g of anhydrous calcium chloride (RH ≈ 0%), with the opening sealed with the test sample, before and after maintaining it to constant mass (72 h) in a desiccator containing a saturated solution of potassium chloride (RH ≈ 80%). $WVTR\ (g \cdot cm^{-2} \cdot h^{-1}) = (m_f - m_i) \cdot 100/t \cdot S$, wherein m_i - is the initial mass of the sample (g), m_f - the final mass of the sample (g), t - time (72 h) and S – the surface of the sample (4.15 cm²).

Evaluation of texture and surface properties: was performed with a CT3 Texture Analyzer (Brookfield Engineering Laboratories, equipped with TexturePro CT V1.5 Software). For each sample, three measurements were carried out and the mean ± standard deviation were reported.

-Hardness force (the resistance of TTS matrix to perforation) - Hf (g) was determined by running the *Rupture Test* in the following conditions: the sample placed between the two plates of the TA-FSF fixture; TA 42 (3 mm Cylinder Probe) as penetration accessory device; target value - 4500 g, trigger load - 10 g, test speed – 0.20 mm/sec; test target – Load (recorded value). One cycle includes all recordings until the rupture of the sample.

-Adhesiveness (the surface stickiness of TTS matrix) - A (mJ) was measured based on the a*dhesive force - Af (g)* determined by running the *Compression Test* in the following conditions: the sample (at two minutes after wetting with 200 µL distilled water) placed into TA-BT-KIT fixture; TA-AACC36 accessory device covered with a natural membrane (intestine porcine membrane); target value - 100 g, hold time - 10 sec, trigger load - 0.5 g, test speed - 1 mm/sec; test target - Load (recorded value).

Statistical analysis: were performed with GraphPad Prism 6 (GraphPad Software, Inc., San Diego, California), considering the statistical significant difference at $p < 0.05$, for the confidence interval (CI) of 95%. The calculated

Table I. Compositions containing 0.5% NSAID proposed in the study

Ingredient (%)	Meloxicam				Tenoxicam				Indomethacin			
	MX 1	MX 2	MX 3	MX 4	TX 1	TX 2	TX 3	TX 4	IND 1	IND 2	IND 3	IND 4
HPMC E5	3.0		-		3.0			-	3.0			-
HPMC 15000	-	1.0	1.5	1.0	-	1.0	1.5	1.0	-	1.0	1.5	1.0
*EC 10				1.0				1.0				1.0
Ethanol - PG (3:1)	40.0											
Tween 20	1.0											
Water	to 100.0											

*dissolved in a small amount of chloroform

descriptive statistic parameters were the followings: *arithmetic mean*; *standard deviation (SD)* and *coefficient of variation (CV)*. In order to test the normality of the dispersion the following inferential tests were applied: *Kolmogorov–Smirnov (KS)*, *D'Agostino & Pearson omnibus* and *Shapiro-Wilk.* The variance analysis and the correlation for association between variables were quantified by: t*wo-way Anova test*; *Tukey test*; *Pearson`s correlation test.*

Results

12 products in form of TTS matrix were prepared by casting on a circular surface of 75.39 cm² each of the homogenous aqueous dispersions containing 0.5% NSAID (MX, TX or IND) in four variants of polymeric composition. The values of the determined parameters of these laboratory products are shown in table II and the texture and surface properties of NSAID TTS matrix prepared in the four polymeric films in table III.

Discussion

The TTSs were obtained as four matrix type (1-4) polymeric films with uniform, porous and lightly sticky surface. The greasy aspect of the EC 10 containing films (type 4) may be explained by the chloroform used to dissolve the polymer before incorporation. The color of the film depends on the NSAID type included in the matrix: those containing meloxicam (MX) are light yellow, tenoxicam (TX) intensive yellow, and indomethacin (IND) white-yellow.

Variance analysis of NSAID TTSs matrix parameters:

Taking into account the variability of compositions, the analysis of three groups of the experimental data expressed as calculated arithmetic averages of data on each group was necessary, in order to identify the parameters (as dependent variables) which statistically are critically influenced by the ingredients associated in the TTSs matrix compositions (as independent variables). These grouped calculated data are shown in table IV.

-The effect of the formulation variables on parameters of the NSAID TTS matrix, based on the analysis of individual data (tables II-III) vs. the average of total products (table IV, group 1):

The average weight (m) of the 12 products is 2.52 ± 0.10 g to a surface of 75.39 cm² (∅ 9.8 cm) and the thickness (T) is 0.32 ± 0.04 mm, favorable for cutaneous administration. The viscosifying capacity of the used HPMC type determines the mechanical resistance of the polymeric matrix. Films based on HPMC E5 have low mechanical resistance, making impossible to measure any elongation at tensile strength. Nevertheless, surface properties (hardness force and adhesiveness) were successfully determined, so the HPMC E5 films were kept in the study. HPMC 15000 combined or not with EC 10 confers flexibility and mechanical resistance (as FE > 150).

Table III. Texture and surface properties of NSAID TTS matrix

TTS matrix	Determined parameter		
	Hf (g) ± SD	Af (g) ± SD	A (mJ) ± SD
MX1	40.2 ± 3.6	60.5 ± 23.0	0.16 ± 0.04
MX2	200.7 ± 13.1	147.1 ± 26.1	0.31 ± 0.05
MX3	473.7 ± 37.0	75.7 ± 26.7	0.16 ± 0.02
MX4	112.8 ± 13.8	185.7 ± 1.0	0.36 ± 0.13
TX1	27.2 ± 1.6	83.7 ± 12.9	0.19 ± 0.01
TX2	154.7 ± 4.8	184.3 ± 14.0	0.20 ± 0.01
TX3	806.2 ± 41.6	63.5 ± 5.3	0.21 ± 0.01
TX4	140.7 ± 10.9	93.2 ± 44.9	0.12 ± 0.03
IND1	70.5 ± 4.4	125.8 ± 11.3	0.14 ± 0.01
IND2	273.7 ± 28	83.5 ± 32.8	0.17 ± 0.04
IND3	505.2 ± 54.5	97.3 ± 21.8	0.12 ± 0.02
IND4	227.5 ± 9.8	93.0 ± 25.2	0.17 ± 0.01

Hf = hardness force; Af = adhesive force; A = adhesiveness
SD = standard deviation (n = 3)

Table II. Bulk viscoelastic properties of NSAID TTS matrix

TTS matrix		Determined parameter							
		m (g) ± SD	T (mm) ± SD	FE (x)	Eb (%)	TS (N mm^{-2})	WVA (%)	WVL (%)	WVTR (g·cm^{-2}·h^{-1})
Meloxicam matrix: *light yellowish*	**MX1**	2.523 ± 0.125	0.296 ± 0.018	-	-	-	2.550	15.346	2.00·10^{-3}
	MX2	2.537 ± 0.106	0.262 ± 0.015	>150	67.5	0.3903	5.543	13.230	2.11·10^{-3}
	MX3	2.733 ± 0.129	0.380 ± 0.012	>150	77.5	0.4900	3.114	11.066	2.05·10^{-3}
	MX4	2.383 ± 0.072	0.354 ± 0.019	>150	40.0	0.2888	4.068	20.808	1.91·10^{-3}
Tenoxicam matrix: *yellowish*	**TX1**	2.617 ± 0.090	0.312 ± 0.015	-	-	-	2.306	15.179	2.02·10^{-3}
	TX2	2.537 ± 0.012	0.260 ± 0.010	>150	62.5	0.4184	4.317	14.753	1.88·10^{-3}
	TX3	2.430 ± 0.078	0.344 ± 0.015	>150	67.5	0.3352	4.670	14.124	2.05·10^{-3}
	TX4	2.490 ± 0.155	0.332 ± 0.013	>150	45.0	0.3080	3.785	20.690	1.89·10^{-3}
Indomethacin matrix: *yellowish white*	**IND1**	2.613 ± 0.030	0.272 ± 0.013	-	-	-	2.238	14.060	1.81·10^{-3}
	IND2	2.433 ± 0.067	0.272 ± 0.013	>150	72.5	0.3999	2.530	12.318	1.69·10^{-3}
	IND3	2.565 ± 0.119	0.356 ± 0.011	>150	80.0	0.3423	3.078	18.805	2.02·10^{-3}
	IND4	2.388 ± 0.109	0.326 ± 0.015	>150	37.5	0.2635	3.787	23.445	1.96·10^{-3}
Sample surface:		75.39 cm² (∅ 9.8 cm)		4 cm²	6 cm² (4.0 cm /1.5 cm)		4.15 cm² (∅ 2.3 cm)		

m = weight uniformity; T = thickness of matrix; FE = folding endurance (x = number of fold pairs until the break); Eb = elongation to break; TS = tensile strength; WVA = moisture vapor absorption; WVL = moisture vapor loss; WVTR = water vapor transmission rate;
SD = standard deviation (n = 3)

Table IV. Groups of data and calculated parameters subjected to analysis by statistical tests

Parameter	Group 1 (total)			Mean value ± SD Group 2			Group 3			
				MX	TX	IND	TTS 1	TTS 2	TTS 3	TTS 4
m	2.52 ± 0.10	a p > 0.10 b p = 0.72 c p = 0.68	a ns b ns c ns	2.54 ± 0.14	2.52 ± 0.08	2.50 ± 0.11	2.58 ± 0.05	2.50 ± 0.06	2.58 ± 0.15	2.42 ± 0.06
T	0.32 ± 0.04	a p > 0.10 b p = 0.54 c p = 0.67	a ns b ns c ns	0.32 ± 0.05	0.31 ± 0.04	0.31 ± 0.04	0.30 ± 0.01	0.27 ± 0.01	0.36 ± 0.02	0.34 ± 0.02
D	1.07 ± 0.14	a p > 0.10 b p = 0.24 c p = 0.16	a ns b ns c ns	1.06 ± 0.18	1.08 ± 0.16	1.08 ± 0.13	1.14 ± 0.04	1.25 ± 0.06	0.94 ± 0.01	0.95 ± 0.05
Eb	61.11 ± 16.21	a p > 0.10 b p = 0.36 c p = 0.17	a ns b ns c ns	61.67 ± 19.42	58.33 ± 11.81	63.33 ± 22.68	-	67.50 ± 5.00	75.00 ± 6.61	40.83 ± 3.82
TS	0.36 ± 0.07	a p > 0.10 b p = 0.78 c p = 0.88	a ns b ns c ns	0.39 ± 0.10	0.35 ± 0.06	0.34 ± 0.07	-	0.40 ± 0.01	0.39 ± 0.09	0.29 ± 0.02
WVA	3.50 ± 1.04	a p > 0.10 b p = 0.68 c p = 0.49	a ns b ns c ns	3.82 ± 1.31	3.77 ± 1.04	2.91 ± 0.68	2.37 ± 0.16	4.13 ± 1.52	3.62 ± 0.91	3.88 ± 0.16
WVL	16.15 ± 3.86	a p = 0.04 b p = 0.49 c p = 0.24	a s* b ns c ns	15.11 ± 4.18	16.19 ± 3.03	17.16 ± 5.01	14.86 ± 0.70	13.43 ± 1.23	14.67 ± 3.90	21.65 ± 1.56
WVTR	1.95 ± 0.12	a p > 0.10 b p = 0.26 c p = 0.49	a ns b ns c ns	2.02 ± 0.08	1.96 ± 0.09	1.87 ± 0.15	1.94 ± 1.12	1.89 ± 0.21	2.04 ± 0.02	1.92 ± 0.04
Hf	252.8 ± 232.3	a p > 0.10 b p = 0.04 c p = 0.04	a ns b s* c s*	206.9 ± 189.6	282.2 ± 354.0	269.2 ± 179.8	46.0 ± 22.2	209.7 ± 60.0	595.0 ± 183.6	160.3 ± 59.8
Af	107.8 ± 43.4	a p = 0.02 b p = 0.31 c p = 0.05	a s* b ns c s*	117.3 ± 59.2	106.2 ± 53.5	99.9 ± 18.2	90.0 ± 33.1	138.3 ± 50.9	78.8 ± 17.1	124.0 ± 53.5
A	0.19 ± 0.07	a p = 0.06 b p = 0.03 c p = 0.02	a ns b s* c s*	0.25 ± 0.10	0.18 ± 0.04	0.15 ± 0.03	0.16 ± 0.03	0.23 ± 0.07	0.16 ± 0.05	0.22 ± 0.13

a = Kolmogorov–Smirnov (KP) test, b = D'Agostino & Pearson omnibus test, c = Shapiro-Wilk test:
ns = statistically insignificant; *statistical significant ($p < 0.05$, for CI of 95%)

For the other products, their viscoelastic properties ensure an elongation of 61.11 % under the action of the downward tensile forces, while the mechanical resistance at break is 0.36 $N \cdot mm^{-2}$ in terms of tensile strength and 252.8 g in terms of hardness force. In the case of the tensile strength, although the value of $p>0.1000$ calculated by Kolmogorov–Smirnov normality test suggests a population with normal distribution, the other two normality tests with $p=0.0360$ (D'Agostino & Pearson omnibus normality test) and $p=0.0374$ (Shapiro-Wilk normality test) indicate the contrary. This anomaly can be explained by the significant influence of composition on the mechanical properties.

Exposed to humidity in form of vapors TTS matrices bound the water in the percentage of 3.5 %, while in dry atmosphere they lose 16.15 % of their weight. The water vapor loss depends on the composition of the matrix, as the individual values vary significantly from a normal distribution ($p<0.05$, KP normality test). Transmission of humidity through the matrix from one to the other surface has a mean rate of $1.95 \cdot 10^{-3}$ $g \cdot cm^{-2}h^{-1}$ water vapors, in case of a moisture loss 5 times greater than the moisture uptake (WVA vs. WVL) under the given circumstances. These data indicate a predominant water loss on the surface exposed to air, even though the other side of the matrix surface is being exposed to humidity.

Adhesiveness of the film surface of 0.19 mJ was obtained by using about 107.8 g adhesive force. The adhesive force is given by the maximum of the negative force recorded on the graph, more negative the values of this parameter meaning better adhesion of the sample. The area under the curve until the zero line is used to calculate the adhesiveness and the force required to break the sample can provide information relating to the cohesion of the molecules in the sample.

The statistical normality tests applied reveal that the individual values of the adhesive force have a significant deviation from the average ($p<0.05$, KS normality test), indicating a powerful influence of films composition on this parameter. As well as in the case of tensile strength, the dispersion from the average of adhesiveness values suggests a normal distribution by KP normality test ($p>0.1000$), while in contrary by the other two tests (D'Agostino & Pearson omnibus test, with $p=0.0291$; and Shapiro-Wilk test, with $p=0.0190$), which also could be explained by the significant influence of matrix compositions on this dependent variable.

-The effect of NSAID type (table IV, group 2) vs. the effect of polymer matrix type (table IV, group 3) on the parameters of the NSAID TTS matrix, based on the analysis of the variance between groups:

For each of the two groups of data arranged in columns in replicate values in side-by-side columns, the variance of individual values to the mean was analyzed by Two-way ANOVA test. Supplementary, each line had been compared (simple effects within columns) by Tukey's multiple comparisons test (figure 1).

In case of data grouped by polymer matrix type, the variance is significantly ($p<0.0001$, $\alpha = 0.05$) determined by the matrix type (3.95%). Type of the film forming polymer influences in an approximately equally measure all the experimental parameters considered as depended variables with the exception of hardness force - the highest variance, adhesive force and elongation to break - with slightly higher different variance (by Tukey test).

In case of data grouped by NSAID type, it can be stated that the effect of the NSAID type is insignificant (0.94%) and appears in the same measure in the values of the analyzed experimental data. All the results suggest that hardness differentiates in a statistically significant way the 12 types of TTSs matrix, the rupture test results as average of data grouped by NSAID type being the following: 206.9 g for MX, 282.2 g for TX and 269.2 g for IND.

Correlation of NSAID TTS matrix mechanical parameters:

Elongation of TTS matrix may be explained by the sliding capacity of matrix building polymeric layers, simultaneously with the resistance to movement of the polymeric chains, which after the elongation caused by a tensile forces, tend to regain their initial form.

The maximum of elongation previous to the rupture causing tension have the following values: 67.5 % - 0.40 $N \cdot mm^{-2}$ for TTS 2 (HPMC 15000 1%), 75.0 % - 0.39 $N \cdot mm^{-2}$ for TTS 3 (1.5% HPMC 15000) and 40.8 % - 0.29 $N \cdot mm^{-2}$ for TTS 4 (1% HPMC 15000 + 1% EC 10), respectively. The correlation grade of the two mentioned parameters was established by Pearson test individually for each product, as it is shown in figure 2.

A significant correlation was demonstrated in all cases, as all Pearson r values are in the range of 0.9818 (the lower, in the case of IND4) to 0.9934 (the highest, in the case of MX3). The average of Pearson coefficients of TTS matrix grouped by NSAID type shows a superior correlation for meloxicam independently of the matrix type: r ± CV (%) = 0.9905 ± 0.2633. On the other hand, in the TTS matrix grouped by polymer matrix type a superior correlation is shown in the case of TTS matrix 3 (formed by 1.5% HPMC 15000): with r ± CV (%) = 0.9919 ± 0.1430.

Conclusions

The texture and the surface properties (resistance to perforation and bioadhesivity) of the 12 products prepared in form of polymeric films are critically (statistically significant) influenced by the ingredients associated in their composition. HPMC 15000 used in concentration of 1 - 1.5 % with 0.5 % MX, TX or IND confers to TTSs matrix adequate mechanical properties for dermal application. MX incorporated in the structure of the polymeric matrix favors its viscoelastic structure. EC 10 functions as plasticizer for the HPMC 15000 matrix and supports its bioad-

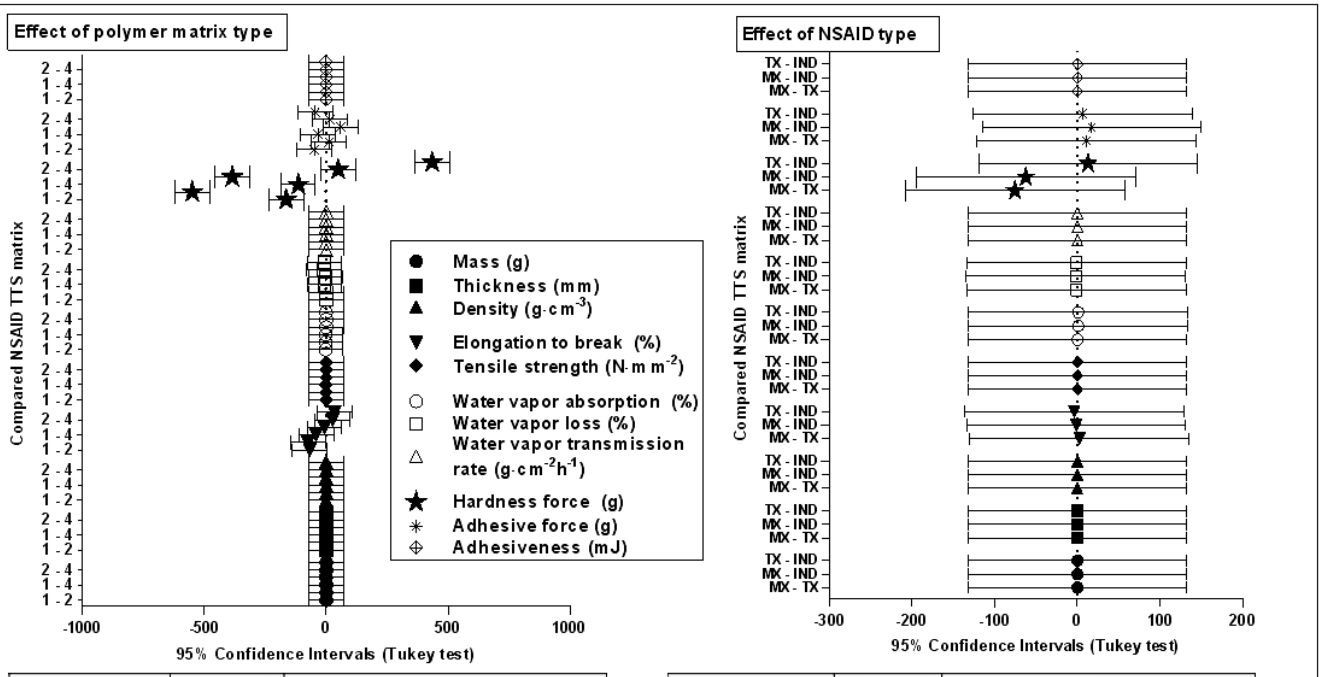

Source of variation	% of total variation	Two-way ANOVA: P value	Summary	Significant?
Interaction	34.98	< 0.0001	****	Yes
Matrix type	3.952	< 0.0001	****	Yes
Parameter type	53.95	< 0.0001	****	Yes

Source of variation	% of total variation	Two-way ANOVA: P value	Summary	Significant?
Interaction	0.9477	> 0.9999	ns	No
NSAID type	0.0571	0.9392	ns	No
Parameter type	53.95	< 0.0001	****	Yes

Fig. 1. Effect of polymer matrix type (group 3) vs. Effect of NSAID type (group 2) on the variance of NSAID TTS matrix parameters value expressed as average of experimental data

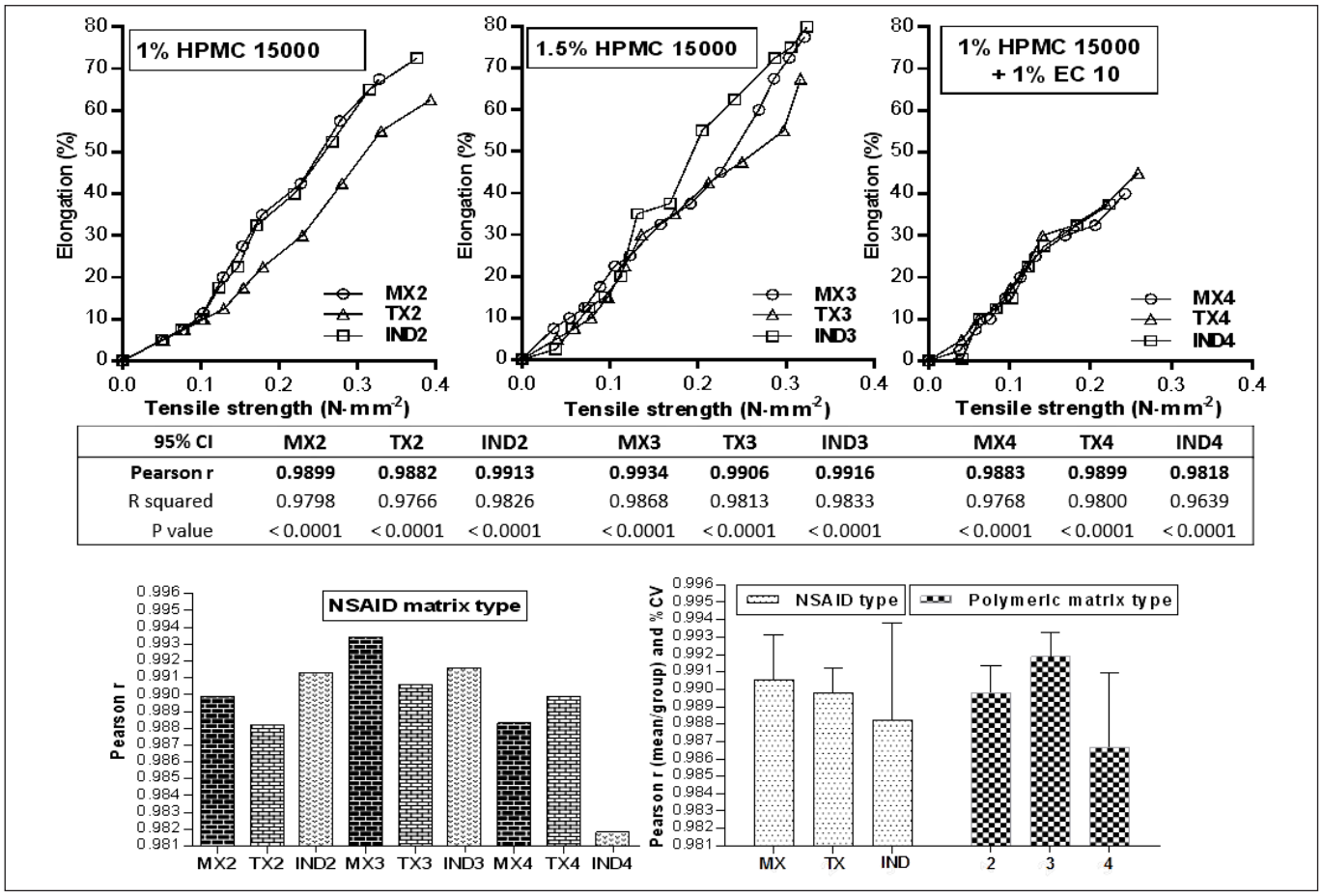

95% CI	MX2	TX2	IND2	MX3	TX3	IND3	MX4	TX4	IND4
Pearson r	**0.9899**	**0.9882**	**0.9913**	**0.9934**	**0.9906**	**0.9916**	**0.9883**	**0.9899**	**0.9818**
R squared	0.9798	0.9766	0.9826	0.9868	0.9813	0.9833	0.9768	0.9800	0.9639
P value	< 0.0001	< 0.0001	< 0.0001	< 0.0001	< 0.0001	< 0.0001	< 0.0001	< 0.0001	< 0.0001

Fig. 2. Elongation of NSAID TSS matrix as function of tensile strength and the statistical significance of correlation by Pearson test: individual and average of grouped data

hesiveness. HPMC E5 3% does not meet the requirements for TTS preparation in the used experimental conditions.

Acknowledgments

Preparation of products and evaluation of bulk viscoelastic properties were carried out with the financial support of *Andofarm S.R.L. Company*, through the internal grant 234/06.01.2016 of *University of Medicine and Pharmacy of Tîrgu Mureș, Romania.*

Evaluation of texture and surface properties were carried out with the support of *"Iuliu Haţieganu"* University of Medicine and Pharmacy Cluj-Napoca, Romania.

Conflict of interest

None to declare.

References

1. Singh I, Morris AP - Performance of transdermal therapeutic systems: Effects of biological factors. Int J Pharm Investig. 2011;1(1):4-9.
2. Popovici I, Lupuleasa D - Tehnologie farmaceutică vol.2, București, Polirom, 2008, 841-888.
3. Patel D, Chaudhary SA, Parmar B, Bhura N - Transdermal drug delivery system: a review. J Pharm Innov. 2012;4:78-87.
4. Yadav V - Transdermal drug delivery system: review. Int J Pharm Sci Res. 2012;3(2):376-382.
5. Ting L, Changshun R, Manli W et al. - Optimized preparation and evaluation of indomethacin transdermal patch. Asian J Pharm Sci. 2007;2(6):249-259.
6. Jadhav JK, Sreenivas SA - Formulation and in vitro evaluation of indomethacin transdermal patches using polymers HPMC E5 and ethyl cellulose. Int J Pharm Pharm Sci. 2012;4(1):550-556.
7. Alladi S, Shastri NR - Semi solid matrix formulations of meloxicam and tenoxicam: an in vitro and in vivo evaluation. Arch Pharm Res. 2015;38(5):801-812.
8. Shirsand SB, Ladhane GM, Prathap S, Prakash PV - Design and evaluation of matrix transdermal patches of meloxicam. RGUHS J Pharm Sci. 2012;2(4):58-65.
9. Nesseem D, Eid SF, El-Hosseny SS - Development of novel transdermal self-adhesive films for tenoxicam, an anti-inflamatory drug. Life Sci. 2011;89:430-438.
10. ElNabarawi MA, Shaker DS, Attia DA, Hamed SA - In-vitro skin permeation and biological evaluation of lornoxicam monolithic transdermal patches. Int J Pharm Pharm Sci. 2013;5(2):242-248.
11. Kavitha K, Rajendra MM - Design and evaluation of transdermal films of lornoxicam. Int J Pharm Bio Sci. 2011;2(2):54-62.
12. Parthasarathy G, Bhaskar Reddy K, Prasanth VV - Formulation and characterization of transdermal patches of naproxen with various polymers. Pharmacie Globale International Journal of Comprehensive Pharmacy. 2011;6(7):1-4.
13. Verma N, Deshwal S - Design and in vitro evaluation of transdermal patches containing ketoprofen. World J Pharm Res. 2014;3(3):3930-3944.
14. Rastogi V, Yadav P - Transdermal drug delivery system: An overview. Asian J Pharm. 2012;6(3):161-170.
15. Snejdrova E, Dittrich M - Pharmaceutical applications of plasticized polymers, in Luqman M (ed.): Recent Advances in Plasticizers, Rijeka, Croatia, InTech Open Access, 2012, 69-84.
16. Güngör S, Erdal SM, Özsoy Y - Plasticizers in transdermal drug delivery systems, in Luqman M (ed.): Recent Advances in Plasticizers, Rijeka, Croatia, InTech Open Access, 2012, 91-105.
17. Kumar SV, Tarun P, Kumar TA - Transdermal drug delivery system for non-steroidal anti-inflammatory drugs: a review. Indo Am J Pharm Res. 2013;3(4):3588-3605.

DE GRUYTER OPEN

Acta Medica Marisiensis 2017;63(2):62-65 DOI: 10.1515/amma-2017-0013

RESEARCH ARTICLE

The Risk of Using Poppy Seed Tea Made from Several Varieties Available on the Romanian Market

Mircea Dumitru Croitoru, Ibolya Fülöp*, Maria-Raluca Irimia-Constantin, Erzsébet Varga, Hajnal Kelemen, Erzsébet Fogarasi, Luana-Maria Faliboga

University of Medicine and Pharmacy of Tîrgu Mureș, Tîrgu Mureș, Romania

Objective: the number of alkaloids like morphine and codeine found in poppy seeds used in food industry are monitored by a directive given by European Food Safety Authority. Based on this regulation the aim of the study was to determine the quantity of morphine and codeine from several brands of poppy seeds. **Methods**: an HPLC-UV method (205 nm) was developed to measure the quantity of morphine and codeine. Sample preparation was made using recipes posted on Drugs Forum by some users. Limits of detection were not determined because the lowest concentration from the reference (0.1 µg/ml) detected morphine concentrations that are far lower than a limit of toxicological concern. **Results**: The concentrations, which were found, ranged between Below the Level of Toxicological Concern (BLTC) - 243.26 mg/kg for morphine and BLTC - 88.58 mg/kg for codeine using several methods of preparation. **Conclusions**: one can observe that there are some brands of poppy seeds which do not respect the regulation about the amount of morphine and codeine. The high amount of morphine in some samples suggests that there are different varieties of poppy seeds, which can be used for an illicit purpose and can lead to addiction or even overdose in some cases.

Keywords: HPLC, morphine, codeine, regulations, poppy seeds

Received 14 December 2016 / Accepted 25 April 2017

Introduction

Morphine is one of the principal ingredients of opium, a drug that has been, by far, one of the most popular and commonly used and abused drug in human history [1]. Nowadays, it is an opiate narcotic painkiller with a high potential for abuse. It belongs to narcotic medication as can cause addiction, overdose and even death [2]. The drug can be used in clinical pain relief but it can be also used illicitly for recreational purpose among drug users. Once administrated, the substance enters the blood stream which carries it to different parts of the body and in brain where it activates opioid receptors. While some effects are beneficial like pain relief due to the activation of µ1 receptors subtype, others are unwanted such as respiratory depression and addiction due to activation of µ2 receptors subtype. Because of its severe effects the substance is regulated worldwide in different classes of risks and it is not available without a medical prescription [3].

Even if the abuse of morphine is no longer as common as in the 19th century [4], drug users search for different methods to obtain morphine without a medical prescription. One of the most popular methods is obtaining morphine from poppy seeds [5]. Drug addicts sustain that making a poppy seed tea is the best solution to obtain doses of morphine large enough for the euphoric effect [6]. However, the concentration of morphine in poppy seed tea can vary enormously so the risk of an overdose is high especially when it is taken with other drugs like benzodiazepines, a combination very popular among the drug consumers [7]. Unfortunately, there are death cases reported worldwide because of the overdoses found in poppy seed tea. One of the cases found on the internet showed that the overdose appeared when using 1.5 kg of poppy seeds for obtaining the tea. Furthermore, it was an unexpected and undesired effect because the consumer had taken poppy seed tea several times, always using the exact amount of seeds and the same preparation method [8].

Based on The European Food Safety Authority`s document about the alkaloids present in the poppy seeds used in food industry, we analysed the amount of morphine from several poppy seeds types available in our country.

The European Food Safety Authority (EFSA) Panel on Contaminants in the Food Chain (CONTAM Panel) established a safety factor of 3 to obtain from the lowest known single oral therapeutic dose of 30 µg morphine/kg body weight (b.w.) an acute reference dose (ARfD) of 10 µg morphine/kg b.w. The safety factor of 3, applied by the EFSA in the case of morphine takes into consideration the acute toxic effect, the lowest active pharmacological dose ever published and the size and type of the population exposed to the substance [9].

The aim of this study was determine the amount of morphine and codeine in poppy seed tea, made from different types of poppy seeds, by four different infusion methods, in order to evaluate if there is a possibility that these poppy seeds can be used for a recreational purpose. We also intended to verify if the regulations regarding the procedures of decreasing the number of alkaloids are taken into consideration. Literature data shows that using the poppy seeds tea for recreational purpose is an easily available and high risk method for opioid users [10].

* Correspondence to: Ibolya Fülöp
E-mail: fulop.ibolya@umftgm.ro

Materials and methods

1.1. Equipment and reagents

Merck HPLS system consisting of: quaternary pump Merck Hitachi L-7100, auto sampler Merck Hitachi L-7200, column thermostat Merck Hitachi L-7360, detector de DAD Merck Hitachi L-7455, interface Merck Hitachi D-7000 I/F, solvent degasser Merck Hitachi L-7612, D-7000 HSM- Manager software, LichroCART 250-4, Rp- Select B (5 μm) column Merck KgA, Germany.

The following reagents were used: purified water (Millipore, USA), H_3PO_4 and K_2HPO_4 (Merck KgA, Germany), morphine hydrochloride (analytical purity), codeine phosphate (analytical purity); commercially available poppy seeds (countries of origin: Romania, Czech Republic, Spain and Turkey).

1.2. HPLC method

The mobile phase composition, gradient and flow rate are shown in Table I.

The injection volume was 100 μl and the full "loop" method was used.

DAD domain: 190-400 nm, best chromatogram extracted at 205 nm, because this wavelength gives the best signal-to-noise noise ratio. Peak purity limit: 95%. Analyse time: 15 minutes.

Retention time:
– morphine 6.70 minutes;
– codeine 10.03 minutes.

1.3. Preparation of the samples

Analyzed poppy seeds recipes are shown in Table II. Four types of sample preparation were used to reproduce recipes taken from Drugs Forum which are provided by some consumers [10].

For a better extraction of alkaloids, an acidic medium (pH = 3) was used for sample preparation. Until analysis, the samples were frozen at -20°C. There were used four methods of preparation: in the first one the seeds were simply washed, in the second one they were left in contact with the extraction solvent and washed, for the third method the seeds were grinded before the washing procedure and for the fourth method the poppy seeds were grinded and left 24 hours in contact with the extraction solvent. After defrosting at room temperature, samples were centrifuged 5 minutes at 5000 rpm, filtered through a 0.5 μm nylon filter and injected into the HPLC system.

Table I. HPLC pump setup

Time (min)	Methanol (%)	20 mM phosphate buffer, pH = 3 (%)	Flow rate (ml/min)
0	5	95	1.000
8.0	30	70	1.000
15.0	30	70	1.000
15.1	5	95	1.000
17.0	5	95	1.000

1.4. Method performance testing

1.4.1. Specificity

To assess the specificity of the method we used a sample of poppy seeds without detectable concentrations of codeine and morphine. All methods of sample preparations showed no peaks with the retention times of morphine and codeine. A typical chromatogram of a sample is shown in Figure 1.

1.4.2. Linearity

To assess the linearity of the method, the following concentration ranges were chosen (N = 3):
– morphine 0.1-15 μg/ml
– codeine 0.1-15 μg/ml

The coefficient of correlation (R) was 0.998 for morphine and 0.998 for codeine (Figure 2). All the residuals (difference between the calculated-from the calibration curve – and theoretic concentration, expressed as a percent of the theoretic concentration) were under 10%. Representing the residuals as a function of the theoretic concentration, no correlating tendency was found.

1.4.3. Accuracy and precision

Spiked sample technique, of a poppy seed type that was found to have undetectable concentrations of morphine and codeine, was used for assessing the accuracy and precision of the method. Three values of concentrations were used (5 mg/kg, 20 mg/kg, 60 mg/kg of poppy seeds, N = 5). Recovery ranged between 81.13-95.30% and the coefficient of variation ranged between 0.28-0.45%. Similar results were obtained in the case of codeine, too.

1.4.4. Limit of detection and quantification

The limit of detection and quantification were not determined. In the case of morphine any peak lower than the lowest point of the calibration curve (0.1 μg/ml corresponding to 1 mg/kg poppy seed) was considered far below of the range of toxicological concern (EFSA RfD would

Table II. The methods of preparation

Series 1	Series 2	Series 3	Series 4
-0.3 g poppy seeds homogenized with 3 ml phosphate buffer pH = 3 -vortex for 1 minute -the solution was centrifuged at 5000 rpm for 5 minutes -the samples were frozen	-0.3 poppy seeds homogenized with 3 ml phosphate buffer pH = 3 and left to rest for 24 hours -vortex for 1 minute - the solution was centrifuged at 5000 rpm for 5 minutes -the samples were frozen	-0.3 g grinded poppy seeds homogenized with 3 ml phospahte buffer pH = 3 -vortex for 1 minute -the solution was centrifuged at 5000 rpm for 5 minutes -the samples were frozen	-0.3 g grinded poppy seeds homogenized with 3 ml phospahte buffer pH = 3 and left to rest for 24 hours -vortex for 1 minute - the solution was centrifuged at 5000 rpm for 5 minutes -the samples were frozen

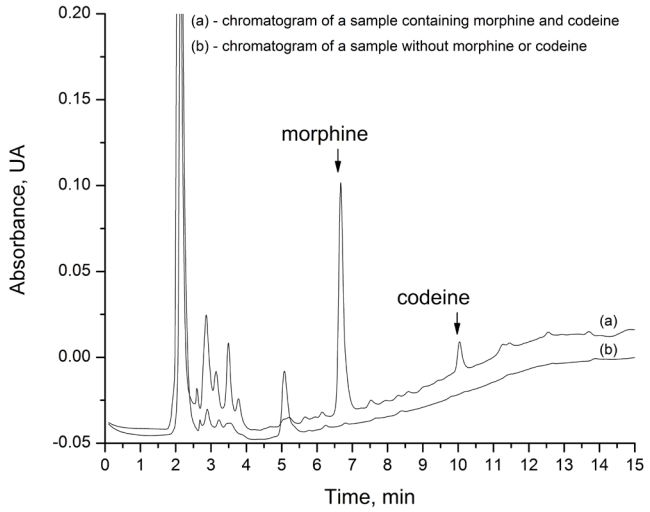

Fig. 1. Comparative chromatogram of a poppy seed tee sample without morphine and codeine, and another one containing both analytes

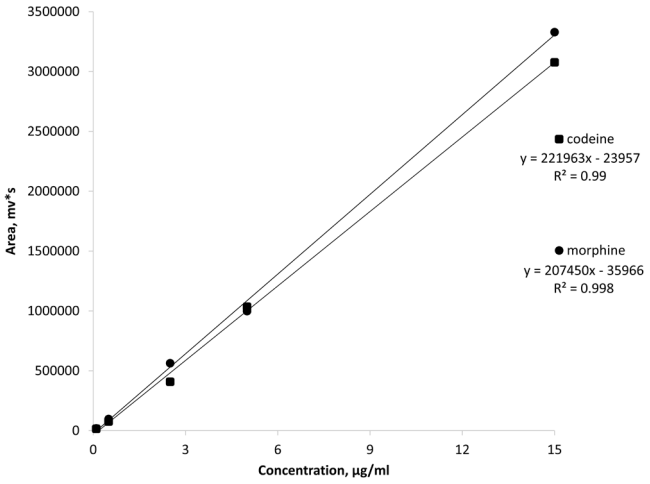

Fig. 2. The linearity curves of morphine and codeine

Table III. The concentration of morphine and codeine from the different types of poppy seeds (mg/kg morphine / mg/kg codeine)

Sample number	Series 1	Series 2	Series 3	Series 4
1	0.10/BLTC	2.04/3.83	1.30/BLTC	22.47/88.58
2	13.75/0.22	3.39/BLTC	0.91/BLTC	8.08/BLTC
3	37.03/0.77	44.16/BLTC	13.86/BLTC	29.06/BLTC
4	0.44/BLTC	2.73/BLTC	BLTC/BLTC	13.30/BLTC
5	0.81/0.26	3.06/BLTC	BLTC/BLTC	28.85/BLTC
6	112.41/16.50	243.26/28.80	117.77/10.51	119.16/9.00
7	7.00/BLTC	8.94/BLTC	8.03/BLTC	42.26/BLTC
8	30.70/3.76	124.84/12.18	98.26/6.59	59.52/BLTC
9	3.82/BLTC	29.90/BLTC	12.00/BLTC	49.43/BLTC
10	8.80/BLTC	15.25/BLTC	4.52/BLTC	29.22/BLTC
11	6.95/0.30	9.61/BLTC	6.81/2.03	11.88/BLTC

Abbreviation: BLTC - Below of Toxicological Concern

be found in 3 kg poppy seeds) and its concentration was noted with BLTC (Below the Level of Toxicological Concern) The codeine is 10 times less potent than morphine, therefore this concentration is even less importation.

Results

Concentrations of morphine and codeine measured in the samples are shown in Table III.

Concentrations for morphine ranged between 0.1 - 112.41 mg/kg for series 1, 2.04 - 243.26 mg/kg for series 2, BLTC - 117.77 mg/kg for series 3 and 8.08 - 119.16 mg/kg for series 4. In the case of codeine the concentrations ranged between BLTC – 16.50 mg/kg, BLTC – 28.80 mg/kg, BLTC – 10.51 mg/kg and BLTC – 88.58 mg/kg, for the series 1, 2, 3 and 4, respectively. For the preparation of the poppy seeds tea, quantities of 200-2000 g seeds are most often used.

Discussions

From the results presented above it is obvious that some of the poppy seed cultivars, easily available on the supermarkets, can be dangerous for human health if they are used in the production of poppy seed tea. Some of the studied samples can produce an overdose and can be possibly deadly (series 1, 2, 4). Even if none of the brands analysed does not contain a quantity of morphine which can have a recreational effect if used as food, there is a high possibility of recreationally use the tea produced from certain seeds. Even overdose and death can result if certain seeds are used in the highest amount recommended by some users for poppy seed tea preparation. Moreover, the methods of preparation are simple and the seeds can be bought freely, therefore, it is obvious that a drug with high addictive and toxic potential can be obtained with very little effort in the lack of a restrictive legislation.

Codeine concentrations in all samples are very low, even undetectable in many cases, and could not be considered to contribute to a recreational or toxic effect of the samples we analysed.

Conclusions

The HPLC method we propose is suitable to detect and measure the quantity of morphine and codeine from the poppy seeds. The method can be used even in emergency situations to confirm the presence of morphine and codeine in liquids suspected to be poppy seed teas. Even if presence of codeine observed in all of our measurements is not of any toxicological concern, its presence can be used to differentiate solutions obtained from analytical purity morphine from those obtained by washing poppy seeds.

Large variation of the morphine content observed in our samples is a high risk of overdose and death especially for young people trying to prepare a poppy seed tea in the lack of a certain degree of tolerance. The presence of samples with such high amounts of morphine suggests that some

poppy seed producers might not wash their products as requested by European authorities.

Acknowledgement

The research was supported by the University of Medicine and Pharmacy of Tîrgu Mureş and Gedeon Richter Romania SA, internal research grant number 15221/02.11.2015.

Conflict of interest

None declared.

References

1. Busse G – Morphine, Drugs The Straight Facts, Chelsea House, USA, 2006.
2. Roland CL, Lake J, Oderda GM - Prevalence of Prescription Opioid Misuse/Abuse as Determined by International Classification of Diseases Codes: A Systematic Review. J Pain Palliat Care Pharmacother. 2016;1:1-11.
3. Yaks TL, Wallace MS – Opioids, Analgesia and Pain Management in Brunton L, Parker K, Blumenthal D, Buxton I (eds.) – Goodman and Gilman's Manual of Pharmacology and Therapeutics, McGraw Hill, London, 2011, 481-526.
4. Ling W, Mooney L, Hillhouse M - Prescription opioid abuse, pain and addiction: Clinical issues and implications, Drug Alcohol Rev, 2011;30:300-305.
5. *** http://www.bluelight.org/vb/threads/696884-Extracting-morphine-from-Poppy-Seed-Tea, accessed on 10.11.2015.
6. *** http://www.bluelight.org/vb/threads/621205-Poppy-seed-tea-is-legitimate-How-to-make-it-work-for-you, accessed on 10.11.2015.
7. *** http://www.bluelight.org/vb/threads/732861-morphine-and-xanax-combo, accessed on 12.11.2015.
8. *** http://www.poppyseedtea.com/, accessed on 12.11.2015.
9. *** EFSA – Scientific Opinion on the risks for public health related to the presence of opium alkaloids in poppy seed, The EFSA Journal, 2011, 11:2405.
10. *** Poppy seeds tea recipe, available at: https://drugs-forum.com/forum/showthread.php?t=131816, accessed on 15.11.2015.

DE GRUYTER OPEN

Acta Medica Marisiensis 2017;63(2):66-69 DOI: 10.1515/amma-2017-0014

RESEARCH ARTICLE

Preparation and Characterization of Levofloxacin-Loaded Nanofibers as Potential Wound Dressings

Noémi Pásztor, Emőke Rédai, Zoltán-István Szabó, Emese Sipos*

University of Medicine and Pharmacy of Tîrgu Mureș, Romania

Objective: The study aimed at obtaining and characterizing levofloxacin-loaded, poly(ε-caprolactone) electrospun nanofiber formulations to be used as antibacterial wound dressings. **Methods**: Drug-loaded nanofibers were obtained by the electrospinning process and their morphology was determined using scanning electron microscopy. Structural analysis of the prepared nanofibers was carried out using differential scanning calorimetry and dissolution testing was performed in order to determine drug release. **Results**: Both nanofiberous formulations (containing 20 % and 50 % w/w levofloxacin) showed dimensions in the range of few hundred nanometers. Thermograms indicated that the formulation containing 20% levofloxacin was totally amorphized, showing a rapid release of the active, in 20 minutes. **Conclusions**: The poly(ε-caprolactone)-based electrospun nanofibers, containing levofloxacin presented suitable characteristics for obtaining potential antibacterial wound dressings.

Keywords: electrospinning, polymer, scanning electron microscopy, differential scanning calorimetry

Received 1 March 2017 / Accepted 26 April 2017

Introduction

Wound dressings can play a major role in the healing process by ensuring a mechanical protection (to prevent secondary infection) and adequate conditions for wound healing. Ideally, wound dressing need to provide a moist environment while absorbing the excessive wound exudates, ensure adequate oxygen supply by allowing gaseous exchange and confer low bacterial exposure by incorporating a broad-spectrum antimicrobial agent [1]. They should also be non-traumatic and should not adhere to the wound, thus at dressing change they will not damage granulating tissue. It is claimed that also the immediate care of skin wounds is important for prevention of microbial infection and trans-epidermal water loss [2]. While the passive dressings fulfil very few of the properties of an ideal dressing and have very limited use as primary dressings, the novel interactive dressings may stimulate activity in the healing cascade and speed up the healing process [3].

Nanofibrous meshes prepared from polymeric materials are interesting alternatives to currently available wound treatments. Being characterized by ultra-fine, fibrous structure, high-surface area and nanoporosity, these meshes are excellent contenders for wound-healing applications [4]. Electrospinning is a simple and widely used technique to produce fibers with diameters in the range of several micrometers down to the few hundreds few hundreds of nanometer range from either polymer solutions or melts [4,5]. In the last decade much attention has been devoted to this technique, not only for the wide range of fiber-forming polymers that can be used, but also because it can consistently produce fibers in the submicron size range and active agents can be easily integrated. The fibers have smaller pore size and higher specific surface area than the ones produced with conventional methods and have been successfully applied in different fields, such as filtration, protective clothing manufacture, nanocatalysis, optical electronics and biomedicine [6–8].

Drug delivery systems based on nanofibers are able to improve therapeutic efficacy, bioavailability, reduce toxicity, and enhance patient compliance by delivering drugs at a controlled rate over a period of time to the site of action [9].

The obtained electrospun nanofibrous scaffolds can be used as a carrier for both hydrophilic and hydrophobic agents, where the drug release can be finetuned by the composition, morphology of the scaffolds and porosity. In the field of wound dressings and tissue engineering different active agents were successfully incorporated in electrospun scaffolds based on biocompatible polymers such as poly(ethylene-co-vinyl alcohol), collagen, polyurethane, poly(vinyl-alcohol), collagen-poly(ethylene-oxid), poly(lactic-co-glycolic acid)(PLGA), polylactic-acid(PLA) and gelatine [4,10,11].

Studies also suggest that polymer matrices may have broad applicability in controlled release technology owing to the simplicity of the electrospinning process and the wide variety of suitable polymer materials[12–14].

These nanofibrous materials should be durable, stress resistant, flexible and elastic in order to be employed as wound dressings. They also should be easy to apply and remove without incurring any trauma during dressing change. Poly(ε-caprolactone) (PCL) based nanofibrous mats fulfil the abovementioned requirements and were

* Correspondence to: Emese Sipos
E-mail: sipos.emese@yahoo.com

successfully applied as wound dressing in numerous studies, showing similar or superior efficacy, when compared to standard therapy [15–17].

The model drug chosen for this research was levofloxacin, which is a water-soluble fluoroquinolone-type antibacterial agent, with broad-spectrum antimicrobial spectrum and enhanced efficacy against Gram-positive and atypical pathogens [18]. Levofloxacin is especially important because of its activity on strains that are resistant to other, widely applied antimicrobial agents. This additional activity is especially useful for developing novel wound dressings for severe bacterial infections of the skin [19].

The aim of the present study was to obtain and characterize levofloxacin-loaded nanofibrous matrices from PCL prepared by electrospinning. The drug release profiles, morphology and thermal properties of the scaffolds are presented herein. Results enable us to understand the effects of the applied polymer and active substance concentrations on the properties of potential wound dressing materials.

Materials and Methods

Materials

The model drug, Levofloxacin (Figure 1) was provided by Richter Gedeon Plc. (Budapest, Hungary).

Poly(ε-caprolactone) (PCL, 50 kDa, Figure 1), ethanol, dichloromethane, sodium hydroxide (NaOH) and phosphate buffer solution (1M, pH 7.4) were purchased from Sigma-Aldrich.

Preparation of PCL dispersions with levofloxacin

As a first step, five different formulations were prepared in order to select a homogeneous PCL dispersion. The exact compositions of dispersions and their aspects are presented in Table I.

As only formulation F5 resulted in a homogenous composition, only this composition was further used for incorporating levofloxacin. The active substance was dissolved in this formulation, obtaining final concentrations of 20% and 50%, respectively. All active substance-related procentual concentrations indicated in the present study are expressed as weight per weight (w/w %).

Electrospinning process

The abovementioned formulations (F5 containing 20% and 50% levofloxacin) were loaded into a 10 mL syringe, which was connected through a 30 cm long silicone tube to a 0.8 mm internal diameter spinneret at the end. The constant flow of the polymeric solution was provided by a SEP 10S Plus automatic syringe pump (Aitecs, Lithuania). The electrostatic spinner was equipped with a NT-35 adjustable high-voltage DC power supply (MA2000, Unitronik, Hungary). A vertically-positioned, grounded collector, covered with aluminium foil was positioned at a distance of 30 cm from the spinneret. The flow rate was set at 10 ml/h, while the applied voltage was 35 kV.

Scanning electron microscopy (SEM)

Morphology of the samples was investigated by a JEOL 6380LVa (JEOL, Tokyo, Japan) type scanning electron microscope. Each specimen was fixed by conductive double sided carbon adhesive tape and sputtered by gold (using JEOL 1200 instrument) in order to avoid electrostatic charging. The diameters of the fibers were determined with the aid of the software provided by the SEM analyzer.

Table I. Compositions of different PCL dispersions

Components	F1	F2	F3	F4	F5
PLC (g)	1.00	2.00	3.00	1.00	0.60
Ethanol (ml)	8	8	8	8	4
Dichloromethane (ml)	-	-	-	8	4
Aspects	Inhomogeneous	Inhomogeneous	Inhomogeneous	Gelling	Homogenous

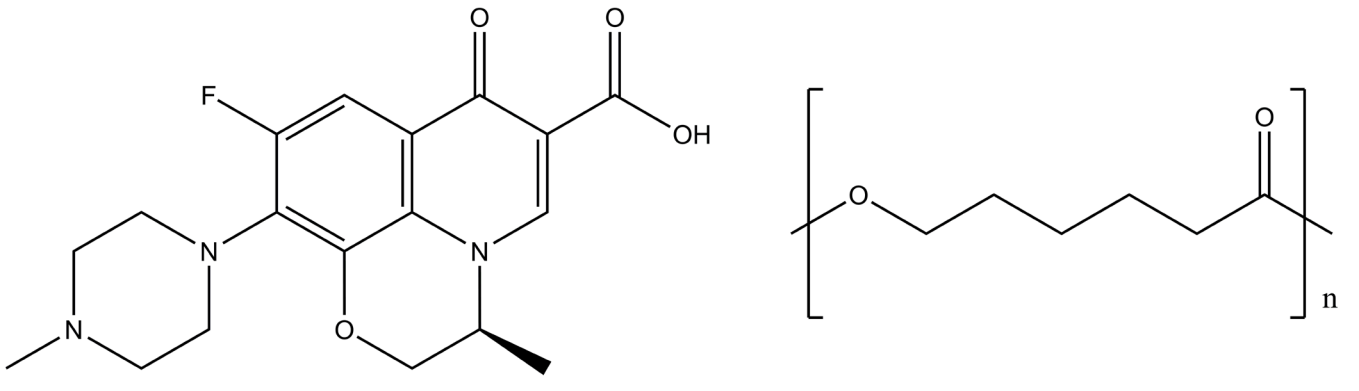

(A) (B)

Fig. 1. Chemical structure of (A) levofloxacin and (B) PCL

Differential Scanning Calorimetry (DSC)

The DSC studies were performed on a Perkin Elmer DSC 7 type device using nitrogen as carrier gas. The weight of the samples varied between 10 and 20 mg. The temperature was raised from -5°C to 300°C with a rate of 10°C/min.

In vitro drug dissolution measurement

The dissolution studies were performed by a Pharmatest IDS 1000 dissolution apparatus equipped with rotating paddles (Pharmatest, Germany). Electrospun samples containing 20% and 50% active were placed in the dissolution vessel filled with 900 ml phosphate buffer solutions with pH=7.4 maintained at 37±0.5°C and stirred at 50 rpm. At the predetermined timepoints, 5 mL samples were withdrawn and analyzed using a Hewlett-Packard HP 8452A UV-VIS spectrophotometer (Palo Alto,USA) at 288 nm. Concentrations were calculated based on a calibration curve (the polymer matrices had no detectable absorbance at this wavelength).

Results and Discussion

Morphology of the electrospun fibers

After preliminary optimization of the solution compositions, the morphology of the produced fibers were examined and compared. Figure 2 represents the SEM images of the PCL fibers without active substance and that of 20% and 50% drug-loaded fibers. In all cases, the obtained fibers presented diameters in the micrometer to few hundreds of nanometer range, suitable for their intended use.

Differential Scanning Calorimetry (DSC) measurements

DSC curves preseted in Figure 3 confirm the crystalline-amorphous transition of levofloxacin through fiber formation. The thermogram of levofloxacin presents a sharp melting endotherm at 235 °C, while the DSC curves of the nanofibrous material show an endothermic peak at 62 °C, characteristic for PCL melting [20]. The sharp endotherm of melting disappears from the thermograms of 20 % drug-loaded nanofibers, while it is greatly reduced and shifted towards lower temperatures at 50 % levofloxacin content. One possible explanation of the abovementioned phenomenon is the amorphisation of the active substance during the electrospinning process.

Dissolution tests of the levofloxacin nanofibers

Figure 4 represents the drug release profiles of nanofibers with 20% and 50% levofloxacin carried out in phosphate buffer pH 7.4.

It can be observed that levofloxacin is totally released from the polymer matrix within 20 minutes and 4 minutes from the 20 % and 50 % levofloxacin-loaded nanofibers, respectively. At the end of the dissolution test, after the release of the active the PCL matrix remained visually unchanged, indicating that it could be a suitable wound dressing, which releases its active content, but does not deteriorate when comes into contact with liquids or body fluids.

Conclusions

This study showed that PCL can be a promising matrix for the preparation of antimicrobial wound dressing. Due

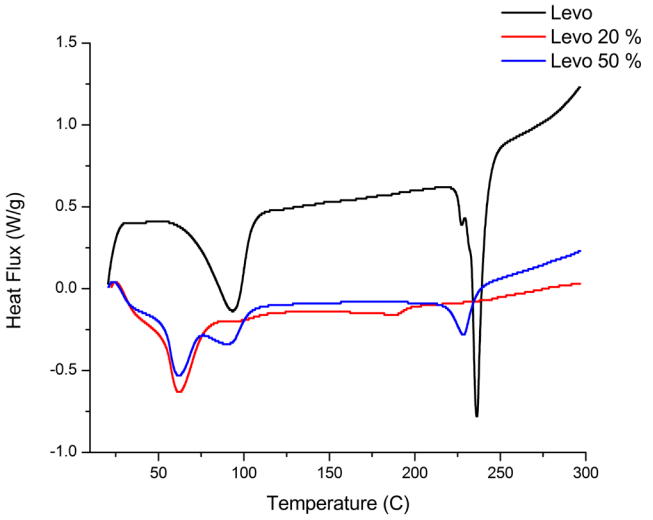

Fig. 3. DSC thermograms of levofloxacin (Levo, upper trace, blue), 50 % levofloxacin-loaded nanofibers (Levo 50%, middle trace, gray) and 20 % levofloxacin-loaded nanofibers (Levo 20%, lower trace, orange).

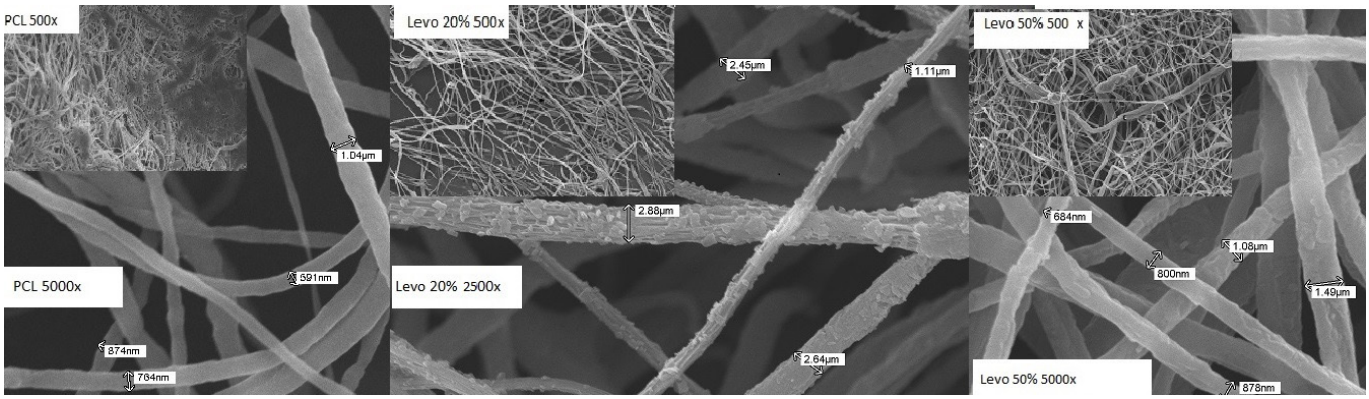

Fig. 2. SEM photographs of the prepared nanofibers using different magnifications: Nanofibers without active substance (PCL), 20 % levofloxacin-loaded nanofibers (Levo 20%) and 50 % levofloxacin-loaded nanofibers (Levo 50%)

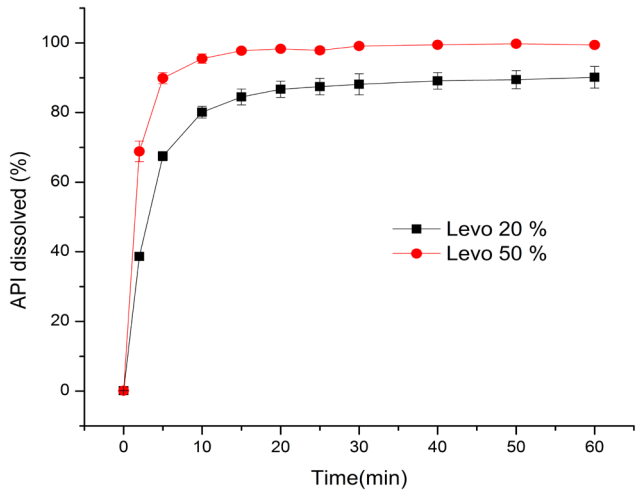

Fig. 4 .Comparative dissolution studies of 20 % (Levo 20%) and 50 % (Levo 50%) levofloxacin-loaded nanofibers

to its stable and elastic structure, the polymer can be suitable for topical application of the manufactured dressings as it fully releases the active and does not degrade when it comes into contact with body fluids. DSC studies confirmed the crystalline-amorphous transition of the active substance during the electrospinning process. The formulated nanofibrous mats may be expected to deliver an attacking dose of levofloxacin, which could be very useful after surgery or in cases of severe topical infections.

Conflict of interest

None declared.

Aknowledgements

This study was supported by an internal research grant of the University of Medicine and Pharmacy of Tirgu Mures and SC Gedeon Richter Romania SA.

References

1. Boateng JS, Matthews KH, Stevens HNE, Eccleston GM - Wound healing dressings and drug delivery systems: a review. J Pharm Sci. 2008; 97: 2892–2923.
2. Sikareepaisan P, Ruktanonchai U, Supaphol P - Preparation and characterization of asiaticoside-loaded alginate films and their potential for use as effectual wound dressings. Carbohydr Polym. 2011; 83: 1457–1469.
3. Queen D, Orsted H, Sanada H, Sussman G - A dressing history. Int Wound J. 2004; 1: 59–77.
4. Abrigo M, McArthur SL, Kingshott P - Electrospun nanofibers as dressings for chronic wound care: advances, challenges, and future prospects. Macromol Biosci. 2014; 14: 772–792.
5. Reneker DH, Yarin AL, Zussman E, Xu H - Electrospinning of nanofibers from polymer solutions and melts. Adv Appl Mech. 2007; 41, 43–346.
6. Subbiah T, Bhat GS, Tock RW, Parameswaran S, Ramkumar SS - Electrospinning of nanofibers. J Appl Polym Sci. 2005; 96: 557–569.
7. Ramakrishna S, Fujihara K, Teo WE, Yong T, Ma Z, Ramaseshan R - Electrospun nanofibers: solving global issues. Mater today. 2006; 9: 40–50.
8. Bhardwaj N, Kundu SC - Electrospinning: a fascinating fiber fabrication technique. Biotechnol Adv. 2010; 28: 325–347.
9. Kenawy ER, Abdel-Hay FI, El-Newehy MH, Wnek GE - Processing of polymer nanofibers through electrospinning as drug delivery systems. Mater Chem Phys. 2009; 113: 296–302.
10. Pham QP, Sharma U, Mikos AG - Electrospinning of polymeric nanofibers for tissue engineering applications: a review. Tissue Eng. 2006; 12: 1197–1211.
11. Supaphol P, Suwantong O, Sangsanoh P, Srinivasan S, Jayakumar R, Nair SV - Electrospinning of biocompatible polymers and their potentials in biomedical applications. Springer Berlin Heidelberg, 2011; pp. 213–239.
12. Thakur RA, Florek CA, Kohn J, Michniak BB - Electrospun nanofibrous polymeric scaffold with targeted drug release profiles for potential application as wound dressing. Int J Pharm. 2008; 364: 87–93.
13. Jannesari M, Varshosaz J, Morshed M, Zamani M - Composite poly (vinyl alcohol)/poly (vinyl acetate) electrospun nanofibrous mats as a novel wound dressing matrix for controlled release of drugs. Int J Nanomedicine. 2011; 6: 993–1003.
14. Feng K, Sun H, Bradley MA, Dupler EJ, Giannobile WV, Ma PX - Novel antibacterial nanofibrous PLLA scaffolds. J. Control Release 2010; 146: 363–369.
15. Duan Y, Jia J, Wang S, Yan W, Jin L, Wang Z - Preparation of antimicrobial poly (ε-caprolactone) electrospun nanofibers containing silver-loaded zirconium phosphate nanoparticles. J Appl Polym Sci. 2007; 106: 1208–1214.
16. Merrell JG, McLaughlin SW, Tie L, Laurencin CT, Chen AF, Nair LS - Curcumin-loaded poly (ε-caprolactone) nanofibres: Diabetic wound dressing with anti-oxidant and anti-inflammatory properties. Clin Exp Pharmacol Physiol. 2009; 36: 1149–1156.
17. Zahedi P, Karami Z, Rezaeian I, Jafari SH, Mahdaviani P, Abdolghaffari AH, Abdollahi M - Preparation and performance evaluation of tetracycline hydrochloride loaded wound dressing mats based on electrospun nanofibrous poly (lactic acid)/poly (ε-caprolactone) blends. J Appl Polym Sci. 2012; 124: 4174–4183.
18. Wimer SM, Schoonover L, Garrison MW - Levofloxacin: a therapeutic review. Clin. Ther. 1998; 20: 1049–1070.
19. Toncheva A, Spasova M, Paneva D, Manolova N, Rashkov I - Polylactide (PLA)-based electrospun fibrous materials containing ionic drugs as wound dressing materials: a review. Int J Polym Mater Polym Biomater. 2014; 63: 657–671.
20. Thomas V, Jose MV, Chowdhury S, Sullivan JF, Dean DR, Vohra YK - Mechano-morphological studies of aligned nanofibrous scaffolds of polycaprolactone fabricated by electrospinning. J Biomater Sci Polym Ed. 2006; 17: 969–984.

DE GRUYTER OPEN

Acta Medica Marisiensis 2017;63(2):70-72 DOI: 10.1515/amma-2017-0018

RESEARCH ARTICLE

Silver Cation Coordination Study to AsW9 Ligand – A Trilacunar Arsenotungstate Compound

Lavinia Berta, Andrei Gâz*, Francisc Boda, Augustin Curticapean

University of Medicine and Pharmacy of Tirgu Mures, Romania

Objective: The main objective of this research is to find the coordination ratio between AsW_9 and Ag^+, as a preliminary study for synthesizing a new silver-arsenotungstate complex. **Material and method**: The ligand:cation molar ratio in complexes was determined by conductometric and potentiometric titrations of AsW_9 with silver salts: CH_3COOAg, $AgNO_3$. **Results**: The ratio was obtained from the inflexion points of the curves when molar ratio was plotted versus conductivity, or from the equivalence point when silver added volume was plotted versus pH value. Each graphic shows one point of inflexion corresponding to 1:1.54 ratio of AsW_9:Ag^+. In the same manner, the equivalent volumes determined by graphical method gave the ratio 1:1.53. The spectral results confirmed that a AsW_9:Ag^+ complex was formed since the ligand absorption maxima values have been changed from 190 nm to 197 nm in the case of using $AgNO_3$ and 196 nm for CH_3COOAg corresponding to the $W=O_d$ bond, and from 246.5 nm to 274 nm ($AgNO_3$) and 270 nm (CH_3COO-Ag^+) for the W-$O_{b,c}$-W bond. **Conclusions**: Silver cation exhibit a preference for AsW_9 in a ratio of 3 to 2. This ratio can be associated to a sandwich type arrangement, with two trilacunary Keggin building blocks incorporating 3 metal cations in a tetrahedral geometry.

Keywords: arsenotungstate ligand, silver complexes, conductometry, potentiometric titration

Received 21 April 2017 / Accepted 30 May 2017

Introduction

Polyoxometalates (POMs) represent a large family of inorganic compounds with a wide range of applications, due to their redox activity, electronic density, structural and configurational diversity [1-4].

One of the widely-used polyoxometalate-ligand is the trilacunary Keggin unit. The $Na_8[HAsW_9O_{33}]_*17H_2O$ (abbreviated as AsW_9 inside the paper) used as ligand in this study, is an unsaturated arsenotungstate (which is a subclass of POMs family, with "*As*" as heteroatom and "*W*" as addenda) compound with a trilacunar Keggin structure. The electronic density of lacunae (one lacunae=six terminal oxygen) enables coordination of different metal cations [5-8].

Construction of multidimensional polyoxometalates structures using transitional metal cations as bounders have shown considerable interest in the research area over last years. New complexes combine intrinsic properties of each component as well as new properties arising from the combination of these components [9].

Among of the reported arsenotungsate complexes, the classical sandwich-type derivatives consist of two trilacunary Keggin building blocks, linked by 2 up to 6 transition metal cations at the equatorial plan [10-12].

Two different salts of the silver cation: $AgNO_3$, which is widely used as a precursor for many silver complexes and CH_3COO-Ag^+ have been chosen. The silver ion is very versatile in creating supramolecular architectures due to its acceptor properties and the flexible coordination sphere. This metal ion can form from 2 up to 8 bonds with various donor atoms in a wide range of coordination geometries [13].

The most important oxidation state for silver in complexes is +1. The silver ion can adopt various coordination geometries such as linear (coordination number CN=2, the characteristic geometry explained by the ion's tendency toward sd-hybridization), trigonal planar (CN=3), tetrahedral (CN=4, as in aqueous ion $[Ag(H_2O)_4]^+$), octahedral (CN=6), even square antiprism (CN=8) geometry [13,14]. In POM complexes silver is generally found in tetrahedral coordinated geometry, being bounded by 2 terminal oxygen atoms from each lacunae of two different Keggin structures.

This paper is focusing on the study of AsW_9 coordination with Ag^+ as a preliminary data for synthesizing new complexes of this arsenotungstate ligand. The synthesis of POMs proceeds by self-assembly with a large variety of structures being obtained, depending on the reaction conditions, the nature and ratio of their constitutive elements, concentration, pH or T [7,9].

Methods

Materials and apparatus

AsW_9 used in this study was synthesized as described earlier [15]. Metal cation salts (CH_3COOAg and $AgNO_3$) were of analytical grade from Alfa Aesar and Merck and were used without any further purification. All solutions were prepared by dissolving samples in purified water (obtained with NanoPure Diamond System (Barnstead, USA)) at a concentration of 10^{-5}M for ligand (at a pH=7.5-8) and $2{,}5*10^{-2}$M for cations. UV spectra were recorded on an Analytik Jena SPECORD 210 spectrophotometer between λ = 190 - 400 nm in standard 1 cm quartz cuvettes. Con-

* Correspondence to: Andrei Gâz
E-mail: andrei.gaz@umftgm.ro

ductometric and potentiometric determinations were performed on an INOLAB 740 multiparameter device.

Analysis method

For every determination series, 40 mL of the ligand solution (10^{-5}M) was placed in the titration cell while the conductance and the pH of the solution was measured. Then, 4 µL 2,5*10^{-2}M cation solution was added drop by drop in a stepwise manner using a calibrated micropipette. During titration conductivity and pH value were recorded after each addition. Titrations were made at 70-80°C. These values will be used in determination of ligand:cation coordination ratio. UV spectra were recorded before and after every titration to highlight modifications which occurred in each case.

Results

Results obtained by conductometry are presented in Figure 1. The graphic shows the conductivity values depending on the added titrant solution moles number.

In Figure 2 we have determined the equivalent volume for both salts by graphical method from potentiometric recorded data.

In Figure 3 we have plotted the overlaid recorded spectra of ligand and titrated solutions.

Discussions

By plotting molar ratio versus conductivity, the ligand:cation ratio was obtained from the inflexion points of the curves. In the same manner plotting pH versus added silver volume we have gathered the equivalence volume which exhibit a 2:3 ratio between ligand and cation. These ratios are presented in Table I. From the plotted data the same ligand:cation combination ratio can be noticed for both salts type.

The structure that correspond to this ratio is an arsenotungstate common sandwich-type structure. Each trilacunar Keggin unit has 6 terminal oxygen which can coordinate metal cations. There are 2 trilacunary Keggin units, one on the top of the other, with 3 silver cations between them, where each cation bound two terminal oxygen atoms per arsenotungstate ligand unit.

The spectral analysis confirm the formation of new complexes between ligand and cation due to a shifting of the peak corresponding to W-$O_{b,c}$-W bonds. The modified ligand absorption peak values are presented in Table II.

UV recorded spectra are characteristic to POM and show intense peak between 185 - 200 nm corresponding to W=O_d bonds. All spectra exhibit only the tail of this peak (Figure 3). This peak does not show large differences for W=O_d bond in these compounds (all having the same addenda, W). The second peak is wider and is characteristic to W-$O_{b,c}$-W bonds (Table II). In complexes spectra, these second peaks move towards higher values of wavelength. This is due to the influence of coordinated cations especially on edges-tricentric bonds from AsW_9 structure [7, 16].

Conclusions

Silver cation exhibit a preference for AsW_9 in a ratio of 3 to 2 (from conductometry determinations) with a sandwich type arrangement. Two trilacunary Keggin building blocks incorporates 3 metal cations, each in a tetrahedral

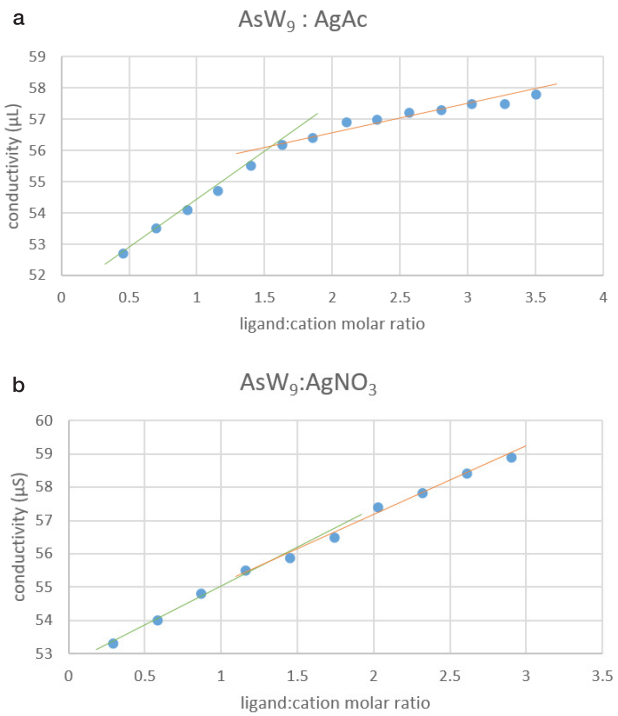

Fig. 1. Determination of inflexion point corresponding to molar ratio by conductometric titration a) CH_3COO Ag, b) $AgNO_3$

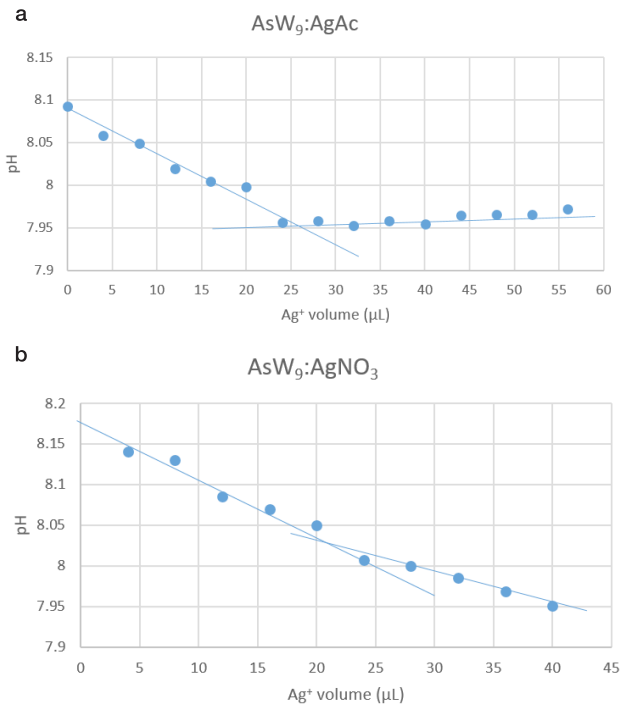

Fig. 2. Determination of equivalent volume by potentiometric titration a) CH_3COO Ag, b) $AgNO_3$

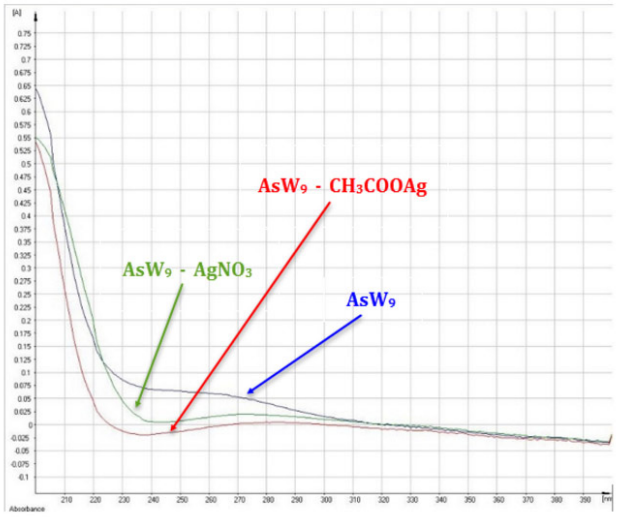

Fig. 3. The overlaid recorded spectra for all coordinative compounds and for the starting solutions of polyoxotungstate and Ag^+ solutions

Table I. AsW_9 : Ag^+ coordination ratio by conductometric and potentiometric titrations

	AsW_9 : Ag^+ coordination ratio	
	Conductometric titration	Potentiometric titration
CH_3COOAg	1:1.59	1:1.51
$AgNO_3$	1:1.5	1:1.56

Table II. Absorption UV maxima values and the corresponding bonds

	$W=O_d$	$W\text{-}O_{b,c}\text{-}W$
AsW_9	190 nm	246.5 nm
$AsW_9 – AgNO_3$	197 nm	274 nm
$AsW_9 – CH_3COOAg$	196 nm	280 nm

geometry and each silver cation being bound by 2 terminal oxygen atoms from each Keggin structure. Data are confirmed by potentiometric analysis where the same ratio was noticed. These are preliminary data and further research will be performed to synthesize new arsenotungstate-silver complexes.

Acknowledgements

The research was partially supported by the UMF Tîrgu Mureş Internal Grant no. 9/23.12.2014.

Conflict of interest

None to declare.

References

1. Gouzerh P, Che M – From Scheele and Berzelius to Müller, Polyoxometalates revisited and the “missing link” between the bottom up and top down approaches. L’actualité chimique. 2006, 298:9-22
2. Chen J J, Symes M D, Fan S C et al. – High-Performance Polyoxometalate-Based Cathode Materials for Rechargeable Lithium-Ion Batteries. Adv Mater, 2015, 27:4649-4654
3. Xing R, Wang F, Zheng A, Wang L, Fei D, Yu Y – Biological evaluation of two Keggin-type polyoxometalates containing glycine as mushroom tyrosinase inhibitors. Biotechnol Appl Biochem, 2015, 63:746-750
4. León I E, Porro V, Astrada S, Egusquiza M G, Cabello C I, Bollati-Fogolin M & Etcheverry S B, Polyoxometalates as antitumor agents: Bioactivity af a new polyoxometalate with copper on a human osteosarcoma model. Chem Bio Interact, 2014, 222:87-96
5. D’Souza L, Noeske M, Richards RM, Kortz U – Polyoxotungstate stabilized palladium, gold, and silver nanoclusters: A study of cluster stability, catalysis, and effects of the stabilizing anions. J Colloid Interf Sci. 2013, 394:157-165
6. Kandasamy B, Bassil BS, Haider A, Beckmann J, Chen B, Dalal NS, Kortz U – Incorporation of organotellurium(IV) in polyoxometalates. J Organomet Chem. 2015, 796:33-38
7. Rusu D, Crăciun C – Cercetări fizico-chimice în domeniul polioxometalaților complecși. Ed. Casa Cărții de Știință, Cluj-Napoca, 2006: 45-49;40-41;73-78,239-243
8. Wang Y, Zou B, Xiao LN, et all. – Two new hybrid compounds assembled from Keggin-type polyoxometalates and transition metal coordination complexes. J Solid State Chem. 2011, 184:557–562
9. Santoni MP, Hanan GS, Hasenknopf B – Covalent multi-component system of polyoxometalates and metal complexes: toward multi-functional organic-inorganic hybrids in molecular and material sciences. Coord Chem Rev. 2014, 281:64-85
10. Xing M, Kaifang S, Jing C, Peijun G, Hailou L, Lijuan C, Junwei Z – Synthesis, structure and electrochemical properties of a FeIII-CeIII heterometallic sandwich-type tungstoantimonate with novel 2-D infinite structure [Ce(H2O)8][Ce(H2O)6][Fe4(H2O)10(b-beta-SbW9O33)2]*16H2O. Inorg Chem Comm. 2015, 60:65-70
11. Bi LH, Huang RD, Peng J, Wang EB, Hu CW – Rational syntheses, characterization, crystal structure, and replacement reactions of coordinated water molecules of [As2W18M4(H2O)2O68]10– (M = Cd, Co, Cu, Fe, Mn, Ni or Zn). J. Chem. Soc. Dalton Trans. 2001, 121-129
12. Yang W, Li H, Li Y, Chen L, Zhao J – Synthesez, structures and properties of a series of 3s-5d-4f mixed metal substituted sandwich-type arsenotungstate. Inorg Chem Comm. 2015, 60:71-76
13. Putaj P, Lefebvre – Polyoxometalates containing late transition and noble metal atoms. Coord Chem Rev. 2011, 255:1642-1685
14. Fox SB, Beyer MK, Bondybey VE – Coordination Chemistry of Silver Cations. J. Am. Chem. Soc. 2002, 124 (45):13613–13623
15. Berta L, Boda F, Borodi Gheorghe et al. Two new sandwich-type compounds based on {AsW9} with Pd2+ and Pt4+ cations - synthesis, characterization and antibacterial activity. Farmacia. 2017, 65(1):63-68
16. Liu J, Wang L, Yu K, Su Z, Wang C, Wang C, Zhou B – Synthesis, crystal structure and properties of sandwich type compounds based on {AsW9} and a hexa-nuclear unit with three supporting TM–triazole complexes. New J Chem. 2015, 39:1139—1147

DE GRUYTER OPEN

Acta Medica Marisiensis 2017;63(2):73-79 DOI: 10.1515/amma-2017-0023

RESEARCH ARTICLE

The Influence of CYP2D6 Phenotype on the Pharmacokinetic Profile of Atomoxetine in Caucasian Healthy Subjects

Ioana Todor[1], Dana Muntean[1], Maria Neag[2], Corina Bocsan[2], Anca Buzoianu[2], Laurian Vlase[1*], Daniel Leucuta[3], Ana-Maria Gheldiu[1], Adina Popa[4], Corina Briciu[4]

1 University of Medicine and Pharmacy "Iuliu Hatieganu", Faculty of Pharmacy, Department of Pharmaceutical Technology and Biopharmaceutics, Cluj-Napoca, Romania
2 University of Medicine and Pharmacy "Iuliu Hatieganu", Faculty of Medicine, Department of Pharmacology, Toxicology and Clinical Pharmacology, Cluj- Napoca, Romania
3 University of Medicine and Pharmacy "Iuliu Hatieganu", Department of Medical Informatics and Biostatistics, Cluj-Napoca, Romania
4 University of Medicine and Pharmacy "Iuliu Hatieganu", Faculty of Pharmacy, Department of Clinical Pharmacy, Cluj-Napoca, Romania

Objective: To analyze a potential phenotypic variation within the studied group based on the pharmacokinetic profile of atomoxetine and its active metabolite, and to further investigate the impact of CYP2D6 phenotype on atomoxetine pharmacokinetics. **Methods**: The study was conducted as an open-label, non-randomized clinical trial which included 43 Caucasian healthy volunteers. Each subject received a single oral dose of atomoxetine 25 mg. Subsequently, atomoxetine and 4-hydroxyatomoxetine-O-glucuronide (glucuronidated active metabolite) plasma concentrations were determined and a noncompartmental method was used to calculate the pharmacokinetic parameters of both compounds. Further on, the CYP2D6 metabolic phenotype was assessed using the area under the curve (AUC) metabolic ratio (atomoxetine/ 4-hydroxyatomoxetine-O-glucuronide) and specific statistical tests (Lilliefors (Kolgomorov-Smirnov) and Anderson-Darling test). The phenotypic differences in atomoxetine disposition were identified based on the pharmacokinetic profile of the parent drug and its metabolite. **Results**: The statistical analysis revealed that the AUC metabolic ratio data set did not follow a normal distribution. As a result, two different phenotypes were identified, respectively the poor metabolizer (PM) group which included 3 individuals and the extensive metabolizer (EM) group which comprised the remaining 40 subjects. Also, it was demonstrated that the metabolic phenotype significantly influenced atomoxetine pharmacokinetics, as PMs presented a 4.5-fold higher exposure to the parent drug and a 3.2-fold lower exposure to its metabolite in comparison to EMs. **Conclusions**: The pharmacokinetic and statistical analysis emphasized the existence of 2 metabolic phenotypes: EMs and PMs. Furthermore, it was proved that the interphenotype variability had a marked influence on atomoxetine pharmacokinetic profile.

Keywords: atomoxetine, 4-hydroxyatomoxetine-O-glucuronide, phenotype, metabolic ratio, pharmacokinetics

Received 28 May 2017 / Accepted 20 June 2017

Introduction

Atomoxetine is the first nonstimulant medication approved by the United States Food and Drug Administration (FDA) for the treatment of attention deficit hyperactivity disorder (ADHD) in children, adolescents and adults [1–3]. The agent is a potent and selective norepinephrine reuptake inhibitor with minimal affinity for the other monoamine transporters or receptors. A second-line approach for ADHD, atomoxetine can be considered as first treatment option when anxiety disorders, major depression, tics or substance abuse problems are diagnosed alongside ADHD and in specific cases in which stimulant medication is not effective or is poorly tolerated [1,4].

Atomoxetine is rapidly absorbed after oral intake and peak plasma concentrations (C_{max}) are reached in approximately 1 to 2 hours [3,5]. The pharmacokinetic studies revealed that three oxidative pathways are involved in the biotransformation of this compound, respectively aromatic-ring hydroxylation, benzylic hydroxylation and N-demethylation. Aromatic ring-hydroxylation is CYP2D6-dependent and results in the formation of the main metabolite, 4-hydroxyatomoxetine, which exhibits similar pharmacological activity to that of the parent compound. Following hydroxylation, the metabolite is subsequently glucuronidated and excreted through urine [3,5,6]. Due to the fact that CYP2D6 is a polymorphic enzyme, differences were noted between phenotypic groups. For example, the absolute bioavailability of atomoxetine ranges from 63% for extensive metabolizers (EMs) to 94% for poor metabolizers (PMs) (3,5). In addition, the mean steady-state plasma concentrations are about 10-fold higher in PMs compared with EMs. Regardless of the metabolic status, the largest fraction of atomoxetine is eliminated into urine, principally as 4-hydroxyatomoxetine-O-glucuronide, while less than 3 % of the initial dose is eliminated unchanged [3,5,7].

Previous studies have revealed that CYP2D6 genotype/phenotype may influence atomoxetine pharmacokinetics in various races and ethnic groups [8–10]. Taking into consideration the complexity of this matter, the aim of the present study was to evaluate a potential phenotypic variation within a certain group based on the pharmacokinetic profile of atomoxetine and to further investigate and

* Correspondence to: Laurian Vlase
E-mail: laurian.vlase@umfcluj.ro

confirm the impact of CYP2D6 metabolic phenotype on atomoxetine pharmacokinetics in Caucasian healthy volunteers.

Material and methods

Subjects

The study was conducted in accordance with Good Clinical Practice guidelines and the principles of Helsinki (1964) and its amendments (Tokyo 1975, Venice 1983, Hong Kong 1989). Moreover, the protocol was approved by the Ethics Committee of the University of Medicine and Pharmacy "Iuliu Hatieganu", from Cluj-Napoca (Romania) and written informed consent was obtained from each volunteer prior to performing any study-related procedures.

Forty-three Caucasian males and females were enrolled in the clinical study. The inclusion criteria required for the study population to comprise healthy subjects between 18 and 55 years of age and to have a body mass index (BMI) between 19 and 25 kg/m^2. Their health status was assessed based on their medical history, physical examination and routine laboratory investigations (hematology, biochemistry and serological tests). Subjects were excluded if they were smokers, they had a history of substance or alcohol abuse, a history of documented allergy or if they took regular medication, except for oral contraceptives. Any medical condition or lifestyle factors that may influence drug response were also considered exclusion criteria.

Study design

The study was designed as an open-label, non-randomized clinical trial during which every subject received a single oral dose of atomoxetine (25 mg). The study drug was administered in the morning, after an overnight fast of at least 12 h and with at least 150 mL of water. Alcohol, beverages or food containing methylxanthines (coffee, tea, cola, etc.) were forbidden starting with 48 h prior to drug intake and until the last blood sample collection. Also, subjects were allowed to drink water only starting 2 h post-dosing and during their 24-h confinement they were provided with standardized meals. The pharmaceutical product used was Strattera® (atomoxetine hydrochloride, 25 mg hard capsules; manufactured by Lilly SA, Hampshire, Great Britain).

Blood plasma samples collection and bioanalytical methods

Venous blood samples (5 ml) were drawn before dosing and at 0.5, 1, 1.5, 2, 2.5, 3, 4, 6, 8, 10, 12, 24, 36 and 48 hours after drug administration and stored in heparin vacutainer tubes. After centrifugation, the separated plasma was stored frozen (-20°C) until analysis.

A validated high-throughput liquid chromatography-mass spectrometry (LC/MS) method was used to determine the plasma concentrations of atomoxetine and 4-hydroxyatomoxetine-*O*-glucuronide. The chromatographic system was an Agilent 1100 series (binary pump, autosampler, thermostat; Agilent Technologies, Santa Clara, CA, USA) coupled with a Brucker Ion Trap SL (BruckerDaltonics GmbH, Bremen, Germany). In addition, the chromatographic column used was a Zobrax SB-C18 (100 mm x 3.0 mm i.d, 3.5 µl; Agilent Technologies) and the mobile phase consisted of 2 mM ammonium formate solution and acetonitrile mixture, elution in gradient: 11 % acetonitrile at start, 41% at 2 minutes. The flow rate was 1 mL/min and the thermostat temperature was set at 48°C. The mass spectrometry detection was in single ion monitoring mode, positive ions, using an electro-spray ionization source. The ions monitored were m/z 256 for the parent dug and m/z 448 for 4-hydroxyatomoxetine-*O*-glucuronide. The retention times for atomoxetine and its glucuronidated metabolite were 4.1 min and 2.2 min, respectively. The analytical method was validated in terms of specificity, linearity, intra- and inter-day precision, accuracy and analyte recovery. The calibration curves for both compounds were linear between 8-600 ng/mL, with correlation coefficients (r) 0.9951 ± 0.0016 (mean ± standard deviation (S.D.), n = 5) for atomoxetine and 0.9982 ± 0.0018 for its glucuronidated metabolite, respectively. For atomoxetine, intra- and inter-day precision was less than 8.2%, the accuracy (bias) less than -11.5% and the recovery ranged between 89-103%, respectively. As for 4-hydroxyatomoxetine-*O*-glucuronide, intra- and inter-day precision was less than 10.7%, the accuracy less than 9.3% and the recovery ranged between 91-105%, respectively.

Pharmacokinetic analysis

The pharmacokinetic parameters of atomoxetine and 4-hydroxyatomoxetine (glucuronidated form) were estimated using noncompartmental methods. The analysis was performed using Phoenix WinNonlin software, version 6.3 (Pharsight Co., Mountain View, Calif., USA). The maximum plasma concentration (C_{max}, ng/mL) and the time to reach C_{max} (t_{max}, h) were obtained directly by visual inspecting the plasma concentration-time profiles. The area under the plasma concentration–time curve from time zero to the last measurable concentration (AUC_{0-t}) was calculated by using the linear trapezoidal rule. Furthermore, the area was extrapolated to infinity (AUC) by dividing last measurable concentration by the elimination rate constant (C_t/ k_{el}) and adding this value to AUC_{0-t}. kel was determined by log-linear regression analysis of the terminal portion of the plasma concentration-time curve and the half-life ($t_{½}$) was calculated using the following formula $t_{½} = 0.693/k_{el}$.

After defining the CYP2D6 metabolizer status, the analysis of variance (ANOVA) was employed to compare the pharmacokinetic profile of atomoxetine and its main metabolite, corresponding to each phenotypic group (EMs versus PMs), with the purpose of identifying any potential differences. t_{max} was an exception in this case, as the values corresponding to this parameter were compared by using a

non-parametric test (Friedman). A *p value <0.05* was considered to be statistically significant.

Statistical analysis

The AUC metabolic ratio (MR_ AUC = AUC atomoxetine/AUC 4-hydroxyatomoxetine-*O*-glucuronide) was used as a tool in order to identify the CYP2D6 metabolic phenotype. After calculating the MR_ AUC for each subject, the lower values were associated with the EM phenotype, while the higher values were attributed to the PM phenotype.

Lilliefors (Kolgomorov-Smirnov) and Anderson-Darling tests were applied to evaluate whether the MR_ AUC data are normally distributed or not. A significance level of 0.05 and a two tailed *p* value was set for all the tests. Moreover, quantile-quantile plot (Q-Q plot) technique was used to provide additional insight regarding intersubject variability. The statistical analysis was performed in R software environment for statistical computing and graphics version 3.2.3.

Results

Assessment of CYP2D6 metabolizer status

The results of the phenotypic analysis are summarized in a series of tables and graphics presented below.

Table I includes the AUC values of atomoxetine and its active metabolite (glucuronidated form, 4-hydroxyatomoxetine-*O*-glucuronide), as well as the MR_ AUC corresponding to each volunteer. Subject no. 5, 15 and 38 presented considerably higher AUC values for the parent drug and much lower values for the glucuronidated metabolite when compared to the remaining 40 individuals. Consequently, the MR_AUC was significantly increased for the aforementioned volunteers, which hinted to the existence of two different phenotypic groups in the study population.

The Q-Q plot (*Figure 1*) offers a visual perspective of the differences that existed between the calculated AUC, emphasizing that the data set was not normally distributed.

Furthermore, the results of the statistical evaluation are included in *Table II* and confirm the intersubject variability, as p value was < 0.05 for both tests.

The impact of phenotype variability on atomoxetine pharmacokinetics

The mean plasma drug concentration-time profiles of atomoxetine and 4-hydroxyatomoxetine-*O*-glucuronide, for each phenotype (EMs and PMs), are illustrated in *Figure 2* (parent drug (A) and active metabolite – glucuronidated form (B)). The plasmatic concentrations of both analytes suffered notable changes in the PM group, compared to EMs. More precisely, atomoxetine plasma levels increased, while the plasma concentrations of 4-hydroxyatomoxetine-*O*-glucuronide were reduced as a consequence of the slow metabolic process. Additionally, the slope of the terminal linear segment from the semi-logarithmic plot was clearly different for the two phenotypic groups, which suggested that in PMs the elimination process of both analytes was altered.

Further on, the mean pharmacokinetic parameters related to each metabolizer status, as well as the statistical interpretation of the results are presented in *Table III*. If considering the parent drug, atomoxetine, most of the calculated parameters, namely C_{max}, AUC_{0-t}, AUC, k_{el} and $t_{½}$ presented marked differences between the two phenotypic groups. As for the glucuronidated form of the active metabolite, statistically significant differences were reported for all pharmacokinetic parameters.

Discussion

The impact of CYP2D6 polymorphism represents a great interest for clinical practice as this isoenzyme is involved in the metabolism of approximately 25% of the drugs available on the market [11]. This genetic feature is responsible for interindividual variability in CYP2D6 enzyme activity which subsequently serves as a criteria for the assignment of individuals in phenotypic groups as follows: ultrarapid metabolizers (UMs – functional copy number duplications), extensive metabolizers (EMs - individuals with two 'wild-type' alleles), intermediate metabolizers (IMs - individuals with one reduced and one loss of function allele) and poor metabolizers (PMs - those with two loss of function alleles) [12–14]. In the Caucasian population, these phenotypes account for approximately 3-5 % (UMs), 70-80 % (EMs), 10-17 % (IMs) and 5-10 % (PMs) [12]. While the majority of people possess a normal CYP2D6 activity and are designated as CYP2D6 EMs [3], a study that aimed to analyze the CYP2D6 diversity in the world found that Europe has the highest prevalence of PM phenotypes [11]. Drugs thought to be primarily affected by the CYP2D6 polymorphism are those for which this isoenzyme represents the major metabolic pathway and include antidepressants (tricyclic antidepressants, selective serotonin reuptake inhibitors), antipsychotics, opioids, antiemetics, antiarrhythmics, beta-blockers, tamoxifen and atomoxetine [12].

The metabolic status can be evaluated either by genotyping, a technique by which the metabolic capacity is predicted after analyzing the functional status of each allele or by phenotyping, a procedure which allows for the phenotype to be established after measuring the metabolic ratio, respectively the substrate test drug/metabolite's concentrations in urine or plasma [15]. The downside of genetic testing is that not all mutations and different variants of alleles are known, which hinders in a certain degree its capacity to predict *in vivo* phenotype. Therefore, there are situations in which the genotype will not accurately predict the phenotype. In some cases, predicted EMs (phenotypes predicted from genotypes) can be phenotypically considered PMs as a result of drug interaction [15,16]. A phenomenon named "phenocopying" can be responsible for such a situation. This process describes the conversion of an EM to a PM as a result of inhibition of the enzyme by another drug or by itself [17]. For example, it was concluded that inhibition

Table I. The individual values of AUC and MR_ AUC corresponding to atomoxetine (ATX) and its glucuronidated metabolite, 4-hydroxyatomoxetine-O-glucuronide (HATX-gluc) (n = 43)

Subject no.	AUC _ATX (hr*ng/ml)	AUC _HATX-gluc (hr*ng/ml)	MR_ AUC (ATX/HATX-gluc)
1	2015.26	5887.55	0.34
2	4132.22	5437.91	0.76
3	1519.93	7321.71	0.21
4	566.48	6318.92	0.09
5	7673.04	2591.11	2.96
6	1000.01	5312.52	0.19
7	3098.07	7994.51	0.39
8	1059.93	7990.74	0.13
9	718.89	4745.92	0.15
10	1161.89	7476.28	0.16
11	955.27	4628.99	0.21
12	2558.22	5478.19	0.47
13	1078.82	5103.49	0.21
14	1615.89	6321.87	0.26
15	7688.97	1167.81	6.58
16	890.76	4156.67	0.21
17	745.38	4413.7	0.17
18	2045.92	4970.07	0.41
19	3050.25	4418.4	0.69
20	281.61	5607.42	0.05
21	1799.88	5268.02	0.34
22	3317.53	5167.65	0.64
23	982.13	5770.4	0.17
24	362.52	4120.32	0.09
25	953.85	6187.12	0.15
26	2118.73	4533.94	0.47
27	861.76	4643.69	0.19
28	1698.9	6342.91	0.27
29	719.85	4596.24	0.16
30	2020.11	5004.72	0.40
31	1715.43	3689.51	0.46
32	2051.61	3285.21	0.62
33	374.17	5670.81	0.07
34	398.28	4408.64	0.09
35	458.87	5623.28	0.08
36	1206.36	6373.5	0.19
37	936.4	4842.81	0.19
38	8473.9	3215.38	2.64
39	1748.95	5093.13	0.34
40	1263.36	4672.21	0.27
41	485.17	5233.89	0.09
42	822.01	3748.75	0.22
43	745.5	4151.36	0.18

AUC_ATX - area under the plasma concentration–time curve from time 0 to infinity for atomoxetine; AUC_HATX-gluc - area under the plasma concentration–time curve from time 0 to infinity for 4-hydroxyatomoxetine-O-glucuronide; MR_ AUC- metabolic ratio calculated as AUC_ATX / AUC_HATX-gluc

of CYP2D6 by paroxetine markedly affected atomoxetine disposition, resulting in a pharmacokinetic profile of this drug similar to PMs of CYP2D6 substrates [18]. According to Shah RR *et al.*, the genotype-phenotype mismatch is viewed as an obstacle in achieving personalized medicine and one approach to avoid this situation is to combine genotype studies with routine phenotyping of subjects [19].

Currently, phenotyping is usually preferred for routine in developing countries as genotyping is a more expensive procedure and is not available in most hospitals [20]. Defining the phenotype status of a population is especially important in drug-drug interaction (DDI) studies considering that DDIs involving enzymatic inhibition can occur in EMs, but not in PMs as they do not have CYP2D6 enzymes to compete for [21]. According to Frank *et al.*, debrisoquine, sparteine, metoprolol or dextrometorphan are acknowledged as well-established probe drugs. If the clearance of a drug depends exclusively on CYP2D6, this can be viewed as appropriate to evaluate an individual's enzymatic activity [22]. In the present study, atomoxetine was used as a probe drug considering that it is primarily metabolized by CYP2D6 [6]. In 1985, a study conducted by Farid *et al.* investigated the pharmacokinetic profile of atomoxetine and hinted to the potential influence of CYP2D6 polymorphism on the metabolism of this agent as a bimodal data distribution was reported for its clearance in healthy volunteers [23].

As depicted in *Table I*, a comparison of the MR_ AUC values corresponding to each volunteer showed that subjects 5, 15 and 38 presented higher values in comparison to the rest of the group, which suggested a decreased metabolism of atomoxetine in these particular cases. For this reason, the study population was considered to comprise 2 phenotypes: PMs (3 subjects) and EMs (40 subjects). This hypothesis was also sustained by statistics. The 3 extreme values and the right skewed asymmetry of the Q-Q plot (*Figure 1*) emphasized the presence of a heterogeneous group. In addition, the results of the two statistical tests described in *Table II* ($p<0.05$) showed that the analyzed data (MR_ AUC values) did not follow a normal distribution. Hence, both the MR_ AUC data set and the statistical analysis provided enough evidence to support the existence of two groups within the study population, each corresponding to a different phenotype. More precisely, the PM group included 3 individuals (subject 5, 15 and 38), while the remaining 40 subjects were characterized as EMs. Female subjects using oral contraceptives can be considered a potential interfering factor for this analysis due to the fact that hormones such as progesterone, testosterone, pregnanolone, pregnenolone, 17β-estradiol, and 17β- hydroxyprogesterone competitively inhibit CYP2D6 activity, whereas epiallopregnanolone and alfaxalone noncompetitively inhibit the same isoenzyme [24]. In addition, pharmacological studies revealed that estrogen-induced cholestasis can repress CYP2D6 expression and activity [25]. However, although the study protocol did permit the use of oral contraceptives during the clinical trial, an enquiry revealed that 50 % of the female subjects were using bar-

Table II. Statistical tests for normality considering the MR_ AUC data set

	Anderson-Darling test		Lilliefors (Kolmogorov-Smirnov) test	
MR_AUC (ATX/HATX-gluc)	A = 9.5941*	p<0.001**	D = 0.36037*	p<0.001**

AUC - area under the plasma concentration–time curve from time zero to infinity;
MR_ AUC– metabolic ratio (MR_ AUC = AUC atomoxetine (ATX)/AUC 4-hydroxyatomoxetine-O-glucuronide (HATX-gluc)), *A - test result ; D - test result; **p<0.05 – statistically significant

rier contraceptive methods, while the rest did not report the use of any birth control method. Therefore, there was no need of exclusion of any subject and data related to all subjects was deemed relevant for the present investigation.

Once the metabolizer status of each subject was known, the present research wanted to reveal potential differences in plasmatic profiles and pharmacokinetic parameters between the two phenotypic groups (PMs versus EMs). For this reason, *Figure 2* depicts the plasma concentration-time profiles of atomoxetine (A) and 4-hydroxyatomoxetine-*O*-glucuronide (B) for each CYP2D6 metabolic status. This graphical representation showed that the parent drug presented higher plasma concentrations for PMs than for EMs. On the other hand, the plasmatic profile of 4-hydroxyatomoxetine-*O*-glucuronide displayed lower mean plasma levels in the PM group in comparison with the ones attributed to the EM group. These results demonstrated that, due to the reduced enzymatic activity of CYP2D6, the biotransformation of atomoxetine to its active metabolite (4-hydroxyatomoxetine) was clearly impaired.

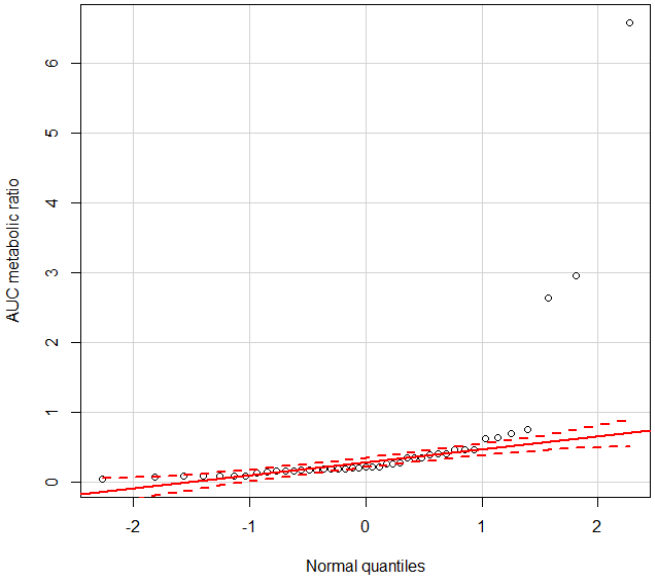

Figure 1. AUC metabolic ratio (MR_AUC) presented as a quantile-quantile plot

Table III. The pharmacokinetic (Pk) parameters of atomoxetine (ATX) and 4-hydroxyatomoxetine-O-glucuronide (HATX-gluc) coresponding to each phenotype (PMs and EMs) and the statistical analysis used to detect potential differences between the groups

Analyte	Pk parameters (mean±SD)	PMs (n=3)	EMs (n=40)	*p value (ANOVAa)
ATX	Cmax (ng/mL)	344.47±36.22	223.58±94.24	0.043,S
	tmax (h)	2.83±2.75	1.46±1.21	Friedman,NS
	AUC0-t (ng*h/mL)	5736.14±1076.97	1291.07±812.28	0.000,S
	AUC (ng*h/mL)	6235.64±641.4	1373±860.48	0.000,S
	kel (1/h)	0.04±0.01	0.22±0.09	0.000,S
	t½ (h)	16.08±2.28	3.95±2.11	0.000,S
HATX-gluc	Cmax (ng/mL)	49.6±15.64	697.39±266.53	0.000,S
	tmax (h)	9.33±1.15	2.36±1.09	Friedman,S
	AUC0-t (ng*h/mL)	1639.43±561.82	5177.35±1101.06	0.000,S
	AUC (ng*h/mL)	1639.43±561.82	5264.73±1113.54	0.000,S
	kel (1/h)	0.04±0.01	0.13±0.03	0.000,S
	t½ (h)	21.46±8.71	5.69±1.52	0.000,S

SD - standard deviation; PMs – poor metabolizers; EMs – extensive metabolizers
*p<0.05 – statistically significant (S); NS - non-significant
aANOVA except where stated otherwise

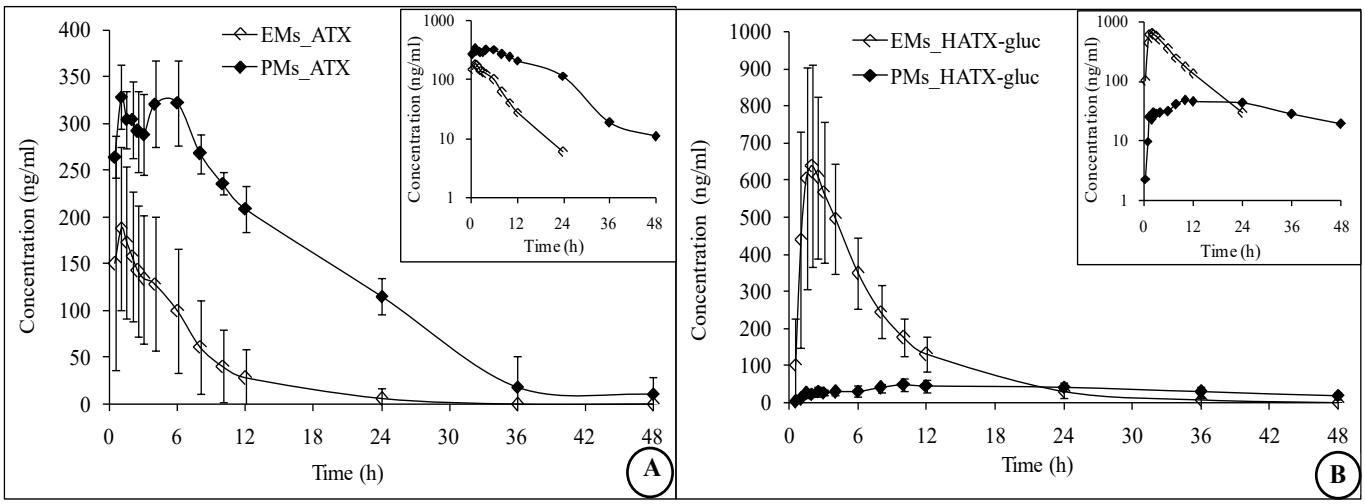

Figure 2. Mean ± SD plasma concentration–time curves of atomoxetine (ATX - (A) and of 4-hydroxyatomoxetine-O-glucuronide (HATX-gluc - (B)) corresponding to each phenotypic group, respectively extensive metabolizers (EMs) and poor metabolizers (PMs). Insert: semilogarithmic presentation

When the pharmacokinetic parameters of atomoxetine were calculated, a marked variability between the 2 phenotypic groups was observed. With regard to the pharmacokinetic data displayed in *Table III*, the mean C_{max} and AUC values were 1.5-fold and 4.5-fold higher, respectively the $t_{½}$ of the parent drug was about 4-fold longer, in subjects characterized as CYP2D6 PMs than in EMs. There were statistically significant differences for all pharmacokinetic parameters, except t_{max}, between the two phenotypic groups. Thus, all data suggest that exposure to atomoxetine is greater in PMs. The role of CYP2D6 in the metabolic fate of atomoxetine was previously investigated in a study conducted by Sauer *et al*. in healthy men. According to that research, after single dose intake (20 mg), the AUC of atomoxetine was 4-fold higher, while the $t_{½}$ was approximately 3.5-fold longer in PMs than in EMs [8], results which are similar with the ones reported in the present study. In addition, the previous investigation concluded that after repeated dosing, a 6-fold higher C_{max} at steady-state and 8-fold higher AUC values were determined for the PM phenotype [8].

The pharmacokinetic parameters of 4-hydroxyatomoxetine-*O*-glucuronide (*Table III*) corresponding to each metabolizer status came to confirm the interphenotype variability. As expected, a decrease in the rate of formation of 4-hydroxyatomoxetine was observed in the PM group. More precisely, for this phenotype, the values of C_{max} and AUC were 14-fold and 3.2-fold lower than the ones determined for EMs. Moreover, the following analysis concluded that the differences between the two groups were statistically different for all the pharmacokinetic parameters of the glucuronidated metabolite. With the exception of $C_{max,}$ these results can be viewed as similar to the ones found by Sauer *et al*. In that particular study, an approximately 4.7-fold decrease in C_{max} was calculated for the PM group after the administration of 20-mg repeated doses of atomoxetine [8]. The exposure to 4-hydroxyatomoxetine-*O*-glucuronide was about 3-fold lower in PMs due to the fact that the clearance of the parent drug was altered [8], a situation comparable with the one seen in the present investigation. Additionally, similarities also reside in the variation of the $t_{½}$ between the two groups. The mean $t_{½}$ of the active metabolite (glucuronidated form) was approximately 6 h in EMs and 21 h in PMs in the present study. Meanwhile, in the past, the same pharmacokinetic parameter was approximately 7 h in EMs and 19 h in PMs [8].

It is already acknowledged that there are pronounced differences not only in the prevalence of PMs, but also in the relative enzyme activity in different ethnic groups. Taking into account this aspect, the present research provided additional insight into the impact of CYP2D6 phenotype on atomoxetine bioavailability and metabolism. Furthermore, according to Teh *et al.*, the comparison of pharmacokinetic parameters between PMs and EMs may suggest the extent of interaction of a CYP2D6 substrate and strong inhibitors of the same isoenzyme and also indicate when clinical pharmacokinetic studies to investigate this aspect should be considered useful or not [21].

Although the present study did not intend to assess clinical aspects, information about the consequences of CYP2D6 polymorphism and on whether the efficacy and safety of atomoxetine are influenced by a certain phenotype, are available in the scientific literature. There is compelling evidence that while CYP2D6 PMs may have a better response to atomoxetine, they may also experience a higher frequency of adverse events as compared to CYP2D6 EMs [14]. Fijal *et al*. analyzed the differences between CYP2D6 PMs and non-PMs (IMs, EMs and UMs combined) in regard to safety and tolerability in a 12-week open-label study which included adult patients with ADHD. This research concluded that PMs had a higher prevalence of side effects such as decreased appetite, dry mouth, hyperhidrosis, insomnia, urinary retention and erectile dysfunction in men. In addition, significantly higher increases in cardiovascular parameters (blood pressure and heart rate) and a greater reduction in BMI were reported for the PM status [26]. Also, Michelson *et al*. evaluated if differences in CYP2D6 genotype/phenotype influence the clinical response to atomoxetine in children and adolescents with ADHD. In terms of efficacy, symptom reduction was greater in PMs versus EMs and fewer patients with a PM status suspended atomoxetine therapy due to lack of efficacy. When safety and tolerability aspects were considered, it was reported that greater increases in heart rate and diastolic blood pressure and smaller increases in weight were attributed to the PM group. Moreover, side effects like decreased appetite and tremor were reported more frequently for PMs [27].

Study limitations

The absence of any reference to the use of herbal medicines and supplements for the exclusion criteria should be acknowledged as a methodological deficiency and subsequently, as a study limit. This aspect needs to be acknowledged in this case as several herbs proved to influence the activity of CYP2D6, including goldenseal and dong quai [28,29]. Still, this interfering factor was later reviewed and no herbal remedy with potential to influence CYP2D6 activity was reportedly used by the study subjects.

Furthermore, lack of genotyping can be regarded as a study limitation, as this procedure could be useful in order to verify and validate the phenotypic data obtained in the present study. Another limit refers to the fact that no clinical monitoring was performed throughout the research. Nonetheless, essential information about the potential clinical consequences associated with atomoxetine intake by PMs was collected from the scientific literature and mentioned in the text.

Conclusion

Based on the MR_ AUC values and statistical tests, it was demonstrated that the study population comprised two phenotypic groups (EMs and PMs). Atomoxetine bioavail-

ability and metabolism were subjected to interphenotypic variation as PMs presented a 4.5-fold higher exposure to the parent drug and a 3.2-fold lower exposure to its metabolite in comparison to EMs.

Acknowledgements and funding

This work was supported by the National Research Council (CNCS) Romania – project PN-II-ID-PCE-2011-3-0731. All authors are full-time employees of the University of Medicine and Pharmacy "Iuliu Hatieganu", Cluj-Napoca, Romania.

Conflicts of interest

The authors declare no conflict of interest.

References

1. Corman SL, Fedutes BA, Culley CM. Atomoxetine: the first nonstimulant for the management of attention-deficit/hyperactivity disorder. Am J Health Syst Pharm. 2004;61(22):2391–99.
2. B Barton J. Atomoxetine: a new pharmacotherapeutic approach in the management of attention deficit/hyperactivity disorder. Arch Dis Child. 2005;90 Suppl 1:i26-9.
3. Sauer J-M, Ring BJ, Witcher JW. Clinical pharmacokinetics of atomoxetine. Clin Pharmacokinet. 2005;44(6):571–90.
4. Findling RL. Evolution of the treatment of attention-deficit/hyperactivity disorder in children: A review. Clin Ther. 2008;30(5):942–57.
5. Yu G, Li G-F, Markowitz JS. Atomoxetine: A review of its pharmacokinetics and pharmacogenomics relative to drug disposition. J Child Adolesc Psychopharmacol. 2016;26(x):1–13.
6. Ring BJ, Gillespie JS, Eckstein JA, Wrighton SA. Identification of the human cytochromes P450 responsible for atomoxetine metabolism. Drug Metab Dispos. 2002;30(3):319–23.
7. Simpson D, Plosker GL. Spotlight on atomoxetine in adults with attention-deficit hyperactivity disorder 1. 2004;18(6):397–401.
8. Sauer JM, Ponsler GD, Mattiuz EL, et al. Disposition and metabolic fate of atomoxetine hydrochloride: The role of CYP2D6 in human disposition and metabolism. Drug Metab Dispos. 2003;31(1):98–107.
9. Matsui A, Azuma J, Witcher JW, et al. Pharmacokinetics, safety and tolerability of atomoxetine and effect of CYP2D6*10/*10 genotype in healthy Japanese men. J Clin Pharmacol. 2012;52(3):388–403.
10. Cui YM, Teng CH, Pan AX, et al. Atomoxetine pharmacokinetics in healthy Chinese subjects and effect of the CYP2D6*10 allele. Br J Clin Pharmacol. Wiley-Blackwell; 2007;64(4):445–49.
11. Sistonen J, Sajantila A, Lao O, Corander J, Barbujani G, Fuselli S. CYP2D6 worldwide genetic variation shows high frequency of altered activity variants and no continental structure. Pharmacogenet Genomics. 2007;17(2):93–101.
12. Zhou S-F. Polymorphism of Human Cytochrome P450 2D6 and Its Clinical Significance. Clin Pharmacokinet. 2009;48(11):689–723.
13. Ingelman-Sundberg M. Genetic polymorphisms of cytochrome P450 2D6 (CYP2D6): clinical consequences, evolutionary aspects and functional diversity. Pharmacogenomics J. 2005;5:6–13.
14. Brown JT, Bishop JR. Atomoxetine pharmacogenetics: associations with pharmacokinetics, treatment response and tolerability. Pharmacogenomics. 2015;16(13):1513–20.
15. LLerena A, Naranjo MEG, Rodrigues-Soares F, Penas-LLedo EM, Farinas H, Tarazona-Santos E. Interethnic variability of CYP2D6 alleles and of predicted and measured metabolic phenotypes across world populations. Expert Opin Drug Metab Toxicol. 2014;10(11):1569–83.
16. Zanger UM, Raimundo S, Eichelbaum M. Cytochrome P450 2D6: Overview and update on pharmacology, genetics, biochemistry. Naunyn Schmiedebergs Arch Pharmacol. 2004;369(1):23–37.
17. Gardiner SJ, Begg EJ. Pharmacogenetics, drug-metabolizing enzymes, and clinical practice. Pharmacol Rev. 2006;58(3):521–90.
18. Belle DJ, Ernest CS, Sauer J-M, Smith BP, Thomasson HR, Witcher JW. Effect of potent CYP2D6 inhibition by paroxetine on atomoxetine pharmacokinetics. J Clin Pharmacol. 2002;42(11):1219–27.
19. Shah RR, Smith RL. Addressing phenoconversion: The Achilles' heel of personalized medicine. Br J Clin Pharmacol. 2015;79(2):222–40.
20. Abraham BK, Adithan C. Genetic Polymorphism of Cyp2D6. Indian J Pharmacol. 2001;33(2):147–69.
21. Teh LK, Bertilsson L. Pharmacogenomics of CYP2D6: molecular genetics, interethnic differences and clinical importance. Drug Metab Pharmacokinet. 2012;27(1):55–67.
22. Frank D, Jaehde U, Fuhr U. Evaluation of probe drugs and pharmacokinetic metrics for CYP2D6 phenotyping. Eur J Clin Pharmacol. 2007;63(4):321–33.
23. Farid NA, Bergstrom RF, Ziege EA, Parli CJ, Lemberger L. Single-dose and steady-state pharmacokinetics of tomoxetine in normal subjects. J Clin Pharmacol. 1985;25(4):296–301.
24. Wang B, Yang L-P, Zhang X-Z, Huang S-Q, Bartlam M, Zhou S-F. New insights into the structural characteristics and functional relevance of the human cytochrome P450 2D6 enzyme. Drug Metab Rev. 2009;41(4):573–643.
25. Pan X, Jeong H. Estrogen-induced cholestasis leads to repressed CYP2D6 expression in CYP2D6-humanized mice. Mol Pharmacol. 2015;88(1):106–12.
26. F Fijal BA, Guo Y, Li SG, et al. CYP2D6 predicted metabolizer status and safety in adult patients with attention-deficit hyperactivity disorder participating in a large placebo-controlled atomoxetine maintenance of response clinical trial. J Clin Pharmacol. 2015;55(10):1167–74.
27. Michelson D, Read H, Ruff DD, Witcher J, Zhang S, McCracken J. CYP2D6 and clinical response to atomoxetine in children and adolescents with ADHD. J Am Acad Child Adolesc Psychiatry. 2007;46(2):242–51.
28. Wanwimolruk S, Prachayasittikul V, Phopin K, Prachayasittikul V. Cytochrome P450 enzyme mediated herbal drug interactions (Part 1). Excli J. 2014;13:347–91.
29. Wanwimolruk S, Phopin K, Prachayasittikul V. Cytochrome P450 enzyme mediated herbal drug interactions (Part 2). Excli J. 2014;13:869–96.

DE GRUYTER OPEN

Acta Medica Marisiensis 2017;63(2):80-86 DOI: 10.1515/amma-2017-0022

RESEARCH ARTICLE

Letrozole Determination by Capillary Zone Electrophoresis and UV Spectrophotometry Methods

Aura Rusu[1*], Maria-Alexandra Sbanca[2], Nicoleta Todoran[3], Camil-Eugen Vari[4]

1 Department of Pharmaceutical Chemistry, University of Medicine and Pharmacy of Tîrgu Mureş
2 University of Medicine and Pharmacy of Tîrgu Mureş
3 Department of Pharmaceutical Technology, University of Medicine and Pharmacy of Tîrgu Mureş
4 Department of Pharmacology and Clinical Pharmacy, University of Medicine and Pharmacy of Tîrgu Mureş

Objective: Letrozole is a highly potent oral nonsteroidal aromatase inhibitor triazole derivative. The aim of this study was to quantify letrozole from bulk, pharmaceutical formulation, and spiked urine samples by developing a simple, rapid and cost effective capillary electrophoresis method. **Methods**: A capillary zone electrophoresis method was optimized and validated. Additionally, an UV spectrophotometry method was used for comparing results. **Results**:The capillary zone electrophoresis method using a 90 mM sodium tetraborate background electrolyte proved to be an efficient method for determination of letrozole in a very short time, less than 2 minutes, using 20 kV voltage, 50 mbar/2 seconds pressure and 50°C temperature as optimum parameters. Additionally, the UV spectrophotometry method proved to be simple and efficient to quantify letrozole from bulk material and pharmaceutical formulation with linearity of response between 5 to 20 $\mu g \cdot mL^{-1}$ concentrations. For both methods, validation parameters, including linearity, detection and quantification limits were determined. Also we proved that our electrophoretic method has potential in analyzing letrozole from biological samples, obtaining encouraging results on estimation of letrozole from spiked urine samples without any special treatment. **Conclusions**: To quantify letrozole from bulk material, pharmaceutical preparations, and spiked urine samples the capillary zone electrophoresis method using a tetraborate sodium background electrolyte has proven to be simple and appropriate. Also a simple UV spectrophotometric method has been developed and validated for the same purposes.

Keywords: letrozole, aromatase inhibitors, capillary zone electrophoresis, UV spectrophotometry

Received 19 May 2017 / Accepted 20 June 2017

Introduction

Letrozole (LET) is a nonsteroidal triazole derivative (Figure 1) classified as a highly potent and selective aromatase inhibitors [1] from the third generation**.** LET inhibits aromatase enzyme which catalyzes the synthesis of estrogens from the androgen precursors. Aromatase expression occurs in many organs, including ovary, placenta, hypothalamus, liver, muscle, adipose tissue, and breast cancer itself. Aromatase catalyzes three separate steroid hydroxylation's which are involved in the conversion of androstenedione (an androgenic precursor) to estrone and testosterone (estrogenic hormones) to estradiol [2-4]. LET offer new treatment options for breast cancer [5]. Unfortunately, LET is also used by doped athletes as post cycle therapy in order to promote restoration of hypothalamic-pituitary-testicular axis integrity [6]. A topical issue has emerged with the manufacture of "counterfeit" drugs by unregulated on-line pharmacies, which are tainted with impurities, contain no medication, or are potentially harmful [7].

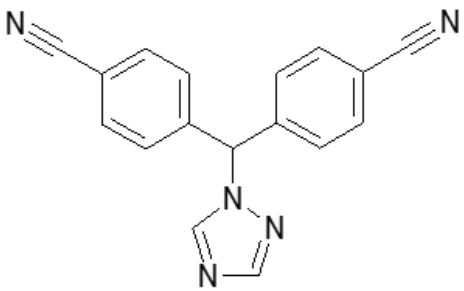

Fig. 1. Letrozole (IUPAC name: 4,4'-((1H-1,2,4-triazol-1-yl)methylene)dibenzonitrile).

Biotransformation of LET. LET is completely absorbed from the gastrointestinal tract. The biotransformation occurs by cytochrome P-450 isozymes (CYP2A6 and CYP3A4) into carbinol (Figure 2), an inactive metabolite [8-10]. CYP2A6 isozyme seems to be the principal clearance mechanism for LET*in vivo* [11].

LET is excreted into urine, approximately 70% of the administered dose is eliminated as unchanged LET (6.0 ± 3.8%) or as the glucuronide of the major, pharmacologically inactive metabolite carbinole (CGP44645) (64.2 ± 22.7%) [13,14]. Similar data has been previously obtained at the administation of a single dose of letrozole (2.5 mg) with 14C-labeled within two weeks when the recovered radioactivity from urine was 88.2 ± 7.6% (5.0 ± 2.4% unmetabolized letrozole, 63.2 ± 11.2% carbinole glucuronide and about 8% other metabolites) [15]. A few capillary electrophoretic (CE) methods for LET determination have been already reported in the literature, mainly micellar electrokinetic capillary chromatographic (MEKC) [16-19]. The electrophoretic methods are more advantageous through accessibility than other expensive analytical methods as HPLC and RP-HPLC, LC-MS/MS or SPE-UPLC-MS/MS [20-24]. For determination of LET in bulk and

* Correspondence to: Aura Rusu
E-mail: aura.rusu@umftgm.ro

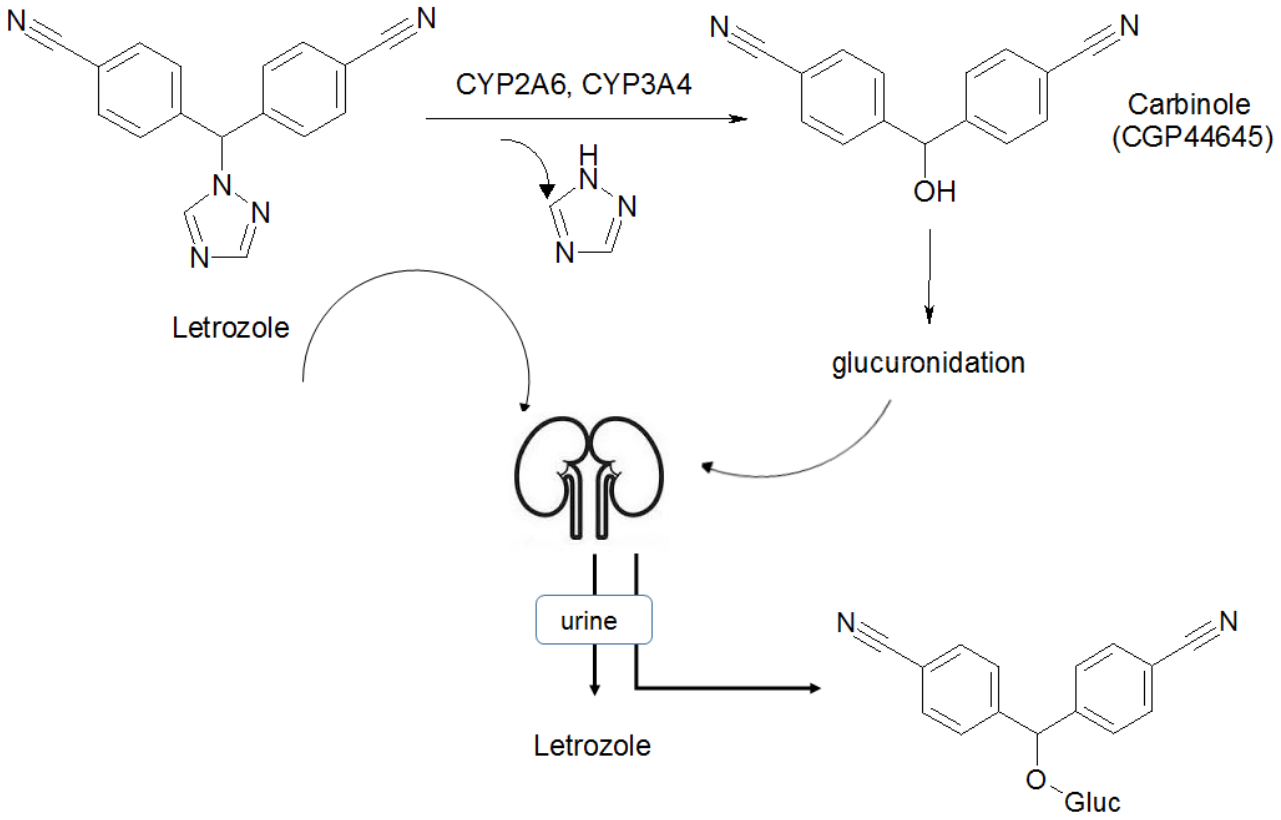

Fig. 2. Biotransformation of LET (*Gluc – glucuronic acid) [12].

pharmaceutical formulations spectrophotometric method are also frequently used [25-27].

The aim of the present study was to develop and validate two simple methods for the determination of LET from bulk materials, pharmaceutical products, and biological samples by capillary zone electrophoresis (CZE) and UV spectrophotometry.

Experimental

Analytical instruments. The CE experiments were performed on an Agilent 6100 CE system equipped with diode-array detector and results were processed with Chemstation 7.01 software (Agilent). All experiments were performed using a hydrodynamic sample injection. Uncoated fused-silica capillaries of 32.5 x 50 µm I.D (effective length 24,5 cm) (Agilent) was used. An Analytik Jena UV-VIS Specord 210 spectrophotometer and WinASPECT software were used for recording UV spectra. The pH adjustments were performed using a Hanna Instruments HI2215 pH-meter. The spiked urine samples was centrifuged in a Centurion Scientific Ltd. Centrifuge.

Chemicals and reagents. LET was supplied by Sigma Aldrich and ciprofloxacin hydrochloride (CIP) (used as internal standard) by Ranbaxy Laboratories Limited. Pharmaceutical product Letrozole 2.5 mg (tablets) were supplied from Teva. All chemicals and solvents were of analytical reagent grade. The deionized water was obtained using a Millipore Direct-Q™ system.

Standard stock solution preparation. The LET stock solution was prepared daily at a 1 mg mL^{-1} concentration in methanol, treated in an ultrasonic bath for 10 min at room temperature and stored in the refrigerator at +4°C, and diluted to an appropriate concentration with methanol.

Biological samples treatment. Fresh human urine samples were acquired from different healthy volunteers. The urine samples were spiked with LET stock solution, centrifuged (4800 rpm, 10 minutes) and the supernatant was filtrated (0.45 µm Whatman filter). The percentage of solvent (methanol) was identically for all spiked urine samples as the the ratio solvent:urine (1:4).

Methods

Nowadays, the CZE method is sometimes more attractive comparative to the more frequently used HPLC methods. The main advantages of CZE are: rapid method development, speed of analysis, and relatively low costs derived from the low required amount of sample and reagents [20]. Also, to compare the results we developed a simple and reliable UV spectrophotometry method appliable to estimate the amount of LET in pharmaceutical formulations.

Results and discussion

A. Capillary zone electrophoresis

The detection was carried out in UV at 240 nm, in accordance with our recorded UV absorption spectra of LET and data previously reported in literature [25-28]. In CZE capillary preconditioning is necessary for removing adsorbed material from the capillary wall [29]. At the be-

ginning of each day of experiments the capillary was conditioned with 1M NaOH (30 min), deionized water (5 min) and BGE (30 min) than at the beginning of each experiment was preconditioned with water (1 min) and BGE (2 min). The preconditioning before experiments is very important because capillary surface is re-equilibrated by rinsing with BGE [33].

Preliminary considerations. Regarding the p*K*a value of LET there are no published studies in the literature. It was found only a calculated pKa value 2.17 (strongest basic) via ChemAxon database [30]. By using MarvinSketch 17.1.2 (ChemAxon) [31] it was found that p*K*a of LET is 1.89. LET can accept protons at the nitrogen atoms of the triazole ring. Thus, major microspecies in the range of pH 5 - 13 are neutral (100%). It is already known that for conventional CZE method, phosphate and borate buffers can be considered suitable because of their low absorbance at the detection wavelength [32]. Initially, we choose to start with a 25 mM phosphate buffer, an acidic background electrolyte (BGE), but the electrophoretic signal of the substance was difficult to detect (low value of area and height). A standard BGE containing 25 mM borax (pH 9.3) was than selected, taking in consideration also previous electrophoretic studies, however the disadvantage in a basic environment was that LET migrated very close to the electroosmotic flow (EOF) [16-19]. Adding sodium dodecyl sulfate (SDS) in the 25 mM borax BGE did not resolved the problem.

Optimization of CZE method. To increase the method performance the external parameters such as BGE characteristics (BGE concentration and pH) and specific internal capillary electrophoretic system parameters (temperature, injection time, applied voltage, and pressure) were analysed and optimezed in order to improve separation (Figure 3) [33].

Effect of the Ionic Strength of BGE. Generally, the BGE concentration change the electrophoretic behavior of the analytes by influencing the selectivity of separation and EOF velocity [32]. The effect of BGE concentration was studied between10 mM to 100 mM. The increase of the BGE concentration lead to an increase of LET migration times, due to a decrease of EOF with the increase in ionic strength. The 90 mM concentration was set as optimum (best height, area and peak symmetry); the use of BGE with high concentration is limited by the generation of high currents which leads to instability of the electrophoretic system.

Effect of the pH of BGE. In order to obtain an adequate peak the variation of pH was analyzed on a pH interval between 8.7 – 10.32 by adding small amounts of 1M NaOH

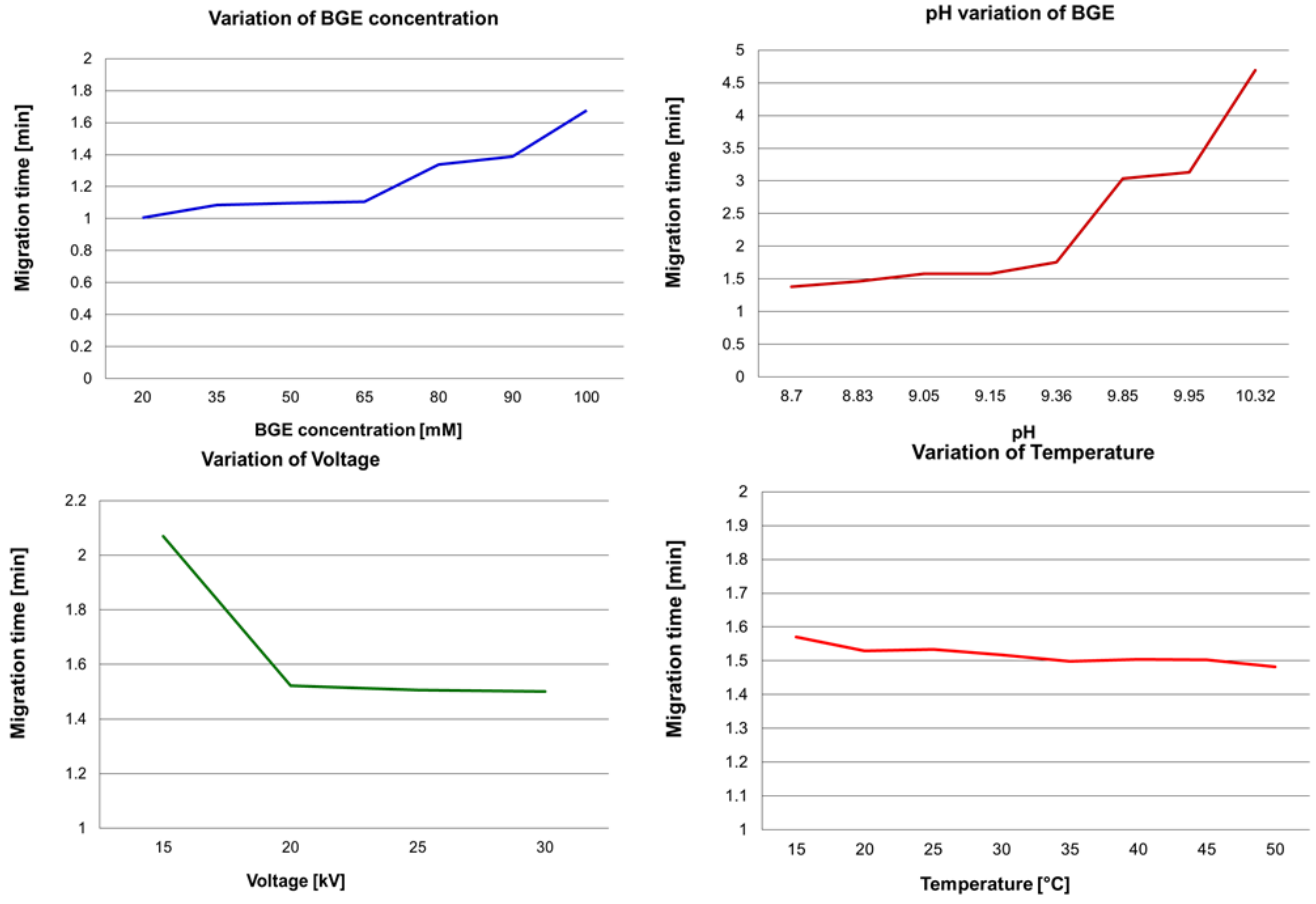

Fig. 3. Variation of the migration time depending on the A) BGE concentration (applied voltage: + 20 kV, temperature: 25°C, injection pressure 30 mbar/2 sec); B) pH of BGE (BGE 90 mM borax, applied voltage: + 20 kV, temperature: 25°C, injection pressure 30 mbar/2 sec); C) voltage (BGE 90 mM borax, temperature: 25°C, injection pressure 30 mbar/2 sec); D) temperature (BGE 90 mM borax, applied voltage: + 20 kV, injection pressure 30 mbar/2 sec).

and 1M boric acid in BGE. The LET migration times increased with pH values. At higher pH values the registered peaks were very broad. In consequence, the optimum pH of BGE was set at value 9.36.

Effect of Voltage. The migration times decreased with the increase of voltage so that we set the optimum value at 20 kV to obtain good peak shapes and amplitudes.

Effect of Temperature. Regarding the influence of temperature on LET migration times slightly decreased with the increase of cassette temperature, the limiting factors being the BGE viscosity and the Joule heating which are directly connected with temperature.The temperature was selected at 50°C for best shape and high value of the LET peak.

Effect of Injection Pressure and Time. Hydrodynamic injection mode because is more precise and robust than electrokinetic injection. In general, analysts prefer hydrodynamic to electrokinetic injection, especially when analyzing biological matrices (e.g. plasma or urine) with varying composition and conductivity [29].

Injection pressure and time modify the migration time of the analyes, but we have noticed that these parameters have influence on the shape of the peaks. Thus, a high injection pressure (50 mbar) and a short injection time (2 s) were preferred in order to avoid peak splitting or broadening.

It was established that LET can be determinate in a very short time, less than 2 minutes (Figure 4**).** To obtain the best peak shapes with the shortest analysis time, 90 mM borax, 20 kV voltage, 50^{0}C, 50 mbar pressure, 2 seconds injection time and 50 °C were set as optimum parameters.

CZE method validation. The method was validated and validation parameters were calculated (Table I). The selected internal standard was CIP, a stable compound with a good signal on sodium borate BGE, which migrates after LET and EOF [34].

Specificity. LET could be quantified from tablets without any interference with other present components.

Linearity. The linearity response for LET was assessed in the range 5 - 875 µg mL^{-1}. The linear regression equations were calculated using six concentration levels and three replicates per concentration. Correlation was over 0.99, which demonstrates a good linearity of the method. LOD and LOQ parameters were calculated by using the signal-to-noise ratio 3:1 and 10:1, respectively.

Precision. The repeatability of migration time and peak area measurement was performed by six replicate injections containing 62.5µg·mL^{-1} of LET, three consecutive days.

These results prove that our developed CZE method can be applied for identification and quantitative determination of LET from bulk materials. Until now, on a base of detailed literature survey, it was found that LET could be estimated along with other compounds only by MEKC [16-19].

Determination of LET in tablets. A total of 20 tablets were weighed and powdered. An equivalent of about 10 mg LET was weighed accurately and transferred into a

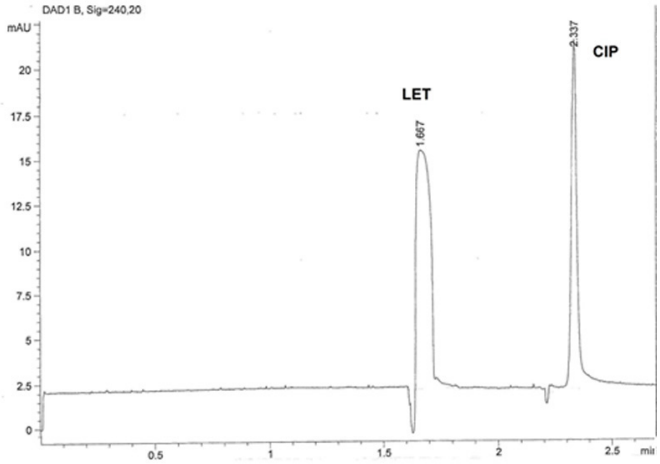

Fig. 4. Electrophoregram of LET. Working parameters: BGE 90 mM borax, 20 kV applied voltage, 50 mbar/2 seconds pressure, temperature 50 °C, UV detection at 240 nm, capillary: 32.5 cm (24.5 cm effective length) x 50 µm, LET concentration: 62.5 µg·mL^{-1}, internal standard CIP concentration 125 µg·mL^{-1}.

Table I. Statistical parameters of CZE method
(working concentration range: 5 - 875 µg·mL^{-1}, internal standard CIP) (T = migration time, A = area, H = height)

Regression equation			Correlation coefficient	LOD (µg·mL^{-1})	LOQ (µg·mL^{-1})
LET	y = 486.01x + 22.875		0.9997	20.43	68.10
			T	A	H
Internal standard CIP 125 µg mL^{-1} (n = 6)		**Average**	2.37	57.67	30.43
		SD	0.05	3.24	2.65
		RSD(%)	2.05	5.62	8.72

Repeatability LET concentration 62.5 µg·mL^{-1}

n = 6	Day 1			Day 2			Day 3		
	T	**A**	**H**	**T**	**A**	**H**	**T**	**A**	**H**
Average	1.67	46.07	11.96	1.67	40.05	10.86	1.74	44.08	11.10
SD	0.036	1.663	0.537	0.008	1.404	0.197	0.027	2.307	0.316
RSD(%)	2.15	3.61	4.49	0.5	3.5	1.81	1.60	5.23	2.84

LET concentration (µg·mL^{-1})	Intra-day precision (RSD%) n=6			Inter-day precision (RSD%) n=18 Days 3		
	T	**A**	**H**	**T**	**A**	**H**
125	2.34	3.00	2.83	2.40	7.18	5.67
62.5	1.60	5.23	2.84	2.35	7.19	5.44
31.25	2.47	2.35	2.93	2.28	5.75	6.22

100 mL volumetric flask with 50 mL methanol. After 30 minutes ultrasonic vibration, the mixture was diluted to volume with methanol and then filtrated. A concentration of 100 µg·mL^{-1} of LET was set. The amount of LET from pharmaceutical tablets and standard deviation (SD) were calculated using linear regression equation of the standard curve (Table I) [26]. The recovery (%) from pharmaceutical formulation was 99.63 ± 1.51 (average of three replicates). Therefore our method has potential to be successfully used to determine LET from counterfeit drugs.

Determination of LET from spiked urine samples. Analytical performance of our CZE method was evaluated on spiked urine from healthy volunteers.

Specificity. LET could be quantified from spiked urine samples without any interference with other present urine components (Figure 5).

Linearity and detection limits. The linearity response and detection limits for spiked with LET urine samples are presented in Table II.

The linear regression equations were calculated using six concentration levels and three replicates per concentration. Correlation was over 0.99, which demonstrates a very good linearity of the method.

Precision. The precision of our CZE method was investigated in repeatability and intermediate precision terms for migration times and peak areas of LET in spiked urine samples (Table II).

Regarding determination of LET our result was satisfactory as respect to selectivity and had a short migration time.

Our validated CZE method is therefore simple but also reliable, with the potential of being used to determinate LET in bulk material, pharmaceutical formulations, counterfeit medicines and urine samples.

B. UV spectrophotometry method

The UV spectra of samples were recorded in methanol in according with data previously reported from literature [25-28].

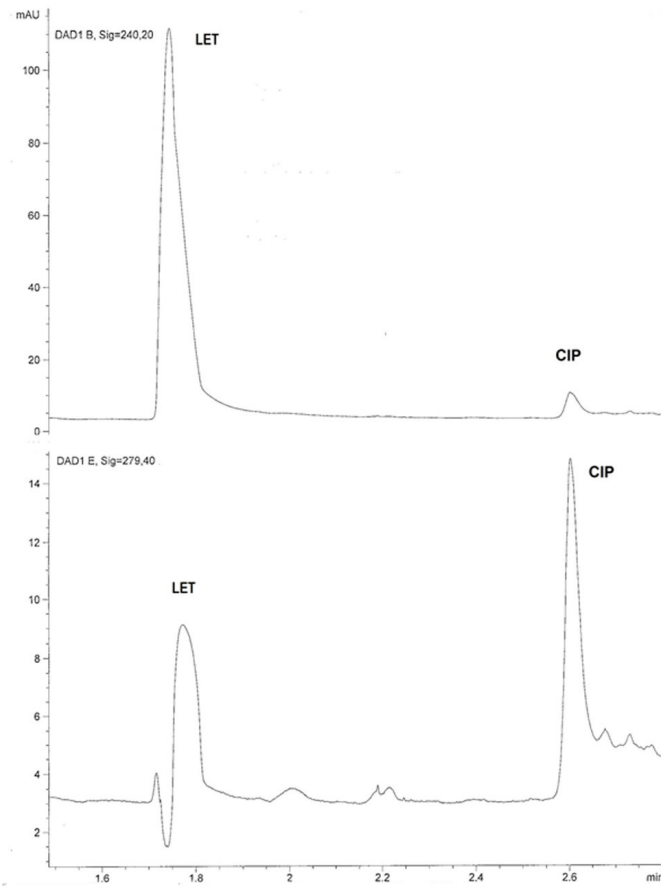

Fig. 5. Electrophoregram of LET form spiked urine sample (LET concentration: 25 µg·mL^{-1}, internal standard CIP concentration 50 µg·mL^{-1}), UV detection at 240 nm and 279 nm. Working parameters: BGE 90 mM sodium tetraborate, 20 kV applied voltage, 150 µA current, 50 mbar/2 seconds pressure, temperature 50 °C, capillary: 32.5 cm (24.5 cm effective length) x 50 µm.

Determination of λ_{max} *(nm).* A 10µg·mL^{-1} concentration was prepared from II stock solution by dilution with methanol. This solution was then scanned at wavelength of 190 to 500 nm against blank (methanol). The λ_{max} was found to be at 240 nm. Hence this was considered as

Table II. Statistical parameters of the CZE method for LET determination from urine spiked samples, internal standard CIP (T - migration time, A – area, H = height).

Conc. domain (µg·mL^{-1})	Regression equation	Correlation coefficient	LOD (µg·mL^{-1})	LOQ (µg·mL^{-1})
0.015 – 0.15	y = 896.82x + 176.49	0.992	14.98	49.94
Internal standard CIP		**T**	**A**	**H**
125 µg mL^{-1}	**Average**	2.37	56.03	29.33
(n = 6)	**SD**	0.05	4.29	2.78
	RSD(%)	2.05	7.66	9.49

Repeatability LET concentration 75 µg·mL^{-1}									
n = 6	**Day 1**			**Day 2**			**Day 3**		
	T	**A**	**H**	**T**	**A**	**H**	**T**	**A**	**H**
Average	1.733	418.8	112.8	1.786	458.9	121.58	1.783	454.81	121.56
SD	0.02	10.76	1.16	0.001	9.215	1.082	0.001	5.26	0.89
RSD(%)	0.13	2.56	1.02	0.06	2.00	0.89	0.10	1.15	0.73

LET concentration (µg·mL^{-1})	**Intra-day precision – RSD(%) n=6**			**Inter-day precision – RSD(%) n=18 Days 3**		
	T	**A**	**H**	**T**	**A**	**H**
125	0.12	3.11	0.92	2.19	6.79	1.76
75	0.13	2.56	1.02	1.43	4.62	3.67
25	0.14	1.86	1.20	1.15	4.56	1.89

Table III. Statistical parameters of the UV spectrophotometric method for LET

Conc. domain (μg·mL^{-1})	Regression equation	Correlation coefficient	LOD (μg·mL^{-1})	LOQ (μg·mL^{-1})
0.005 – 0.020	y = 0.1114x – 0.0239	0.9986	0.99	3.29

	Intra-day precision n= 6			Inter-day precision n=18 Days 3		
LET concentration (μg·mL^{-1})	Mean	SD	RSD(%)	Mean	SD	RSD(%)
7.0	0.738	0.010	1.35	0.761	0.022	2.94
10.0	0.976	0.010	1.02	1.014	0.035	3.46
13.0	1.360	0.015	1.14	1.389	0.025	1.79

absorption maxima which was then used for the calibration curve.

Preparation of standard stock solution

I Stock solution. LET standard solution was prepared by dissolving 10 mg of LET in 10 mL methanol (1mg·mL^{-1} concentration).

II Stock solution. From I stock solution 1 mL solution was taken and then diluted up 10 mL with the same solvent in a volumetric flask (100 μg·mL^{-1} concentration).

Linearity study. From II stock solution aliquots were prepared in the range of 5 - 20 μg·mL^{-1}.The absorbances were measured at 240 nm and used for the linearity calibration plot (Table III). Our experimental detection limits were set between 1 and 30 μg·mL^{-1}.

Intra-day and inter-day precision study. Aliquots of II stock solution were taken and respectively diluted to obtain three concentrations of 7.0, 10.0 and 13 μg·mL^{-1}, respectively. Triplicate absorbance measurements of each sample were registered and the mean, SD and RSD calculated. The selected concentrations for intra-day precision study were again analyzed the following 2 days and the standard deviation (SD) and relative standard deviation (RSD) were calculated (Table III).

Determination of LET in tablets

For the determination of LET from commercial preparation we prepare the samples similar to previous CZE method [26]. The recovery (%) from pharmaceutical formulation Letrozol was 97.8 ± 0.098 (average of three replicates).

Conclusions

CZE was proven to be a simple, rapid and appropriate method to quantify LET from bulk material, pharmaceutical preparations and spiked urine samples. The analytical parameters were optimized to achieve the determination of LET in a very short time analysis using a 90mM borax BGE. Validation parameters were also determined, linearity, LOD, LOQ, inter-day and intra-day precision. Also for comparing results a simple, rapid and sensible UV spectrophotometric method for determination of LET in bulk material and pharmaceutical dosage form has been developed and validated. Our methods could be useful in analyzing LET in the pharmaceutical industry, clinical studies and have potential in identifying counterfeit products marketed on-line used by athletes that doping.

Acknowledgement

The study was supported by a project funded through Internal Research Grants (grant contract for execution of research projects no. 17/23.12.2014) by the University of Medicine and Pharmacy of Tîrgu Mures¸ Romania.

Conflict of interest

None to declare.

References

1. Bhatnagar AS, Häusler A, Schieweck K, Lang M, Bowman R - Highly selective inhibition of estrogen biosynthesis by CGS 20267, a new non-steroidal aromatase inhibitor. J Steroid Biochem Mol Biol. 1990;37:1021–1027.
2. Bhatnagar AS - The discovery and mechanism of action of letrozole. Breast Cancer Res Tr. 2007;105(Suppl 1):7-17.
3. Santen RJ, Harvey HA - Use of aromatase inhibitors in breast carcinoma. Endocr-Relat Cancer. 1999;6:75–92.
4. Torrisi R, Rota S, Losurdo A, Zuradelli M, Masci G, Santoro A - Aromatase inhibitors in premenopause: Great expectations fulfilled? Crit Rev Oncol Hematol. 2016;107:82-89.
5. Berry J - Are all aromatase inhibitors the same? A review of controlled clinical trials in breast cancer. Clin Ther. 2005;27:1671-1684.
6. Vari CE, Ősz BE, Miklos A, Berbecaru-Iovan A, Tero-Vescan A - Aromatase inhibitors in men – off-label use, misuse, abuse and doping, Farmacia, 2016;64: 813-818.
7. Baron DA, Martin DM, Abol Magd S - Doping in sports and its spread to at-risk populations: an international review. World Psychiatry. 2007;6:118-123.
8. Sioufi A, Gauducheau N, Pineau V et al. - Absolute bioavailability of letrozole in healthy postmenopausal women. Biopharm Drug Dispos. 1997;18:779-789.
9. Sioufi A, Sandrenan N, Godbillon J, et al. - Comparative bioavailability of letrozole under fed and fasting conditions in 12 healthy subjects after a 2.5 mg single oral administration. Biopharm. Drug Dispos. 1997;18:489-497.
10. Tao X, Piao H, Canney DJ, Borenstein MR, Nnane IP - Biotransformation of letrozole in rat liver microsomes: effects of gender and tamoxifen. J Pharm Biomed Anal. 2007;43:1078-1085.
11. Desta Z, Kreutz Y, Nguyen AT, et al. - Plasma letrozole concentrations in postmenopausal women with breast cancer are associated with CYP2A6 genetic variants, body mass index, and age. Clin Pharmacol Ther. 2011;90:693-700.
12. Precht JC, Schroth W, Klein K, et al. -The letrozole phase 1 metabolite carbinol as a novel probe drug for UGT2B7. Drug Metab Dispos. 2013;4:1906-1913.
13. Pfister CU, Martoni A, Zamagni C, et al. - Effect of age and single versus multiple dose pharmacokinetics of letrozole (Femara) in breast cancer patients. Biopharm Drug Dispos. 2001;22:191-197.
14. Letrozole, BCCancer Agency Cancer Drug Manual, Developed: 2001, Page 1-5, Limited revision: 1 May 2006; 1 November 2010, 1 April 2011 (http://www.bccancer.bc.ca/drug-database-site/Drug%20Index/Letrozole_monograph_1April2011.pdf Accessed 14 May 2017)
15. Femara (http://www.accessdata.fda.gov/drugsatfda_docs/nda/97/20726_FEMARA%202.5MG_BIOPHARMR.PDF Accessed 14 May 2017)
16. Rodríguez Flores J, Berzas Nevado JJ, Castañeda Peñalvo G, Rodríguez Cáceres MI - Micellar electrokinetic capillary chromatographic method for simultaneous determination of drugs used to treat advanced breast cancer, Chromatographia. 2002;56:283-288.

17. Rodríguez-Flores J, Contento Salcedo AM, Villaseñor Llerena MJ, Muñoz Fernández L - Micellar electrokinetic chromatographic screening of letrozole and its metabolite in human urine: validation and robustness/ruggedness evaluation. Electrophoresis. 2008;29:811-818.
18. Rodríguez Flores J, Salcedo AM, Llerena MJ, Fernández LM - Micellar electrokinetic chromatographic method for the determination of letrozole, citalopram and their metabolites in human urine. J Chromatogr A. 2008;1185:281-290.
19. Rodríguez-Flores J, Contento Salcedo AM, Muñoz Fernández L. Rapid quantitative analysis of letrozole, fluoxetine and their metabolites in biological and environmental samples by MEKC. Electrophoresis. 2009;30:624-632.
20. Suntornsuk L - Recent advances of capillary electrophoresis in pharmaceutical analysis. Anal Bioanal Chem. 2010; 398:29-52.
21. Zarghi A, Foroutan SM, Shafaati A, Khoddam A. - HPLC Determination of Letrozole in Plasma Using Fluorescence Detection: Application to Pharmacokinetic Studies. Chromatographia. 2007;66: 747-750.
22. Mondal N, Pal TK, Ghosal SK - Development and validation of RP-HPLC method to determine letrozole in different pharmaceutical formulations and its application to studies of drug release from nanoparticles. Acta Pol Pharm. 2009;66:11-17.
23. Shao R, Yu LY, Lou HG, Ruan ZR, Jiang B, Chen JL - Development and validation of a rapid LC-MS/MS method to quantify letrozole in human plasma and its application to therapeutic drug monitoring. Biomed Chromatogr. 2016;30:632-637.
24. Vanol PG, Singhal, P, Shah PA, Shah JV, Shrivastav PS, Sanyal M - SPE-UPLC-MS/MS assay for determination of letrozole in human plasma and its application to bioequivalence study in healthy postmenopausal Indian women. JPA. 2016;6:276-281.
25. Mondal N, Pal TK, Ghosal SK - Development and Validation of a Spectrophotometric Method for Estimation of Letrozole in Bulk and Pharmaceutical Formulation, Pharmazie. 2007;62:597-598
26. Acharjya SK, Mallick P, Panda P, Kumar KR, Annapurna MM - Spectrophotometric methods for the determination of letrozole in bulk and pharmaceutical dosage forms. J Adv Pharm Tech Res. 2010;1:348-353.
27. Patil SM, Galatage ST, Choudhary AU - Development of UV spectrophotometric method for estimation of letrozole in pure and pharmaceutical dosage form, Indo American Journal of Pharmaceutical Research. 2013;3:5541-5548.
28. UV and IR Spectra, Pharmaceutical Substances (UV and IR) and Pharmaceutical and Cosmetic Excipients (IR), in Dibbern HW, Müller RM, Wirbitzki E(eds): Editio Cantor Verlag, Aulendor, 2002, 873.
29. Mayer BX - How to increase precision in capillary electrophoresis. J Chromatogr A. 2001;907:21-37.
30. Letrozole - DrugBank (https://www.drugbank.ca/drugs/DB01006 Accessed 14 May 2017)
31. MarvinSketch - ChemAxon (https://www.chemaxon.com/products/marvin/marvinsketch/)
32. Orlandini S, Gotti R, Furlanetto S - Multivariate optimization of capillary electrophoresis methods: a critical review. J Pharm Biomed Anal. 2014;87:290-307.
33. Varenne A, Descroix S - Recent strategies to improve resolution in capillary electrophoresis—A review, Anal Chim Acta. 2008;628:9–23.
34. Rusu A, Hancu G, Völgyi G, Tóth G, Noszál B, Gyéresi A - Separation and determination of quinolone antibacterials by capillary electrophoresis. J Chromatogr Sci. 2014;52:919-925.

DE GRUYTER OPEN

Acta Medica Marisiensis 2017;63(2):87-90 DOI: 10.1515/amma-2017-0010

RESEARCH ARTICLE

Short Period Storage Impact on Bioactive Constituents from Bilberries and Blueberries

Ruxandra Emilia Ștefănescu[1]*, Sigrid Eșianu[2], Eszter Laczkó-Zöld[2], Anca Mare[3], Bianca Tudor[3], Maria Titica Dogaru[4]

1 University of Medicine and Pharmacy Tîrgu Mureș
2 University of Medicine and Pharmacy Tîrgu Mureș, Faculty of Pharmacy, Department of Pharmacognosy and Phytotherapy
3 University of Medicine and Pharmacy Tîrgu Mureș, Faculty of Medicine, Department of Microbiology, Virology, and Parasitology
4 University of Medicine and Pharmacy Tîrgu Mureș, Faculty of Pharmacy, Department of Pharmacology and Clinical Pharmacy

Objectives: The aim of this study was to assess storage effects on anthocyanin and total polyphenol content in different bilberry and blueberry extracts and to evaluate the antioxidant and antibacterial activity of these extracts. **Materials and methods:** Total phenolic content, total monomeric anthocyanin content and antioxidant activity were determined in the first month and after three months storage of berries at either -20 °C or -50 °C. Two different solvents were used (methanol and 50% ethanol). Antibacterial activity was determined for the 3 months stored fruits using a microdilution method and was expressed as the minimum inhibitory concentration. **Results**: There were significant differences between the concentration in the first month and after three months storage in both types of fruit extracts. Regarding the extracting solvent, we noticed that total phenols were better extracted with 50% ethanol, while the total monomeric anthocyanin content was higher in the methanolic extracts. No significant or slightly significant differences were observed between the fruits stored at -20 °C or -50 °C. Ethanolic extracts showed the highest scavenging activity. Good antibacterial activity was observed on gram-positive bacteria. **Conclusions**: Storage conditions are an important factor that can influence chemical composition of fruits. Although freezing is a good option for preservation, our study showed a high decrease in the concentration of total phenols and anthocyanins after only three months. The fruits have shown a high antioxidant activity and a good antibacterial effect. Further studies are needed for better understanding the changes that can appear during the storage.

Keywords: blueberry, bilberry, storage conditions, antioxidants, antibacterial

Received 3 January 2017 / Accepted 13 April 2017

1. Introduction

Vaccinium berries are widely consumed worldwide because of their nutritional properties. As main components they contain polyphenolic compunds, among them polyphenolcarboxilic acids, flavonoids and anthocyanins, mainly in their glycosylated form. These berries have been studied for the last ten years because of their complex composition and multiple health-beneficial effects [1]. Researches conducted in different geographical areas have revealed great differences among berries collected from various areas, and also great differences have been noticed among different cultivars [2, 3]. This is why it is quite important to evaluate each regional fruit before carrying out any other determination. Bilberries are European wild berries collected from *Vaccinium myrtillus* L., they contain a bigger amount of anthocyanins comparative with the cultivated species. Blueberries are the fruits of a cultivated species, *Vaccinium corymbosum*, also called highbush blueberry. Researches conducted on the effects of storage conditions on active constituents from fruits are still unclear. There are many studies conducted on the storage conditions of different types of processed berries, but only few of them evaluated the changes during freezing of unprocessed berries [4, 5].

The aim of this study is to assess whether the freezing temperature influences the composition and the free radical scavenging activity of two types of fruits from *Vaccinium* species collected from Mureș county area, comparative with the composition and antioxidant activity determined on the freshly harvested fruits. Antibacterial activity on six bacterial strains was determined for the stored fruits.

2. Materials and methods

2.1. Plant material

Bilberries (*Vaccinium myrtillus* L.) were collected from their natural habitat in Lunca Bradului area, Mureș county, Romania. Blueberries (*Vaccinium corymbosum* L.) were collected from a culture near Trei Sate village area, Mureș county, Romania. The fruits were collected at their commercial harvest maturity according to ground color, in July 2016. After harvesting, the fruits from each species, were divided in three samples: the first sample was immediately prepared for analysis (VC 1; VM 1), the second and the third were stored for three months at either -20 °C (VC 3; VM 3), or at -50 °C (VCF 3; VMF 3).

2.2. Chemicals

Gallic acid, Folin-Ciocâlteu reagent, 1,1-Diphenyl-2-picrylhydrazyl (DPPH) and 2,2'-Azinobis [3-ethylbenzothiazoline-6-sulfonic acid] (ABTS) tablets were purchased from Sigma-Aldrich (Sigma-Aldrich Chemie GmbH,

* Correspondence to: Ruxandra Emilia Stefanescu
E-mail: ruxandra.stefanescu@umftgm.ro

Steinheim, Germany). Other chemicals used were of analytical grade.

2.3. Extraction procedure

Berries were crushed extemporaneously, and the crushed fruits were mixed with quartz sand (1:1 w/w) at room temperature for 5 minutes. This procedure was based on the sea sand disruption method (SSDM) [6]. The mixture was extracted with either methanol (MeOH) or 50% ethanol (EtOH) with a solid to solvent ratio of 1:10 (w/v, on a fresh weight basis). The extractions were carried out on an ultrasonic water bath at 40°C for 30 minutes, after which they were vortexed at high speed for 10 minutes and the extract was separated from the residue by filtration through a 0.45 μm filter, giving a number of 12 samples as they appear in Table I.

2.4. Phytochemical analysis

2.4.1 Total phenolic content

The total phenolic content (TPC) of the extracts has been measured spectrophotometrically according to a previously described protocol, using Folin-Ciocalteu reagent and gallic acid as reference. All samples were analyzed in three replicates. The results were expressed as mg gallic acid equivalents / 100 g fresh weight (R = 0,99714) [7,8].

2.4.2. Total monomeric anthocyanin content

Total monomeric anthocyanins (TMAC) were determined using the pH-differential method [9]. The extracts were diluted with 0.025 M potassium chloride (adjusted with HCl to pH 1.0) and 0.4 M sodium acetate (pH 4.5) and the absorbance was measured at 520 and 700 nm. The absorbance values were calculated as follows: $A = (A_{520} - A_{700})_{pH\ 1} - (A_{520} - A_{700})_{pH\ 4,5}$. TMAC was calculated with the formula:

$$TMAC = \frac{A \times MW \times DF \times 1000}{\varepsilon \times 1}$$

The results were expressed as mg cyanidin-3-glucoside equivalents / 100 g fresh weight, using the molecular weight (MW) of 449.2 for cyandin 3-glucoside, the dilution factor (DF), molar extinction coefficient (ε) of 26,900 L x mol^{-1} x cm^{-1} and the pathlength (1, in this case). All samples were analyzed in three replicates.

Table I. List of tested samples

	Sample	Solvent	Abbreviation
1.	Blueberries freshly harvested	50% Ethanol	VCE1
2.	Blueberries freshly harvested	Methanol	VCM1
3.	Blueberries stored at -20 °C	50% Ethanol	VCE3
4.	Blueberries stored at -20 °C	Methanol	VCM3
5.	Blueberries stored at -50 °C	50% Ethanol	VCEF3
6.	Blueberries stored at -50 °C	Methanol	VCMF3
7.	Bilberries freshly harvested	50% Ethanol	VME1
8.	Bilberries freshly harvested	Methanol	VMM1
9.	Bilberries stored at -20 °C	50% Ethanol	VME3
10.	Bilberries stored at -20 °C	Methanol	VMM3
11.	Bilberries stored at -50 °C	50% Ethanol	VMEF3
12.	Bilberries stored at -50 °C	Methanol	VMMF3

2.5. Antioxidant activity

2.5.1. DPPH Radical Scavenging Activity

The antiradical capacity of each sample was tested using a series of dilutions. Briefly, an aliquot of 150 μL of sample solution at different concentrations was mixed with 3000 μL DPPH solution (0,1 mmol/L in methanol) [10]. The reaction mixture was incubated for 30 minutes in the dark at room temperature and the absorbance was measured at 517 nm. The percentage of DPPH inhibition at different concentrations of each sample was plotted and the concentration of extract required to inhibit oxidation by 50% (IC_{50}) was obtained by interpolation. Results were expressed as mg/ml and all samples were analyzed in three replicates. Ascorbic acid was used as positive control.

2.5.2. Scavenging effect on ABTS• radical

The scavenging effect of all extracts against the radical cation $ABTS^{\bullet+}$ was determined according to a procedure described previously [11, 12]. Briefly, a stock solution of 2,45 mM potassium persulfate was prepared as well as an ABTS stock solution of 7 mM, which was left to react at room temperature in the dark for 12 hours. The ABTS solution was diluted with methanol to the appropriate absorbance. A volume of 100 μL for different concentrations of samples was added to 2500 μL diluted ABTS solution and then, the mixture was allowed to react in the dark at room temperature for 30 minutes and the absorbance was read at 734 nm. The controls contained the extraction solvent instead of the test sample. The percentage of ABTS inhibition at different concentrations of each sample was plotted and the concentration of extract required to inhibit oxidation by 50% (IC_{50}) was obtained by interpolation. Results were expressed as mg/ml and all samples were analyzed in three replicates.

2.6. Antibacterial activity

For this determination, ethanolic extracts of the fruits stored for three months, were used after a prior evaporation of the ethanol, at 40°C using an Ika rotary evaporator RV 05-ST with a vacuum controller, giving a final concentration of 200 mg fresh fruits/mL. The antibacterial activity of the extracts was tested on six bacterial strains: *Staphylococcus aureus* ATCC 25923, MRSA ATCC 43300, *Enterococcus faecalis* ATCC 29212, *Escherichia coli* ATCC 25922, *Klebsiella pneumoniae* ATCC 13883, *Pseudomonas aeruginosa* ATCC 27853.

The antibacterial activity was determined by a microdilution method and the minimum inhibitory concentration (MIC) was interpreted as the last dilution without bacterial growth.

2.7. Statistical analysis

All the data were statistically evaluated and the significance of various treatments was calculated. The results were expressed as mean ± standard deviation (SD) and comparison between the groups was made by Analysis of variance (one-way ANOVA), followed by a Tukey-Kramer test, using GraphPad Prism (version 7.0b, 2016). Pearson's linear correlation was calculated using StatPlus:mac (statistical analysis program for Mac OS®, Version v6 AnalystSoft Inc.).

3. Results

The results of total phenolic content, total monomeric anthocyanin, DPPH free radical scavenging activity and ABTS scavenging activity are presented in Table II and Table III.

The highest total phenolic content was found in 50% ethanolic extracts for both bilberries and blueberries, but the difference between 50% EtOH and MeOH is not statistically significant. The highest total monomeric anthocyanin content was found in the methanolic extracts.

All extracts have shown a high scavenging activity, which decreases in the following order: VME1 > VMM1 > VME3 > VMEF3 > VMMF3 > VMM3 > VCE1 > VCM1 > VCE3; VCEF3 > VCM3 > VCMF3.

The susceptibility of bacteria against tested samples are presented in Table IV. Of the tested gram-negative microorganisms, bilberries were active on *Escherichia coli* and *Klebsiella pneumoniae*, while blueberries were active only on *Klebsiella pneumoniae*. *Pseudomonas aeruginosa* was not susceptible to any of the samples at the given concentration. Both berries had an inhibitory effect on all tested gram-positive microorganisms.

4. Discussion

As it is known, bilberries contain higher amounts of phenolic compounds than blueberries. Regarding the extracting solvent there can be observed that in both types of fruits there is no or just a small statistically significant difference in TPC between methanolic and ethanolic extracts, but there are significant differences in methanolic and ethanolic extracts regarding total monomeric anthocyanin content, which leads us to the conclusion that anthocyanins are better extracted with methanol. This is a long debate between different studies, some being in accordance with our results. This could be explained by the different chemical profile and concentration of phytoconstituents between fruits collected from different area or from different cultivars. Compared with freshly harvested fruits, the fruits that have been stored for three months have lost a great percent of compounds. Similar results have been reported by Giovanelli G. et al [13]. In case of further use of the extracts for animal or human studies, ethanolic extracts should be used due to the high toxicity of methanol.

Our results (determined per 100 g fresh weight) show a higher TP and TA content than in other reported data

Table IV. Assessment of MICs for bilberry and blueberry ethanolic extracts

Microorganisms	MIC (mg/ml)	
	Bilberry	Blueberry
Gram-positive		
Staphylococcus aureus	25	25
MRSA	25	50
Enterococcus faecalis	25	50
Gram-negative		
Escherichia coli	100	-
Klebsiella pneumoniae	50	100
Pseudomonas aeruginosa	-	-

Table II. Bioactive compounds and antioxidant activity of Vaccinium corymbosum

Sample	TPC mg GAE / 100 g FW	TMAC mg C3GE / 100g FW	DPPH IC50	ABTS IC50
VC-E1	427.32 ± 14.4^{a}	262.08 ± 14.29^{a}	1.47±0.12	0.139±0.002^{b}
VC-M1	392.73 ± 8.7^{a}	323.12 ± 11.58^{b}	1.85±0.01^{a}	0.207±0.003^{acd}
VC-E3	311.94 ± 4.8^{b}	170.46 ± 2.75^{c}	1.91±0.04^{a}	0.172±0.021^{abc}
VC-M3	251.26 ± 0.5^{c}	267.83 ± 13.2^{a}	1.99±0.09^{a}	0.216±0.02^{ad}
VC-EF3	343.27 ± 14.7^{b}	172.43 ± 13.77^{c}	1.91±0.06^{a}	0.153±0.008^{bc}
VC-MF3	306.27 ± 14.^{b}	226.66 ± 10.37^{a}	2.05±0.1^{a}	0.236±0.014^{d}

Means sharing the same superscript are not significantly different from each other (Tukey's HSD, P<0.05).

Table III. Bioactive compounds and antioxidant activity of Vaccinium myrtillus

Sample	TPC mg GAE / 100 g FW	TMAC mg C3GE / 100g FW	DPPH IC50	ABTS IC50
VM-E1	636.63 ± 7.45^{a}	520.81 ± 9.57^{a}	0.175±0.03^{a}	0.106±0.004^{a}
VM-M1	534.34 ± 3.17^{b}	576.86 ± 65.26^{a}	0.33±0.03^{a}	0.129±0.005^{ac}
VM-E3	484.87 ± 23.6^{c}	277.86 ± 26.73^{b}	1.03±0.08^{b}	0.138±0.003^{bc}
VM-M3	443.53 ± 13.7^{cd}	396.43 ± 8.94^{c}	1.19±0.01^{b}	0.161±0.002^{bd}
VM-EF3	465.98 ± 3.92^{cd}	293.37 ± 6.13^{b}	1.09±0.12^{b}	0.134±0.003^{c}
VM-MF3	426.32 ± 6.98^{d}	367.18 ± 10.89^{bc}	1.18±0.09^{b}	0.166±0.013^{d}

Means sharing the same superscript are not significantly different from each other (Tukey's HSD, P<0.05).

from Romanian bilberries [14]. The high difference between our results and the other results reported could be explained by the extraction using quartz sand. The extraction method using quartz sand also known as sea sand disruption method (SSDM) is a simple and cheap process, which due to the abrasive character of the sand, facilitates the extraction [15].

Other factors that could have influenced the chemical content are the storage period and the time of harvest. Our own results indicate that the content may decrease by almost 27% for TP and by 46% for TMA in only three months. It has been previously reported that increased maturity of fruits influences their chemical profile and their antioxidant activity [16]. Several researches concluded that the higher the content of anthocyanins in fruits, the higher the stability of the extract [17]. In the case of frozen fruits we recorded the higher lost of anthocyanins in the fruits with the highest content. The difference in the stability between extracts and unprocessed fruits could be explained by the antioxidant activity of the total polyphenols from the extract.

The concentration determined in our study for IC_{50} is lower than in other studies [18], which shows a higher antioxidant activity even in the fruits stored for 3 months. Using Pearson's correlation we noticed a highly negative correlation between DPPH IC_{50} and TPC ($r = -0,8247$, $p < 0,05$) in fruit extracts of *Vaccinium corymbosum*. For *Vaccinium myrtillus* fruit extracts, DPPH IC_{50} is highly correlated with TPC ($r = -0,9149$, $p < 0,05$) and TMAC ($r = -0,868$, $p < 0,05$) while for the ABTS IC_{50} the correlation coefficient shows a highly negative correlation with TPC ($r = -0,9474$, $p < 0,05$). The antioxidant activity of plant extracts containing phenolic compounds is attributed to their ability to donate hydrogen atoms or electrons, and therefore scavenging free radicals.

Regarding the microbiological study, a good antibacterial activity was observed on Gram-positive bacteria, with a higher activity for bilberry extracts, as it was expected. Previous studies have shown that phenolic compounds posses antibacterial activity and it is believed that these compounds suppress virulence factors of bacterial pathogens or have a direct antimicrobial effect [19, 20]. This antibacterial activity needs to be further tested with more concentrated extracts for a better evaluation, and also the bactericidal and bacteriostatic effect should be assessed.

5. Conclusions

This study shows important data regarding the impact of short time storage conditions on active constituents from *Vaccinium* berries. Our results demonstrated that freezing is not sufficient for anthocyanin preservation; other treatments could be needed to avoid degradation. Regarding the overall results we may conclude that both types of berries collected from our area contain a high amount of polyphenolic compounds, and, although the level of main active constituents decreased during the storage period, we could record a high antioxidant activity, and an antibacterial activity. These are important findings for the future use of our local fruits as nutraceuticals in prevention and treatment of different illnesses.

Conflict of interest

None to declare

References

1 Norberto S, Silva S, Meireles M, Faria A, Pintado M, Calhau C - Blueberry anthocyanins in health promotion: A metabolic overview. J Funct Foods. 2013;5(4):1518–1528.

2 Mikulic-Petkovsek M, Schmitzer V, Slatnar A, Stampar F, Veberic R - A comparison of fruit quality parameters of wild bilberry (Vaccinium myrtillus L.) growing at different locations. J Sci Food Agric. 2015;95:776–785.

3 Makus DJ, Morris JR - A Comparison of Fruit of Highbush and Rabbiteye Blueberry Cultivars. J Food Qual. 1993;16:417–428.

4 Dinkova R, Heffels P, Shikov V, Weber F, Schieber A, Mihalev K - Effect of enzyme-assisted extraction on the chilled storage stability of bilberry (Vaccinium myrtillus L.) anthocyanins in skin extracts and freshly pressed juices. Food Res Int. 2014;65:35–41.

5 Syamaladevi RM, Andrews PK, Davies NM, Walters T, Sablani SS - Storage effects on anthocyanins, phenolics and antioxidant activity of thermally processed conventional and organic blueberries. J Sci Food Agric. 2012;92(4):916–924.

6 Manhita AC, Teixeira DM, da Costa CT - Application of sample disruption methods in the extraction of anthocyanins from solid or semi-solid vegetable samples. J Chromatogr A. 2006;1129(1):14–20.

7 Singleton VL, Orthofer R, Lamuela-Raventos RM - Analysis of total phenols and other oxidation substrates and antioxidants by means of folin-ciocalteu reagent. Methods Enzymol. 1998;299(1974):152–178.

8 Waterhouse AL - Determination of Total Phenolics. Curr Protoc Food Anal Chem. 2002 I1.1.1.-I1.1.8,.

9 Giusti E, Wrolstad R - Characterization and measurement of anthocyanins by UV- Visible spectroscopy. Curr Protoc Food Anal Chem. 2005:19–31.

10 Bondet V, Brand-Williams W, Berset C - Kinetics and Mechanisms of Antioxidant Activity using the DPPH.Free Radical Method. Food Sci Technol. 1997;30(6):609–615.

11 Re R, Pellegrini N, Proteggente A, Pannala A, Yang M, Rice-Evans C - Antioxidant Activity Applying an Improved Abts Radical Cation Decolorization Assay. Free Radic Biol Med. 1999;26(9):1231–1237.

12 Kim DO, Chun OK, Kim YJ, Moon HY, Lee CY - Quantification of Polyphenolics and Their Antioxidant Capacity in Fresh Plums. J Agric Food Chem. 2003;51(22):6509–6515.

13 Giovanelli G, Buratti S - Comparison of polyphenolic composition and antioxidant activity of wild Italian blueberries and some cultivated varieties. Food Chem. 2009;112(4):903–908.

14 Oancea S, Stoia M, Coman D - Effects of extraction conditions on bioactive anthocyanin content of Vaccinium corymbosum in the perspective of food applications. Procedia Eng. 2012;42:489–495.

15 Wianowska D - Application of sea sand disruption method for HPLC determination of quercetin in plants. J Liq Chromatogr Relat Technol, 2015;38(10):1037–1043.

16 Prior RL, Cao G, Martin A et al - Antioxidant capacity as influenced by total phenolic and anthocyanin content, maturity, and variety of Vaccinium Species. J Agric Food Chem. 1998;46:2686–2693.

17 Cevallos-Casals BA, Cisneros-Zevallos L - Stability of anthocyanin-based aqueous extracts of Andean purple corn and red-fleshed sweet potato compared to synthetic and natural colorants. Food Chem. 2004;86(1):69–77.

18 Pranprawit A, Heyes JA, Molan AL, Kruger MC - Antioxidant Activity and Inhibitory Potential of Blueberry Extracts Against Key Enzymes Relevant for Hyperglycemia. J Food Biochem. 2015;39:109–118.

19 Daglia M - Polyphenols as antimicrobial agents. Curr Opin Biotechnol. 2012;23:174–181.

20 Nohynek LJ, Alakomi HL, Kähkönen MP et al - Berry Phenolics: Antimicrobial Properties and Mechanisms of Action Against Severe Human Pathogens. Nutr Cancer. 2006;54:18–32.

DE GRUYTER OPEN

Acta Medica Marisiensis 2017;63(2):91-96 DOI: 10.1515/amma-2017-0020

RESEARCH ARTICLE

Flow Cytometry Assessment of Bacterial and Yeast Induced Oxidative Burst in Peripheral Blood Phagocytes

Floredana-Laura Şular[1,2*], Minodora Dobreanu[1,2]

1 Discipline of Laboratory Medicine, University of Medicine and Pharmacy of Tîrgu Mureş, Romania
2 Central Laboratory, Emergency Clinical County Hospital of Tîrgu Mureş, Romania

Objective: The aim of this study was to verify in our laboratory conditions the performance criteria of a commercial kit (Phagoburst™, Glycotope Biotechnology) as described by the producers. We have also partially altered the use of the available kit by introducing a non-opsonized *Candida albicans* stimulus, in addition to the opsonized *Escherichia coli* stimulus provided by the manufacturer. **Material and methods**: The peripheral blood samples of 6 clinically healthy adults were tested in triplicate according to the manufacturer recommendations. The intra-assay imprecision as well as the ranges of neutrophil and monocyte burst activation triggered by various stimuli were assessed. **Results**: The activation range of granulocytes and monocytes was similar to the one described by the producer in the presence of *E. coli* (granulocytes: 78.45-99.43% versus 99.6-99.95%, average %CV of 1.53% versus 0.1%, monocytes: 54.63-92.33% versus 81.80-96.67, average %CV 6.92% versus 1.1%). The leukocyte range of activation in the presence of non-opsonized *C. albicans* was comparable to the one triggered by the fMLP (N-formyl-methionyl-leucyl-phenylalanine) stimulus. **Conclusion**: The intra-assay precision obtained in our laboratory conditions, as well as the ranges of activated leukocytes, are comparable to the ones described by the producer when using *E. coli* as a stimulus. The present study shows that introducing an extra fungal stimulus for burst oxidation assessment could provide additional information regarding the non-specific cellular immune response, particularly in patients at risk for candidemia.

Keywords: flow cytometry, method verification, intra-assay precision, reactive oxygen species, fungal bloodstream infection

Received 23 April 2017 / Accepted 4 June 2017

Introduction

The peripheral blood phagocytes (PBP) have long been acknowledged as key factors in bacterial and fungal infections. As first line of defense, they phagocyte and kill microorganisms through a combination of mechanisms that include the production of reactive oxygen species (ROS) [1].

Along the years, flow cytometry methods have been developed in order to quantify the production of ROS using bacteria as stimulus [2,3]. Different authors have described methods for burst oxidation assessment in peripheral blood mononuclear cells (PBMC) using isolated leukocytes and different strains of *Candida* as stimuli as well as different incubation periods [4-8]. Recent years have seen the development of several commercial kits that use whole blood, not isolated PBMC as many methods used before, and unlabeled opsonized *Escherichia coli* as stimulus for PBP activation besides other chemical stimulants [9]. Up to the present moment none of the available commercial kits used fungi as stimulus.

The aim of the present study was to verify in our laboratory conditions the performance criteria of the commercial kit Phagoburst ™ (Glycotope Biotechnology) as recommended by the producers. We have also partially altered the use of the available kit by introducing a non-opsonized *Candida albicans* suspension for testing as stimulus with the purpose to assess the cellular immune response in fungal bloodstream infections.

* Correspondence to: Floredana-Laura Şular
E-mail: floredana.sular@gmail.com

Materials and methods

We conducted a study that aimed to verify the performance parameters of the *Phagoburst ™ (Glycotope, Biotechnology)* commercial kit in our laboratory conditions and to validate as well the use of a new stimulus – a non-opsonized *C. albicans* suspension in order to verify the PBP innate immune response to fungal stimuli.

The study was conducted according to the World Medical Association Declaration of Helsinky and was approved by the Ethics Committee of the Emergency Clinical County Hospital of Tîrgu Mureş, No.19204/29th of September 2014 as well as the Ethics Committee of the University of Medicine and Pharmacy of Tîrgu Mureş, No.53/22nd of April 2015. Informed consent was given by each enrolled adult.

Blood samples

Whole venous blood specimens were collected from 6 healthy adults on BD sodium heparin tubes as recommended by the producers of the *Phagoburst ™* (Glycotope Biotechnology) commercial kit. The volunteers were chosen by absence of infectious history and clinical signs of infection. All samples were tested in triplicate within one hour after collection, being kept meanwhile on a covered ice bath.

Assay for the evaluation of cell burst activity

Phagoburst ™ was created to investigate the altered oxidative burst activity present in various pathologies and to evaluate the effects of drugs. It allows quantitative assess-

ment of PBP oxidative burst. The kit contains an unlabeled opsonized *E. coli* bacteria as particulate stimulus, the protein kinase C ligand phorbol 12-myristate 13-acetate (PMA) as high stimulus, the chemotactic peptide N-formyl-MetLeuPhe (fMLP) as low physiological stimulus, dihydrorhodamine 123 (DHR 123) as a fluorogenic substrate and necessary reagents.

In order to quantify the production of ROS by PBP that could be triggered by a fungal pathogen in neonates which are known to have low opsonin concentration and degree of activation [10], we introduced an extra fungal stimulus for testing in the form of a *C. albicans* yeast suspension. The reference strain *C. albicans ATCC 10321* was cultured aerobically on Sabouraud chloramphenicol agar for 18 hours at 35°C. An 0.5 optical density inoculum of *C. albicans* (approximate cell concentration of 1-5 x 10^6 colony forming units/mL) was prepared for each testing round by Using Vitek2 Densichek densitometer (Biomerieux, France). The yeast suspension was not exposed to any supplementary opsonins then those present in the 100 µL whole blood used for testing. The yeast cells underwent no inactivation prior to exposure to whole blood. May Grunwald Giemsa stained blood smears performed after a 10 minutes period of incubation of whole blood with the yeast stimulus showed no budding, pseudohyphae or hyphal growth.

Heparinized whole blood (100 µL) within 1 hour after sampling was incubated with 20 µl of each of the above mentioned stimuli for 10 minutes at 37°C on a water bath. The ROS produced during the oxidative burst by the phagocytes was monitored by oxidation of 20 µl DHR 123 which served as an oxidative fluorogenic substrate. A volume of 2 ml lysing solution which removed the erythrocytes and resulted in a partial fixation of the leukocytes was added to stop the burst oxidation reaction. After centrifugation and one washing step, 200 µL DNA staining solution was added to exclude aggregation artifacts of bacteria, fungi or cells. The DNA staining required 10 minutes incubation at 0°C, protected from light. Samples were thus ready for FACS analysis that was performed within 30 minutes following DNA staining.

Flow cytometry analysis

Each blood sample was tested in triplicate. Cells were analyzed by flow cytometry using a 488 nm argon-ion excitation laser. As recommended by the producer, during data acquisition a "live gate" was set in the red fluorescence histogram on the events that had at least the same DNA content as a human diploid cell with the purpose of precluding bacteria or fungi aggregates that had the same scatter light properties as the leukocytes from analysis. An average number of 15000 leukocytes per sample were collected.

The percentage of cells that produced ROS (recruitment) as well as their mean fluorescence intensity (MFI) (activity, amount of cleaved substrate) was quantified. The relevant leukocyte cluster was gated in the software program in the scatter diagram (linear FSC vs linear SSC) and its rhodamine 123 green fluorescence was collected in the FL1 channel (standard FITC filter set) and analyzed. A negative control sample without any stimulus was always run as a negative background control to set a marker for fluorescence (FL1) so that less than 3% of the events were positive. The percentage of activated cells in the test samples was then set by counting the number of events above this threshold. The mean fluorescence correlates with oxidation quantity per individual leukocyte.

Data collection and analysis

Results for every round of tests of each replicate of the six samples were collected. For data entry and analysis Microsoft Excel® (Microsoft Corporation, Redmond, WA, USA) and its tools were used. The coefficient of variance of each sample, as well as the minimum-maximum range of the percentage of activated cells and their MFI was assessed for each of the used stimuli.

Results

Figure 1 shows the "live gate" (viability assessment) set on leukocyte DNA which is meant to distinguish between those events which have at least the same DNA content as a human diploid cell thus excluding aggregates of bacteria and fungi having the same scatter light properties as the leukocytes. Leukocyte viability decreases as burst oxidation intensity triggered by the used stimuli increases: viability of the negative control tube (97.87%) is followed by opsonized *E. coli* as particulate stimulus (70.43%) and then by the protein kinase C ligand PMA as high stimulus (45.93%).

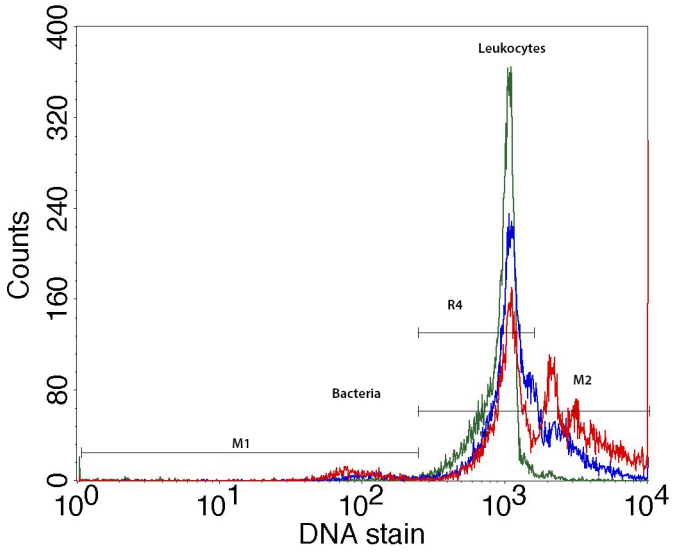

Fig. 1. Viability of assessed leukocyte population of the control sample (green), compared to the cell viability of the samples that were exposed to *E. coli* (blue) and PMA (red). A "live" gate (M2) was set on those events that have at least the same DNA content as a human diploid cell with the purpose of precluding from analysis bacteria or fungi (M1) which had the same scatter light properties as the leukocytes.

Figure 2 row 1 presents typical FSC/SSC dot plot sets of one of the tested subjects. The gate is set on granulocytes and monocytes stimulated with *E. coli* (1A), fMLP (1B), PMA (1C) and *C. albicans* (1D).

Figure 2 row 2 displays the degree of granulocyte (R2) and monocyte (R3) activation (recruitment) and production of ROS when using the same stimuli as mentioned above. *E. coli* (2A) and PMA (2C) trigger a similar intense PBP activation, while the burst activation triggered by the unopsonized *C. albicans* (2D) is similar to the one generated by the presence of low fMLP stimulus (2B). The burst activity (amount of DHR 123 cleaved substrate) of the two studied leukocyte populations was also quantified as mean fluorescence intensity (MFI) for each stimulus as depicted in *Figure 2* 3A, 3B, 3C, 3D for granulocytes, and *Figure 2* 4A, 4B, 4C, 4D for monocytes.

Table I shows the activation range of granulocytes and monocytes as percentages and MFI when verifying in our

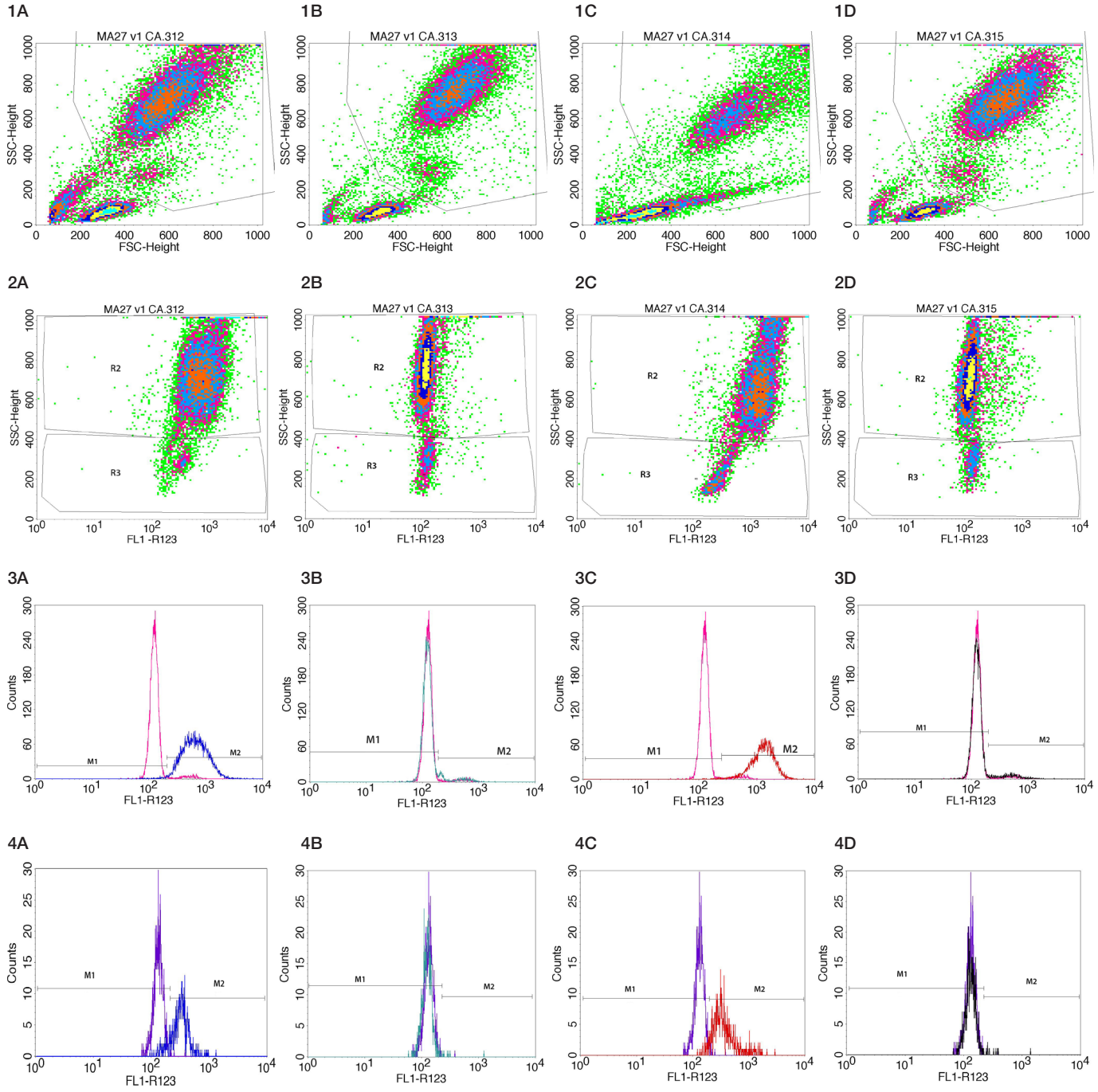

Fig. 2. Flow cytometry analysis results. Row 1 displays the typical FSC/SSC dot plots when adult PBP cells are stimulated with *E. coli* (1A), fMLP (1B), PMA (1C) and *C. albicans* (1D) (gate set on granulocyte and monocyte populations). Row 2 displays the dot plot lin SSC/log FL1-R123 of test samples stimulated with *E. coli* (2A), fMLP (2B), PMA (2C) and *C. albicans* (2D). Row 3 shows the typical FL1-DHR123 histogram that depicts granulocyte activation of the control sample (pink) compared to activation triggered by *E. coli* (blue) (3A), fMLP (green)(3B), PMA (red)(3C) and *C. albicans* (black) (3D). Row 4 illustrates the typical FL1-DHR123 histogram that shows monocyte activation of the control sample (violet) compared to burst activation triggered by *E. coli* (blue) (4A), fMLP (green)(4B), PMA (red)(4C) and *C. albicans* (black) (4D).

laboratory the intra-assay precision, as well as the average CV that resulted after testing in triplicate each of the 6 whole blood samples as recommended by the producers.

The activation range of granulocytes and monocytes, though having a broader lower limit in our laboratory conditions, was similar to the one described by the producer in the presence of *E. coli* (granulocytes: 78.45-99.43% versus 99.6-99.95%, average %CV of 1.53% versus 0.1%, monocytes: 54.63-92.33% versus 81.80-96.67, average %CV 6.92% versus 1.1%).

We obtained similar ranges of activation as the producers did for fMLP and PMA in the case of granulocytes, while for monocytes data for these stimuli were not provided by the producer.

When assessing the PBP burst oxidation triggered by *C. albicans*, our data revealed acceptable variation of mean %CV for granulocytes (6.46% for oxidizing cells and 7.54% for MFI). Due to low monocytes activation, during the 20 minutes incubation time, the resulting average %CV showed higher but acceptable values for validation (8.80 % for oxidizing cells and 11.61% for MFI).

Discussion

The *Phagoburst ™ (Glycotope Biotechnology)* kit that we used for our study is already validated for in vitro diagnostic testing with the above mentioned stimuli. According to professional standards, it is recommended that the performance criteria of each test to be verified in the user's own laboratory conditions. We performed this verification and then we tried to validate a new fungal stimulus by quantifying the intra-assay imprecision and the ranges of neutrophil and monocyte burst activation triggered by various stimuli.

According to the Practice guidelines from the ICSH and ICCS-part V- Assay performance criteria [11] recommended for validation of cell-based fluorescence assays, for the quantification of the intra assay imprecision, we used the same assay matrix (whole blood) originating from 6 patients (a minimum of 5 samples being required) tested in triplicate in a single analytical run [12]. We used samples only from healthy patients due to the laboratory's inability to access samples from patients with altered oxidative burst activity such as chronic granulomatous disease. We made this choice in order to be also able to compare our laboratory's results to the ones provided by the producer of the commercial kit which tested only healthy subjects.

The mean and %CV for each sample tested in triplicate was calculated. As recommended [12], percent CV (%CV), rather than standard deviation (SD) was used as acceptance criteria due to the fact that %CV normalizes variations at lower levels of event detection as it happened in our case of monocyte activation when using the low stimuli fMLP and *C. albicans*.

The level of acceptable imprecision in flow cytometry techniques for an reportable result depends upon the frequency of the population and the total number of events acquired [13]. As stated by the guidelines [11], a desirable target for assay imprecision is a CV of less than 10%, while for less abundant populations (frequency at 1:1000 (0.1%)) a CV of less than 20% is acceptable [14].

Table I. Verification performance parameters of the Phagoburst™ Glycotope Biotechnology commercial kit

Cell Type	Stimulus		Oxidizing cells (%)		GeoMean FL1 (MFI)	
			Producer	Own Laboratory	Producer	Own Laboratory
Granulocytes	*E. coli*	(min-max)	99.6-99.95	78.45-99.43	154.5-395.75	400-735
		mean		91.96		538
		average CV	0.1	1.53	4.8%	6.84%
	fMLP	(min-max)	1-10	1.53-12.95		320-496
		Mean		6.35	NA	387
		average CV	NA	18.61		4.08%
	PMA	(min-max)	98-100	95.83-99.77	300-1000	907-1528
		Mean		98.57		1215
		average CV	NA	0.78	NA	6.21%
	C. albicans	(min-max)		2.18-8.80		371-519
		mean	NA	5.68	NA	458
		average CV		6.46		7.54
Monocytes	*E. coli*	(min-max)	81.80-96.67	54.63-92.33	49.60-88.65	278-349
		mean		69.18		307
		average CV	1.1	6.92	6.5%	5.57%
	fMLP	(min-max)		0.61-4.52		236-410
		mean	NA	2.14	NA	283
		average CV		56.59		18.23
	PMA	(min-max)		29.15-95.89		285-383
		mean	NA	70.89	NA	356
		average CV		7.57		4.41
	C. albicans	(min-max)		1.04-10.63		239-347
		mean	NA	3.6	NA	299
		average CV		8.80		11.61

CV= coefficient of variance (mean of the %CV), min=minimum value, max= maximum value, NA= non-available, MFI=mean fluorescence intensity

The results obtained in our own laboratory conditions for the intra-assay precision are acceptable according to the guidelines [11] when assessing the %CV of oxidizing granulocytes and monocytes in the presence of *E.coli*, PMA and C. *albicans*. Also the ranges of values for oxidizing leukocytes that we obtained when assessing imprecision were similar to the ones described by the producer though having an acceptable lower reference range.

We did get a high %CV for granulocyte and monocyte activation as well as a high %CV for monocyte MFI when fMLP was used as stimulus. This situation that can be easily explained by the fact that considering the very low degree of PBP activation, very small variations generated large %CVs. Nevertheless, a value for fMLP %CV hasn't been provided for comparison not even by the kit manufacturer. A borderline value of 11.61%, slightly above the acceptable criteria, was also obtained for the MFI in the case of *C. albicans*.

When examining the MFI, in our laboratory conditions and flow cytometer settings, the value ranges, thought proportional to the ones described by the producer, were higher. It is one of the producer's recommendations that laboratories should establish their own normal reference ranges using their own testing conditions.

In the experiment we conducted in healthy adults, the particulate opsonized stimulus *E. coli* generated a similar activation of the PBP as the high stimulus (PMA), though with larger lower ranges in our laboratory conditions. MFI in our experiment, as described by the producer, reached higher values when PMA was used in comparison to the opsonized particulate stimulus *E. coli*.

The burst activation generated by incubation with *C. albicans* was similar in granulocytes and slightly lower in monocytes than the one generated by the low stimulus (fMLP).

C. albicans can reside as a lifelong commensal on or within the human host for a long time. Still, literature describes a number of pathogenic mechanisms that render *C. albicans* virulent when alterations in the host environment occur [15]. One of these mechanisms is represented by the robust stress response *C. albicans* displays against the oxidative and nitrosative stresses of the phagocyte cells [16,17]. Studies show that *C. albicans* mutants that lack genes that encode regulators of stress response or detoxifying enzymes have an attenuated virulence [18]. The ability of *C. albicans* to produce antioxidant enzymes like catalase Cta1 as well as the intracellular and extracellular superoxide dismutases (Sods) to counteract the respiratory burst [17,19], represents a viable explanation of the low activation and ROS production by neutrophils and monocytes in our study. Previous studies have shown that Sod1 interacts with macrophages while Sod2 is required to resist neutrophil attack [19]. Sod4, Sod5 [20] and Sod6, along with the catalase Cta1 detoxify extracellular ROS produced by macrophages [21].

According to previous studies described by Mayer at al. [17], due to quorum sensing, a low yeast density (<10^7 cells/mL), as in our case (1-5 x 10^6 cells/mL), favours hyphal formation. Though we did not submit the *C. albicans* yeast cells to any inactivation process prior to whole blood exposure, the smears performed after 10 minutes of incubation at 37°C showed no budding, pseudohyphae or hyphal growth. Still, hyphae could have formed during the next 10 minutes of incubation with the DHR123 prior to burst oxidation assessment. Studies have shown that regardless of the fungal morphology, Sods are expressed: yeast cells express Sod4 while hyphal forms express Sod5. Neutrophils also induce the expression of Sod5 although they inhibit the yeast-to-hyphal formation in *C. albicans* [19,20].

Other studies have shown the enhanced capacity of the human neutrophils from healthy patients in the presence of opsonins to inhibit germination of *C. albicans* into clusters of hyphae in overnight assays as well as to kill *Candida* conidia (2 hours). The killing of the unopsonized *C. albicans* was found to be dependent solely on the complement receptor 3 (CR3) and the signaling proteins phosphatidylinositol-3-kinase and caspase recruitment domain-containing protein 9 (CARD9), but completely independent of NADPH oxidase activity, as opposed to opsonized *C. albicans* whose killing was dependent upon production of ROS by the NADPH oxidase system [22].

Consequently, all these mechanism could explain the low production of ROS by phagocytes in the presence of unopsonized *C. albicans.*

Study limitations

The lack of supplementary opsonins in our study in the case of *C. albicans* stimulus, coupled with the relatively short incubation time (20 minutes), compared to other studies that used isolated PBMC might have led to a lower degree of burst activation than in the case of opsonized *E. coli*.

Conclusions

The performance parameters for the *Phagoburst ™ (Glycotope Biotechnology)* kit obtained in our laboratory compared to the ones provided by the producer as well as the professional guidelines allow us to safely use the kit for burst oxidation assessment in human PBP. Our study suggests also that introducing an extra fungal stimulus for burst oxidation assessment could provide additional information regarding the non-specific cellular immune response, particularly in patients at risk for fungal bloodstream infection.

Acknowledgements

This study was partially financed by Internal Research Grants of the University of Medicine and Pharmacy of Tîrgu Mureş, Romania, Project number 15/23.12.2014.

Conflict of interests

The authors declared no potential conflicts of interest with respect to this research, authorship and/or publication of this article.

References

1. Fradin C, De Groot P, MacCallum D, Schaller M, Klis F, Odds FC, et al. Granulocytes govern the transcriptional response, morphology and proliferation of Candida albicans in human blood. Mol Microbiol 2005 Feb 18,56(2):397–415.
2. Gille C, Leiber A, Mundle I, Spring B, Abele H, Spellerberg B, et al. Phagocytosis and postphagocytic reaction of cord blood and adult blood monocyte after infection with green fluorescent protein-labeled Escherichia coli and group B Streptococci. Cytom Part B - Clin Cytom 2009,76(4):271–84.
3. Martin E, Bhakdi S. Flow cytometric assay for quantifying opsonophagocytosis and killing of Staphylococcus aureus by peripheral blood leukocytes. J Clin Microbiol 1992,30(9):2246–55.
4. Wellington M, Dolan K, Krysan DJ. Live Candida albicans suppresses production of reactive oxygen species in phagocytes. Infect Immun 2009 Jan,77(1):405–13.
5. Schuit KE. Phagocytosis and intracellular killing of pathogenic yeasts by human monocytes and neutrophils. Infect Immun 1979,24(3):932–8.
6. Destin KG, Linden JR, Laforce-Nesbitt SS, Bliss JM. Oxidative burst and phagocytosis of neonatal neutrophils confronting Candida albicans and Candida parapsilosis. Early Hum Dev 2009 Aug,85(8):531–5.
7. Martin E, Bhakdi S. Quantitative analysis of opsonophagocytosis and of killing of Candida albicans by human peripheral blood leukocytes by using flow cytometry. J ClinMicrobiol 1991,29(0095–1137 SB–IM):2013–23.
8. Salih HR, Husfeld L, Adam D. Simultaneous cytofluorometric measurement of phagocytosis, burst production and killing of human phagocytes using Candida albicans and Staphylococcus aureus as target organisms. Eur Soc Clin Infect Dis 2000,6:251–8.
9. Vitro I, Medical D, Conformity E. Instructions PHAGOBURST™ Version 04/09 page 1 of 9. :1–9.
10. Grumach AS, Ceccon ME, Rutz R, Fertig A, Kirschfink M. Complement profile in neonates of different gestational ages. Scand J Immunol 2014,79(4):276–81.
11. Yan M, Jacobs P, Wood B, Jevremovic D, Marie CB, Nancy D, et al. Validation of Cell-based Fluorescence Assays : Practice Guidelines from the ICSH and ICCS – Part V – Assay Performance Criteria n e. 2013,323(May):315–23.
12. O'Hara DM, Xu Y, Liang Z, Reddy MP, Wu DY, Litwin V. Recommendations for the validation of flow cytometric testing during drug development: II assays. J Immunol Methods 2011 Jan,363(2):120–34.
13. Wang L, Gaigalas AK, Marti G, Abbasi F, Hoffman RA. Toward quantitative fluorescence measurements with multicolor flow cytometry. Cytom Part A 2008 Apr,73A(4):279–88.
14. Barnett D, Granger V, Kraan J, Whitby L, Reilly JT, Papa S, et al. Reduction of intra- and interlaboratory variation in CD34+ stem cell enumeration using stable test material, standard protocols and targeted training. Br J Haematol 2000 Mar,108(4):784–92.
15. Dühring S, Germerodt S, Skerka C, Zipfel PF, Dandekar T, Schuster S. Host-pathogen interactions between the human innate immune system and Candida albicans-understanding and modeling defense and evasion strategies. Front Microbiol 2015,6(JUN):1–18.
16. Cheng SC, Joosten LAB, Kullberg BJ, Netea MG. Interplay between Candida albicans and the mammalian innate host defense. Infect Immun 2012,80(4):1304–13.
17. Mayer FL, Wilson D, Hube B. Candida albicans pathogenicity mechanisms. Virulence 2013,4(2):119–28.
18. Brown AJP, Budge S, Kaloriti D, Tillmann A, Jacobsen MD, Yin Z, et al. Stress adaptation in a pathogenic fungus. J Exp Biol 2014,217(Pt 1):144–55.
19. Miramón P, Kasper L, Hube B. Thriving within the host: Candida spp. interactions with phagocytic cells. Med Microbiol Immunol 2013 Jun 25,202(3):183–95.
20. Frohner IE, Bourgeois C, Yatsyk K, Majer O, Kuchler K. Candida albicans cell surface superoxide dismutases degrade host-derived reactive oxygen species to escape innate immune surveillance. Mol Microbiol 2009,71(1):240–52.
21. Lopez CM, Wallich R, Riesbeck K, Skerka C, Zipfel PF, Soloviev D. Candida albicans Uses the Surface Protein Gpm1 to Attach to Human Endothelial Cells and to Keratinocytes via the Adhesive Protein Vitronectin. Stevenson B, editor. PLoS One 2014 Mar 13,9(3):e90796.
22. Gazendam RP, Hamme JL Van, Tool ATJ, Houdt M Van, Verkuijlen PJJH, Herbst M, et al. Two independent killing mechanisms of Candida albicans by human neutrophils : evidence from innate immunity defects. 2017,124(4):590–8.

DE GRUYTER
OPEN

DOI: 10.1515/amma-2017-0019

Retraction

By the request of corresponding author Fogarasi Erzsébet, the article „Could Codeine Containing OTC Analgesics Sold in Romania be Used as Recreational Drugs?" published in Acta Medica Marisiensis, 2016;62(3):309-312 (DOI 10.1515/amma-2016-0031) was retracted, due to identified Conflicts of Interest.

As an immediate consequence of the aforementioned retraction, the accompanying editorial "The Culprit Coffee Filter and Freezer?" published in Acta Medica Marisiensis, 2016;62(3) had to be retracted for lack of object. This does not mean that we deny or back off the content of the editorial.

Statement of ethics

The journal observes and values the principles of ethics in scientific research, as previously highlighted in the main document on the topic: "The code of ethics for scientific research of the Târgu Mureș University of Medicine and Pharmacy" and according to all the documents enlisted as source of our code. We promote innovative research and original articles are thus prioritized. The editors adhere to the views and recommendations of the International Committee of Medical Journal Editors.

All forms of plagiarism will be exposed when and if evidenced. Therefore, we discourage ghost writing and guest authorship, including the situation when the author was unaware of being enlisted as co-author and as such, the cover letter is invalidated.

The peer-review process is intended to be a complimentary supplemental investment of expertise and is highly valued when well accomplished. The best peer-reviewers will be acknowledged by the editors and we promise to drop out the peer-reviewers who repeatedly acted as if their task was burdensome or annoying, and came up with shallow reports.

The journal encourages PhD students to publish their research. Reviews and "state of the art" articles will be hosted upon invitation. When judging the quality of the research, double standards are not an option.

Our retraction policy is intended to the articles inadvertently published, due to an unfair submittance, by this defining any form issue that trespasses our statement of ethics.

Errata will be inserted as soon as an error is detected, either spontaneously or by authorized notice.

Instructions for authors

All submitted manuscripts must be written in English. All authors should sign a *Licence to publish*, according to the model available here. This license to publish signed by all authors should be uploaded together with the manuscript on the editorial manager platform at the time of submission.
The corresponding author must complete and sign a *Cover Letter*, on behalf of all authors. This must contain the title of article, the name(s) of all author(s). The Cover Letter should attest that:

1. The manuscript is not submitted for publication elsewhere; in this case the cover letter must include the topic: "this paper has not been published previously" or "the results presented in this paper have not been published previously in whole or in part, except in abstract form";
2. The manuscript is an original work without fabrication, fraud, or plagiarism;
3. The author has read the complete manuscript and takes responsibility for the content of the manuscript;
4. Authors are required at the time of submission to disclose any potential conflict of interest (employment, consultancies, stock ownership, equity interests, and patent-licensing arrangements);
5. In the Cover letter must be included a description of each author's contribution. Authorship credit should be based on (a) substantial contributions to conception and design, acquisition of data, or analysis and interpretation of data; (b) drafting the article or revising it critically for important intellectual content; and (c) final approval of the version to be published. Authors should meet conditions a, b, and c. (See *Uniform Requirements for Manuscripts Submitted to Biomedical Journals: Ethical Considerations in the Conduct and Reporting of Research: Authorship and Contributor ship*).

Manuscripts that do not conform to the format guidelines will be returned to the authors for reformatting.
Manuscripts should respect all the requirements outlined below.
Acta Medica Marisiensis accepts for publication the following types of articles: original research, review, brief report, case presentation, case series, state of the art, letter to editor, editorial.

Font size and style, page layout and manuscript lenght. The text of the manuscript should be typed double spaced in 12 point font using 2 cm wide margins all around. Do not write with "Caps lock" on, not even for names and titles. For emphasys use only italics (no bold, no underline). All pages should be numbered consecutively. As a guide for manuscript length, there should be no more than 1 figure or 1 table for every 500 words.

Copyright. If any tables, illustrations or photomicrographs have been published elsewhere, written consent for re-publication must be obtained by the author from the copyright holder and the author(s) of the original article.
The signed permissions must be submitted with the manuscript and be identified as to the relevant item in the manuscript (e.g., "permissions for Figure 1").

Abbreviations. Except for units of measurement, abbreviations are strongly discouraged. Don not use abbreviations unless absolutely necessary. In order to abbreviate – the first time an abbreviation appears, it should be preceded by the words for which it stands.

Manuscript style. Assemble manuscripts in the order listed:

1. Title page, without author information. Do not write with "caps lock" on!
2. Abstract and keywords
3. Introduction
4. Methods
5. Results
6. Discussion
7. Acknowledgements and funding page
8. References
9. Appendices
10. Tables (including titles)
11. Figures (including titles and legends)

The format may be altered for review articles and case reports, if necessary.

Title page. The title page should contain only the title of the article, without any information related to name of authors, their affiliation or the address for correspondence. These information will be uploaded directly on editorial manager platform and their appearance in the text of the manuscript should be avoided, in order to ensure a blinded review process.
Use titles that stimulate interest, are easy to read and concise and contain enough information to convey the essence of the article. Title must not contain abbreviations. Do not write with „caps lock" on. Do not use symbols, special characters, or math formulas.

Abstract. Include no more than 250 words with the following headings: Objective, Methods, Results, and Conclusions. Insert a hard return (press the Enter key) before each heading. References should not be cited in the Abstract. Do not use acronyms or abbreviations. Do not use symbols, special characters, or math formula or spell them out (i.e.: alpha, beta, microns, etc.) or translate them (mean, chi square, etc.). Abstract should be written on a separate page following the title page.

Keywords: not more than 5, characterizing the scope of the paper, the principal materials, and main subject of work. Keywords must be written in small letters and separated by commas. Please use academically accepted keywords.

Manuscript text. Original research articles must include five main headings: Introduction, Methods, Results, Discussion, and Conclusion.

The presentation must be clear, concise and logically organized.
Introduction. Use very short introductions for presenting the context of the research for readers. Always end the introduction section with a clear statement of the study's objectives or hypotheses.
Methods. This section must describe the design of the study (selection/recruitment of patients, the number of patients), the study procedures including any interventions, measurements and data collection techniques and also the methods used for the statistical analysis.
For all manuscripts reporting data from studies involving human participants or animals, formal review and approval by an appropriate institutional review board or ethics committee is required and should be described in the Methods section. For those investigators who do not have formal ethics review committees, the principles outlined in the Declaration of Helsinki should be followed. For investigations of humans, state in the Methods section the manner in which informed consent was obtained from the study participants (i.e., oral or written). Editors may request that authors provide documentation of the formal review and recommendation from the institutional review board or ethics committee responsible for oversight of the study.
Results. In this section, the main characteristics of participants and your major findings must be presented.

Tables. Tables should not be embedded in the text of the article. Each table should have a brief descriptive title placed above the table. The approximate position of each table should be indicated in the manuscript (i.e.: Insert Table I). Tables must not duplicate material in text or figures. Cite each table in text in numerical order. Tables should be numbered consecutively with Roman numerals and must be cited exactly as "(Table I, Table II, etc)". All explanatory information and abbreviations should be given in a footnote below the table. Tables should be submitted as editable text and not as images. Each table should be typed single-spaced on a separate page after the Reference section in the submitted manuscript.

Figures. Figures should not be embedded in the text of the article. Each figure should have a brief descriptive title placed below the figure. The approximate position of each figure should be indicated in the manuscript (i.e.: Insert Figure 1). Figures must be numbered as they appear in the text and numbered consecutively with Arabic numerals (Figure 1, Figure 2, etc). Letters of permission from the copyright holder must accompany submission of borrowed material. Each figure should be presented on a separate page after the Reference section in the submitted manuscript. Figure legends should be typed single-spaced consecutively on a separate page.
Photomicrographs should include stain and magnification data at the end of the legend for each part of the figure. A magnification bar should be added to each photomicrograph. If no scale marker appears in the figure, the original magnification should be reported in the legend.
Figures are either black and white drawings, halftones (photographs), or com-

puter (laser) graphs or prints. Authors are responsible for the cost of printing color illustrations. Authors are also responsible for obtaining from the copyright holder permission to reproduce previously published figures. Where photographs of patients are included, consent to publish the photograph, signed by the patient must accompany the manuscript.
All figures should be submitted at a proper resolution as follows: monochrome images (images such as line graphs) will be submitted at a resolution of a minimum 900 DPI; black/white or color images will be submitted at a resolution of 300 DPI; combination halftones (images containing both pictures and text labeling) should be submitted at minimum of 600 DPI. Acceptable figure formats are JPEG and TIFF. Labels should be written using a font size appropriate for easy reading at a printed width of 87 mm for single-column fitting figures or 180 mm for 2-column fitting figures.
When submitting bar graphs, it should be taken into consideration that various patterns of black do not reproduce well.
All figures submitted for the review process must be in digital format, must be sent separately from the text file and must be named as Figure 1, Figure 2, etc.

Identification of Patients in Descriptions and Photographs. A signed statement of informed consent to publish (in print and online) patient descriptions and photographs should be obtained from all persons (parents or legal guardians for minors) who can be identified (including by the patients themselves) in such written descriptions, photographs and should be submitted with the manuscript and indicated in the Acknowledgment section of the manuscript.
Names of Drugs, Devices, and Other Products. Use only generic names of drugs, devices, and other products, unless the specific trade name of a drug is essential to the discussion.

Reproduced Materials. When previously published figures or tables are used, the author must obtain written permission from the copyright holder (usually the publisher) to reproduce the material in print and online. An appropriate credit line should be included in the figure legend or table footnote, and full publication information should be cited in the reference list.
Discussion. Provide a brief synopsis of your major findings, with particular emphasis on how the findings add to the body of pertinent knowledge, discuss possible mechanisms and explanations for the findings, compare study results with relevant findings from other published work, and discuss the limitations of the present study.

Conclusions. Provide only conclusions of the study directly supported by the results, along with implications for clinical practice, avoiding speculation and over-generalization. \

References. Authors are responsible for the accuracy and completeness of their references and for correct text citation.
The references should be numbered in the text between square brackets in citation order, making sure each is quoted in sequence in the text. In-text reference numbers may be repeated but not omitted. References cited in a table or figure legend should also be numbered.
The references list should give the name and initials of surname of all authors unless there are more than six, when only the first three should be given followed by et al. The authors' names should be followed by the title of the article, the title of the Journal abbreviated according to the style of Index Medicus, the year of publication, the volume number and complete page numbers.
For books one should give the name and initials of surname of all authors, the title of the book, which should be followed by the place of publication, the publisher, the year and the relevant pages.
For book chapters one should provide the name and initials of surname of all authors of the chapter, the title of the chapter, which should be followed by the name of editors, the name of the book, the place of publication, the publisher, the year and the relevant pages.
The titles of the journals should be abbreviated according to the style used in Index Medicus. Names of journals that are not cited should be entirely spelled out. Avoid using abstracts as references. Avoid citing a "personal communication".
The format for journal article, chapter, book, and publish-ahead-of-print journal article references is exactly as below:
For journals:
Hammermeister KE, Dodge HT – Evidence from a nonrandomized study that coronary surgery prolongs survival in patients with two-vessel coronary disease. Eur Heart J. 1979;59:1430-1435.
For book chapters:
Franz M – Monophasic action potential mapping, in Shenasa M, Borggrefe M, Breithardt G (eds): Cardiac Mapping. Futura Publishing Co.Inc. Mount Kisco, NY, 1993, 2565-2583
Acknowledgments. The Acknowledgments section may acknowledge contributions from non-authors, list funding sources, and should include a statement of any conflicts of interest.
Acta Medica Marisiensis considers all authors to be responsible for the content of the entire paper.

Other types of articles
a. Reviews. Review articles should include a brief abstract of no more than 200 words and the text should be limited to 5.000 words including references, tables and figures. Review articles can be submitted by invitation or unsolicited.

b. Case reports and case series. Case reports should be limited to presentation of a single particular and uncommon case, or uncommon presentation of a disease. Case series include description of a series of a maximum of 10 cases with common particularities. The abstract should be limited to 200 words, being divided into introduction, case presentation / presentation of case series and conclusions. The full manuscript should not exceed 2.000 words including references, figures and tables, being divided into sections headed Introduction, Case presentation / presentation of case series, Discussions, Conclusions.

c. Brief reports. Brief reports refer to articles presenting a short communication related to an original preclinical or clinical study which is not a case presentation or a case series report. The abstract should be limited to 200 words and the full text (including references, tables and figures) to 3.000 words.

d. Letter to editor. A letter to the editor may refer to an article recently published by the journal, commenting on the article in a constructive professional manner the content of which, in the opinion of the author(s) would add the current status of knowledge in the field. The letters should be limited to 500 words, 5 references and 3 authors. No abstract is required.

e. Editorial. Editorials should be limited to 2000 words (including references) and should be related to an article published in the current number or to a specific topic that is current and of high interest to the readers.

f. State-of-the-art papers. The journal publishes state-of-the-art articles that aim to provide an update on the current status of areas of high interest. The principal aim of such articles is to offer the specialist and other practitioners a source of continuing education and forum for discussion. A state-of-the-art article should have a full text limited to 4.000 words, in addition to a 200 word unstructured abstract. Sections of the article should be divided using headings relevant to each particular case.

Manscript limits specifications

Article type	Manuscript word limit	Maximum number of references	Maximum number of figures and tables	Abstract (max 250 words)
Review	5000	70	6	Yes
Original article	3500	40	6	Yes
Case report	2000	25	3	Yes
Letter to the Editor	1500	10	1	No

Publication fee. The publication fee for accepted article is 250 RON. The manuscript will be sent to the publication system only after the corresponding author pays the publication fee. The payment should be made in the name of the corresponding author at the University of Medicine and Pharmacy of Tirgu Mures cash desk or by bank transfer to the following account:

RO29TREZ47620F331600XXXX, Trezoreria Tîrgu Mureş, for: Universitatea de Medicină şi Farmacie Tîrgu-Mureş, CF 4322742, Str. Gh. Marinescu nr. 38, Mureş
Please mention "Article publication fee for Acta Medica Marisiensis" or "Taxa publicare articol Acta Medica Marisiensis".

The corresponding author will receive one printed issue of Acta Medica Marisiensis and 10 reprints of the published article. Please send the scanned proof of payment to ammjournal@umftgm.ro, with the subject "Publication fee".

For any further information please contact the Journal's editorial office at ammjournal@umftgm.ro